MONTHLY NOTICES

OF THE

ROYAL ASTRONOMICAL SOCIETY

Vol. 98 No. 7

MEETING OF 1938 MAY 13

Dr. H. Spencer Jones, President, in the Chair.

The President announced the death of Dr. Anders Donner, Associate of the Society.

The election by the Council of the following Fellow was duly confirmed :—

A. L. Narayan, M.A., D.Sc., Director of the Solar Physics Observatory, Kodaikanal, S. India.

The following candidates were proposed for election as Fellows of the Society, the name of the proposer from personal knowledge being appended :—

E. R. Bartlam, M.Eng., M.Inst.Struct.E., F.R.G.S., F.R.S.A., Principal, Ceylon Technical College, Colombo, Ceylon (proposed by F. C. Leonard) ; and

M. H. L. Pryce, Fellow of Trinity College, Cambridge (proposed by R. A. Lyttleton).

One hundred and two presents were announced as having been received since the last ordinary meeting, including :—

Boss (Benjamin) : General Catalogue of 33342 stars for the epoch 1950. Prepared at the Dudley Observatory, Albany, New York. Volumes I, II, III, IV, V. (Presented by the Carnegie Institution of Washington.)

Königsberg, Universitäts-Sternwarte, Astronomische Beobachtungen. Abtheilung 46. Katalog von 2043 Sternen zwischen 50° und 55° nördlicher Deklination für das Aequinoktium 1925.

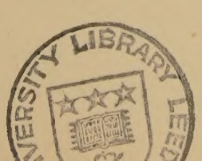

Waterfield (Reginald L.) : A Hundred Years of Astronomy. (Presented by the author.)

Weil (E.) : Albert Einstein. A Bibliography of his Scientific Papers, 1901–1930. (Presented by the author.)

The President announced that there was in stock a large number of aristotype (brown) prints from the Society's collection of celestial photographs, which are now reproduced as black and white bromide prints. These brown prints, so long as the stock lasted, would be offered to Fellows at half-price (6d. each).

Professor Fabry delivered the George Darwin Lecture, taking as his subject "Interstellar Space."

THE DISTRIBUTION OF STARS IN THE CAPE ASTROGRAPHIC ZONE, −40° TO −52°.

J. Jackson, M.A., D.Sc., F.R.S., H.M. Astronomer at the Cape.

The Cape Astrographic Zone, extending from declination −40° to −52°, covers about one-fourteenth of the whole sky. At its northern limit it reaches galactic latitude −78° at $0^h\ 40^m$ of R.A. and +22° at $12^h\ 40^m$. The zone is crossed obliquely by the Milky Way at 9^h and between 16^h and 17^h. The latter is a very interesting region very near to the galactic centre.

This zone has now been photographed four times with overlapping series of plates. Two series were taken with relatively short exposures round about 1900, the second being used in the construction of the Astrographic Catalogue. About the same time a series of plates with longer exposures were taken for the Astrographic Chart. The fourth series of plates was taken in the years 1923–28 for the determination of proper motions in conjunction with the most suitable of the earlier plates.

The proper motions were determined for all stars down to magnitude 9·5 in the *Cape Photographic Durchmusterung* and for 2432 fainter stars which were found to have a proper motion exceeding 5″ per century. The proper motions were measured relatively to stars estimated to be of photographic magnitude 11·9 on the international scale and interpreted as of mean magnitude 11·2 on the visual scale. The motions were made absolute by the application of the parallactic motion, taken as ″·0092 for these stars, and galactic rotation. The necessary constants were taken from *Groningen Publication* No. 45.

The results for the stars down to magnitude 9·0 have already been published and the copy for press for the remainder has been completed. The two catalogues contain respectively 20,843 and 20,554 entries. The actual number of stars is slightly less than 41,397, as occasionally the mass as well as the separate components of multiple stars has been measured. Also, this figure includes the 2432 faint stars of large proper motion.

About one-half of these stars are contained in the Henry Draper Catalogue, so that spectral types were immediately available. Dr. Shapley of the Harvard Observatory was approached with a view to obtaining the spectral classification of as many stars as possible. He and Miss Cannon most willingly agreed to co-operate in the work, as the zone was one for which Harvard Observatory possessed spectrum plates considerably better than the average. The principal difficulty in determining the spectra was the identification of the stars. For this purpose the stars were marked on photographic prints made from the chart plates at the Cape Observatory, and the identification was transferred from these prints to the spectrum plates at Harvard. In the end the spectra of 38,713 stars in the zone were classified by Miss Cannon. This leaves only 2684 entries without spectra, and 1200 of these are of the faint proper motion stars.

For astrophysical discussions we require, besides the proper motions and the spectra, the magnitudes of the stars. These were determined by means of the magnitudes of the C.P.D. and the measured diameters of the Astrographic Catalogue. The scale was based in a sequence of 71 stars from the 5th to the 12th magnitude in the neighbourhood of the south pole. By means of a diffraction grating and series of exposures ranging from 3 seconds to 30 minutes an accurate photographic scale was established amongst these stars and transferred to the Astrographic Zone. The zero point for each of the C.P.D. plates was taken from *Harvard Annals*, **80**, No. 13. The actual details of the determination, which is based on researches by Dr. Halm, are given in a volume entitled *Magnitudes of Stars in the Cape Zone Catalogue.* Although the limit taken throughout was magnitude 9·5 on the C.P.D. scale it varies considerably with the right ascension; in a few regions the correction to the C.P.D. magnitudes is as small as 0·5, but in some sparse regions it amounts to 2·0. For the great majority of regions it exceeds 1·0. The data therefore may be taken as essentially complete to magnitude 10·0, generally nearly complete to 10·5 and sometimes complete to 11·0. These magnitudes are approximately on the international photographic scale.

Star Counts.—Rather extensive star counts have been made of the stars, and these are being published in the volume dealing with 20,554 faint stars in this zone. The number of stars in each hour of R.A. (*i.e.* in an area of 124·8 square degrees) and for each 0·1 magnitude are given. The counts show that from the 8th to the 10th magnitude the galactic concentration does not vary much with the magnitude. There are fully six times as many stars in 8^h–9^h as in the hours of R.A. of high galactic latitude, while in 16^h–17^h there are only four times as many. It may be noted that although the galactic equator crosses the central line of the zone at R.A. $8^h\ 54^m$ the number of stars in 9^h–10^h is much smaller than in 8^h–9^h. The maximum of star density at the second crossing of the galaxy is not nearly so sharp as at the first. An examination of the observational data does not indicate that the difference can be explained by an error in the magnitude scale: it may be due to an obscuring medium.

Table I gives the number of stars per 100 square degrees in different galactic latitudes. In forming this table different hours of R.A. of approximately the same galactic latitude have been combined. No distinction has been made between positive and negative galactic latitudes.

The ratio of the number of stars brighter than magnitude m to the number brighter than magnitude $m - 1$ is called the star ratio. If stars were uniformly distributed throughout a perfectly transparent space the star ratio would be 3·98. The way in which the star ratio falls short of this value is shown in Table II. The last line of the table is affected by incompleteness of the star counts, but the loss of stars near the Milky Way is less than might have been expected. The results agree fairly well with those given by Seares and Van Rhijn (*Transactions of the International Astronomical Union*, **2**, 98, 1925), but not so well with those of Van Rhijn (*Groningen Publications*, No. 43, 1929). The results indicate that for stars in general, when catalogued by apparent magnitude, we reach to such great distances that the star density has con-

TABLE I

The Number of Stars per 100 Square Degrees in different Galactic Latitudes to different Magnitude Limits on the Photographic Scale

Mag. \ Gal. Lat.	−61°	−35°	± 17°	± 10°	± 3°
7·95	38	46	91	123	175
8·45	66	84	148	204	285
8·95	105	136	242	334	462
9·45	162	218	387	533	743
9·95	246	363	607	838	1146
10·45	368	553	903	1307	1763
10·95	527	740	1276	1778	2291

TABLE II

The Ratio of the Number of Stars N(m) brighter than Magnitude m to the Number N(m − 1) brighter than Magnitude m − 1

Mag. \ Gal. Lat.	−61°	−35°	± 17°	± 10°	± 3°	All
8·95	2·74	2·99	2·65	2·71	2·64	2·71
9·45	2·46	2·59	2·60	2·61	2·61	2·59
9·95	2·36	2·66	2·56	2·51	2·48	2·50
10·45	2·28	2·53	2·41	2·45	2·37	2·41
10·95	(2·14)	(2·04)	(2·10)	(2·12)	(2·00)	(2·08)

siderably diminished before magnitude 8. If we assume that the star density falls away as r^{-n} and if a be the star ratio, then

$$n = 3 - 5 \log a,$$

giving for $a = 2{\cdot}7$, 2·6, 2·5 the values of $n = 0{\cdot}84$, 0·92, 1·01. Hence taking the stars as a whole we may consider that between the 9th and 10th magnitude the star density is falling off approximately inversely as the distance if we assume that space is perfectly transparent to these distances. The star density at nearer distances does not fall off so rapidly, and at greater distances it falls off more rapidly.

Distribution of the Spectral Types.—Complete counts have been made of the different spectral types in different magnitude groups. At first each hour of R.A. was kept separate (as shown in fig. 1), but in Table III different hours of approximately the same galactic latitude have been combined. As more than half the spectra refer to stars fainter than magnitude 10·0, the data must be essentially complete to this magnitude, and the data in the faintest magnitude group may be taken as representing stars of magnitude 10·0–10·7 in low galactic latitudes and 10·0–10·9 in high latitudes. (The spectra of

TABLE III

Number of Stars of each Spectral Type arranged according to Galactic Latitude and Apparent Photographic Magnitude

R.A.	0^h–4^h, 21^h–24^h				4^h–6^h, 19^h–21^h				6^h–7^h, 11^h–14^h, 18^h–19^h			
Gal. Lat.	−61°				−35°				±17°			
Mag.	−7·9	8·0–8·9	9·0–9·9	10·0–	−7·9	8·0–8·9	9·0–9·9	10·0–	−7·9	8·0–8·9	9·0–9·9	10·0–
O									1			
B												
B0									2			
B1												
B2									4	1		
B3					1				20			
B5	2				2	1	2		13	3	3	2
B8	7		1		8	3	2		33	20	10	9
B9	5	1	2		12	4	6		53	44	44	26
A			3	1		1	10	6	1		11	39
A0	23	23	33	38	29	41	53	59	113	130	311	332
A2	33	20	24	33	19	33	56	57	54	104	190	272
A3	21	20	21	24	10	20	29	33	22	33	100	157
A5	13	15	31	29	9	12	32	45	19	43	78	127
A7				4			3	8			1	43
F			1	4			2	1			4	21
F0	18	52	56	57	22	45	82	73	21	91	122	205
F2	11	45	62	87	11	33	41	73	25	52	95	193
F5	27	81	131	275	17	45	120	226	26	47	149	360
F8	14	42	134	330	11	30	104	196	20	36	168	352
G			3	20			2	21			4	47
G0	29	50	208	602	12	28	134	321	15	40	166	526
G5	30	71	183	472	14	39	144	258	26	70	218	521
K			1	8				5				18
K0	84	115	223	505	39	85	182	324	78	148	309	666
K2	7	19	80	187	6	11	71	131	14	47	150	302
K5	2	16	18	132	4	9	32	78	8	21	97	230
K7			1	19			1	13			2	25
M	7	12	23	50	5	9	20	27	9	12	23	53
Total	333	582	1239	2877	231	449	1128	1955	577	942	2255	4526
−A3	91	64	84	96	81	103	158	155	316	335	669	837
A5–F5	69	193	281	456	59	135	280	426	91	233	449	949
F8–G5	73	163	528	1424	37	97	384	796	61	146	556	1446
K–	100	162	346	901	54	114	306	578	109	228	581	1294
Percentage of Different Types												
−A3	27·4	11·0	6·8	3·3	35·1	22·9	14·0	7·9	54·8	35·6	29·7	18·5
A5–F5	20·7	33·2	22·7	15·8	25·5	30·1	24·8	21·8	15·8	24·7	19·9	21·0
F8–G5	21·9	28·0	42·6	49·5	16·0	21·6	34·0	40·7	10·6	15·4	24·7	31·9
K–	30·0	27·8	27·9	31·3	23·4	25·4	27·1	29·6	18·9	24·2	25·8	28·6

TABLE III

Number of Stars of each Spectral Type arranged according to Galactic Latitude and Apparent Photographic Magnitude

R.A.	7^h–8^h, 10^h–11^h, 14^h–16^h, 17^h–18^h				8^h–10^h, 16^h–17^h				Total No. of Stars of each Spectral Type			
Gal. Lat.	±10°				±3°							
Mag.	–7·9	8·0–8·9	9·0–9·9	10·0–	–7·9	8·0–8·9	9·0–9·9	10·0–	–7·9	8·0–8·9	9·0–9·9	10·0–
O	1			1	8	2	2		10	2	2	1
B				8	5	9	23	29	5	9	23	37
Bo	6	8	5	2	13	7	18	18	21	15	23	20
B1	3				6				9			
B2	15	2	4	2	14	8	16	9	33	11	20	11
B3	40	7	8	11	63	23	32	36	124	30	40	47
B5	47	23	18	16	55	35	40	61	119	62	63	79
B8	67	85	81	97	80	89	173	179	195	197	267	285
B9	107	143	167	209	84	169	200	226	261	361	419	461
A	4	9	34	144	2	5	26	94	7	15	84	284
Ao	124	282	659	999	81	266	587	742	370	742	1643	2170
A2	63	108	303	615	40	75	264	450	209	340	837	1427
A3	22	42	120	292	21	35	98	231	96	150	368	737
A5	17	29	93	234	15	21	65	189	73	120	299	624
A7			7	74		1	10	62		1	21	191
F			5	21			7	17			19	64
Fo	28	68	181	253	28	46	108	191	117	302	549	779
F2	21	41	100	265	7	23	63	157	75	194	361	775
F5	27	62	167	406	21	28	110	248	118	263	677	1515
F8	15	53	172	386	10	29	95	192	70	190	673	1456
G		3	12	54		1	5	25		4	26	167
Go	19	45	162	518	10	15	95	229	85	178	765	2196
G5	37	77	212	540	20	45	127	208	127	302	884	1999
K		1	5	24				11		1	6	66
Ko	74	145	353	721	48	91	198	390	323	584	1265	2606
K2	14	44	143	303	12	22	79	147	53	143	523	1070
K5	16	22	87	253	10	20	64	139	40	88	298	832
K7			3	54			2	25			9	136
M	8	14	30	73	3	7	17	43	32	54	113	246
Total	775	1313	3131	6575	656	1072	2524	4348	2572	4358	10277	20281
–A3	499	709	1399	2396	472	723	1479	2075	1459	1934	3789	5559
A5–F5	93	200	553	1253	71	119	363	864	383	880	1926	3948
F8–G5	71	178	558	1498	40	90	322	654	282	674	2348	5818
K–	112	226	621	1428	73	140	360	755	448	870	2214	4956
Percentage of Different Types												
–A3	64·4	54·0	44·7	36·4	72·0	67·4	58·6	47·7	56·7	44·4	36·9	27·4
A5–F5	12·0	15·2	17·7	19·1	10·8	11·1	14·4	19·9	14·9	20·2	18·7	19·5
F8–G5	9·2	13·6	17·8	22·8	6·1	8·4	12·8	15·0	11·0	15·5	22·8	28·7
K–	14·4	17·2	19·8	21·7	11·1	13·1	14·3	17·4	17·4	20·0	21·5	24·4

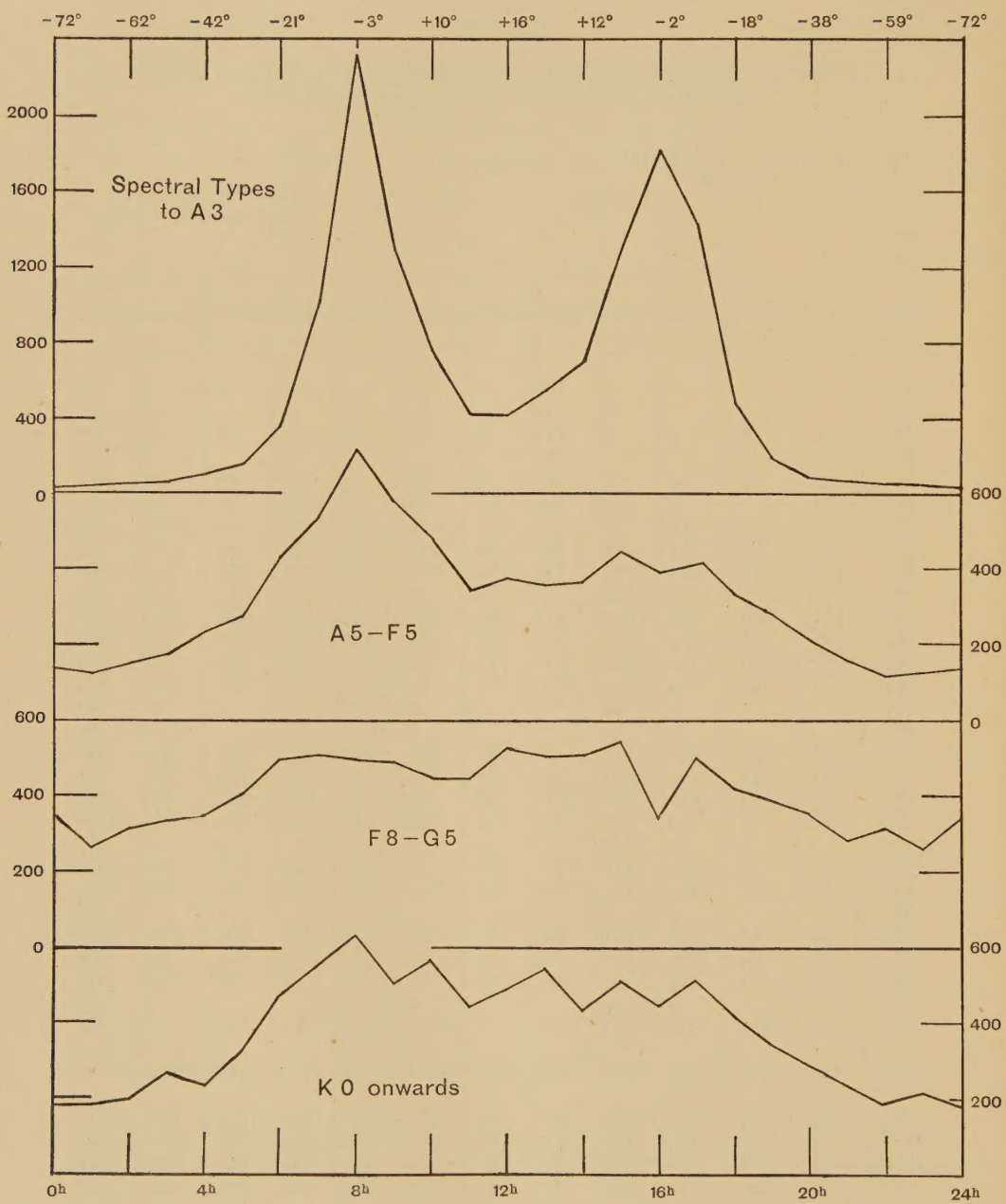

FIG. 1.—*Distribution of stars of different spectral ranges according to R.A. (indicated below where* 0^h *refers to* 0^h *to* 1^h*, etc.) and galactic latitude (indicated at top). The scale for the earliest type stars has been reduced to half that for the others so as to keep the diagram within reasonable size. It will be noted that variation with galactic latitude is least for stars of type F8 to G5. At the crossing of the Milky Way near* 16^h *there appears to be a deficiency of stars of all types. The simplest explanation would be the presence of an obscuring medium, but as the deficiency is most marked for types F8 to G5 this explanation does not appear tenable. This direction is not very different from that to the galactic centre. The actual star counts have been slightly adjusted to make the data complete to magnitude 10·9 for all R.A.'s.*

1232 faint proper motion stars have not been included in this table.) It will be noted that types A7 and K7 are represented only amongst the faintest stars—this results from the fact that these types were not classified in the Draper Catalogue. Also account should be taken of the fact that subdivisions of the spectral class are not given for the faintest stars, so that, for example, stars of type A should be distributed amongst types A0 to A5. But the number of such stars is small, and cannot affect our analysis to any serious extent. The most outstanding feature of Table III is the variation of the number and percentage of early type stars as indicated in Tables IV and V for types earlier than A5 : the result would be even more striking if we dealt with stars earlier than A0.

TABLE IV

Number of Stars earlier than A5 per 100 Square Degrees for different Galactic Latitudes and Ranges of Apparent Magnitude

(The last column is not complete to magnitude 10·9 except in high latitudes)

Gal. Lat. \ Mag.	−7·9	8·0–8·9	9·0–9·9	10·0–
°				
± 3	126	193	395	(554)
± 10	80	103	224	(384)
± 17	51	54	107	(134)
−35	16	21	32	31
−61	10	7	10	11

TABLE V

Percentage of Stars of Types earlier than A5 for different Magnitudes and Galactic Latitudes

Gal. Lat. \ Mag.	−7·9	8·0–8·9	9·0–9·9	10·0–
°				
± 3	72·0	67·4	58·6	47·7
± 10	64·4	54·0	44·7	36·4
± 17	54·8	35·6	29·7	18·5
−35	35·1	22·9	14·0	7·9
−61	27·4	11·0	6·8	3·3

Table VI shows the number of stars to different magnitude limits for each spectral type and also the variation of the star ratio with spectral type and magnitude. This table shows that the star ratio is approximately equal to 1·35 for types up to B3. For later types it is larger, but presents some curious anomalies. For types B8 and B9 the star ratio shows a larger increase for the brighter stars, and this is very marked in stars of type A0. With so many stars the change of the star ratio from 3·01 to 2·50 at magnitude 8·9 may be significant and represent a real phenomenon of stellar distribution. For types A2 to A5 the star ratio is the same for the two magnitude

TABLE VI

Number of Stars N(m) to different Magnitude Limits for each Spectral Type
(Adjusted for Stars of Type B, A, F, G, K, A7 and K7)

Mag. Limit / Spec.	7·9	8·9	9·9	$\frac{N(8\cdot9)}{N(7\cdot9)}$	$\frac{N(9\cdot9)}{N(8\cdot9)}$
O–B2	74	103	153	1·39	1·49
B3	125	157	201	1·26	1·28
B5	120	184	251	1·53	1·36
B8	196	395	667	2·02	1·69
B9	262	625	1049	2·39	1·68
A0	373	1122	2803	3·01	2·50
A2	211	555	1414	2·63	2·55
A3	97	249	629	2·57	2·53
A5	74	197	520	2·66	2·64
F0	117	419	982	3·58	2·34
F2	75	269	635	3·59	2·36
F5	118	381	1063	3·23	2·79
F8	70	260	937	3·71	3·60
G0	85	265	1043	3·12	3·94
G5	127	431	1328	3·39	3·08
K0	323	908	2177	2·81	2·40
K2	53	196	720	3·70	3·67
K5	40	128	433	3·20	3·38
M	32	86	202	2·69	2·35
Total	2572	6930	17207	2·70	2·48

limits. It would, of course, be possible to smooth out the results by a slight alteration in the spectral classification which may not be quite independent of apparent magnitude.

For stars of type F0 to F5 the value of $N(8\cdot9)/N(7\cdot9)$ is definitely nearer the theoretical ratio than for stars a magnitude fainter. The number of stars of type F8 approaches fairly closely to that resulting from uniform distribution, while for type G0 there is an inversion of the normal variation of the star ratio with magnitude. Type K0 shows a sudden drop in the star ratio which is not shown by stars of type K2 and K5, but again appears in the latest type stars.

Much of this data can be fitted into the recognised division of stars into giants and dwarfs. When stars are counted by apparent magnitudes we include intrinsically bright stars at very great distances, and even when they are relatively rare in a given volume of space the volume concerned is so great that they appear relatively numerous. For a difference of 5 magnitudes the volume of space is increased 1000-fold. The interpretation of these figures is therefore that for types such as F8 we are dealing with a small enough volume of space to reveal little change in the star density with distance (or with small enough distances for absorption of light to be ignored). It is

known that for K-type stars there is a great range in the real brilliancy of the different members, and the low value of the star ratio for type Ko indicates that the majority of the stars are giants similar in real brightness to the Ao stars. The K2 stars, on the other hand, appear to include a large proportion of near stars. It may be mentioned here, however, that Ko and K2 stars show very similar distribution of proper motions quite different from that for the Ao stars. The large difference in the star ratio between Ko and K2 stars may be due to a difference in the classification of bright and faint stars.

The subdivision of the stars into giants and dwarfs can be accomplished for individual stars by means of their parallax, proper motion or spectral peculiarities. Generally, however, such a subdivision has only been attempted for selected stars and there is very little information regarding the stars as a whole to some definite apparent magnitude. We know that even when we limit ourselves to naked-eye stars there is a large proportion of them of great luminosity and situated at such great distances that they are outside a region of space for which the star density is uniform, and indeed at distances where the star density is a small fraction of what it is in our neighbourhood. On the other hand, dwarf stars must lie in a relatively small volume of space, and we can consider that for them the star ratio reaches its theoretical value. We have already noted on this account that stars of type F8 are on the whole the most uniformly distributed and therefore intrinsically the faintest. As an hypothesis for determining the number of giants and dwarfs in any group we can assume that the dwarfs are distributed uniformly with the star ratio equal to 3·98, while the giants have the same distribution as the stars earlier than A5, which we take to be all giants. Consider, for example, the stars in the highest galactic latitudes. Let x be the number of dwarfs and y the number of giants brighter than apparent magnitude 8·0 and of spectral types A5 to F5. Then from the data of Table III we have

$$\begin{aligned} x+y &= 69 \\ 2{\cdot}98x+\tfrac{64}{91}y &= 193 \\ 11{\cdot}86x+\tfrac{84}{91}y &= 281. \end{aligned}$$

In these equations 2·98 and 11·86 ($=3{\cdot}98\times 2{\cdot}98$) represent the volumes of space involved by the magnitude limits on the assumption of uniform distribution, while 91, 64, 84 are the number of stars of types earlier than A5 and are supposed to determine the relative proportion of giants to the different limits of apparent magnitude. In this way we get three equations for two unknowns and the question of weighting the equations arises. We might solve for x and y from two of the equations and test the suitability of the hypothesis by the accuracy with which the third is satisfied. Actually we have solved the equations by least squares, giving to each equation a weight inversely proportional to the coefficient of x, *i.e.* by multiplying the equations throughout by a factor to reduce the coefficient of x to unity and considering the three resulting equations of equal weight. The results obtained in this way are shown in Table VII, where the headings "d" and "g" denote the number of dwarfs and giants in the various groups. The

TABLE VII

Separation of Stars into "Dwarfs" and "Giants" by Means of Counts of Stars according to Magnitude

Gal. Lat.	Stars Brighter than 8·0				Magnitude 8·0–8·9				Magnitude 9·0–9·9			
	Computed			Obs.	Computed			Obs.	Computed			Obs.
	d	*g*	*d*+*g*	*d*+*g*	*d*	*g*	*d*+*g*	*d*+*g*	*d*	*g*	*d*+*g*	*d*+*g*
					A5–F5							
−61°	37	35	72	69	111	25	136	193	440	32	472	281
−35	22	39	61	59	65	50	115	135	260	76	336	280
± 17	42	53	95	91	125	56	181	233	499	111	610	449
± 10	35	59	94	93	105	84	189	200	418	165	583	553
± 3	14	56	70	71	41	86	127	119	165	176	341	363
All	137	259	396	383	407	343	750	880	1620	672	2292	1926
					F8–G5							
−61	45	29	74	73	134	20	154	163	531	26	557	528
−35	31	6	37	37	92	7	99	97	366	11	377	384
± 17	43	18	61	61	129	19	148	146	514	37	551	556
± 10	42	30	72	71	126	42	168	178	501	84	585	558
± 3	22	18	40	40	65	27	92	90	260	55	315	322
All	176	106	282	282	526	140	666	674	2096	275	2371	2348
					K–							
−61	30	71	101	100	89	50	139	162	356	66	422	346
−35	22	33	55	54	65	42	107	114	260	64	324	306
± 17	44	67	111	109	131	71	202	228	521	142	663	581
± 10	36	77	113	112	108	109	217	226	431	215	646	621
± 3	16	57	73	73	48	88	136	140	191	180	371	360
All	128	325	453	448	383	431	814	870	1524	844	2368	2214

agreement between the computed $d+g$ and the actual number of stars indicates the extent of fit of the hypothesis with the data. The fit is best for spectral types F8–G5, where the proportion of dwarfs to giants is greatest. This does not mean that the distinction between dwarfs and giants is most clear cut in this spectral range—we know that the range in magnitude is greatest for the late type stars. The fit is somewhat better near the galaxy than away from it. There is a distinct systematic difference between the computed and the observed numbers in the sense that for the faintest magnitudes the computed numbers are too great. This can be attributed to a slight error in our magnitude scale or to a slight fall in the star density of the "dwarf stars" at the distances involved. The table indicates that for types F8 to G5 there are 5 dwarfs to 3 giants brighter than 8·0, but a proportion of nearly 8 to 1 for magnitudes 9·0–9·9. For other classes there are more

giants than dwarfs for the brighter stars, but the ratio is reversed at the 8th magnitude.

When we restrict the typical giants to stars of type A0 and earlier we get similar results. If an attempt were made to extrapolate the formula to magnitude 10·9 we would find that the computed number of dwarfs was greater than the total number of stars. The only way to fit the star counts into a formula is to take account of the actual fall in star density, except for a comparatively small proportion of the stars we have been considering. The fact that our analysis fits best for the lowest latitudes indicates a uniform distribution to a greater distance in the galactic plane. The failure of the late type stars to fit the formula very well throws doubt on the assumption of a similar distribution of late and early type giants, or indicates the existence of stars of intermediate intrinsic brightness.

In the analysis we have been dealing with areas of different size in the different galactic latitudes, the counts for galactic latitude −61° extend over 7 hours of R.A., while those for ± 3° extend over 3 hours only. Table VIII gives the computed number of dwarfs and giants together with the observed total brighter than magnitude 8·0 for each 1000 square degrees of the sky.

TABLE VIII

Number of Stars per 1000 *Square Degrees brighter than* 8·0 *Photographic Magnitude*

Gal. Lat.	−A3	A5–F5			F8–G5			K–		
	Obs.	*d*	*g*	Obs. *d*+*g*	*d*	*g*	Obs. *d*+*g*	*d*	*g*	Obs. *d*+*g*
−61°	104	42	40	79	51	33	83	34	82	114
−35	162	44	78	118	62	12	74	44	66	108
± 17	506	67	84	146	69	28	98	70	107	175
± 10	800	56	94	149	68	48	114	58	123	180
± 3	1260	37	150	190	58	47	107	43	154	195
All	487	46	87	128	59	35	94	43	109	150

The interest in this table lies in the variation of the numbers with galactic latitude. As our classes of dwarfs and giants are to a large extent classes of near and distant stars, we should expect that the number of the former should not vary much with galactic latitude, while for the latter there should be a concentration to the galaxy. This is what we find, although there is a tendency for the number of dwarfs of all types to increase in intermediate latitudes. For the group of stars F8–G5 the concentration of giants to the galactic plane is not so marked as for the other types, but for none of the later types is the concentration so marked as for the earliest types to A3—a result distinctly opposed to our hypothesis that the distribution of the earliest type stars may be assumed as the same as the distribution of the giants of other types.

Colour Index.—From a knowledge of the proportion of stars of different spectral types we can calculate the mean colour index if we assume the relationship between colour index and spectral type to be known. As there is a variation of colour index with absolute magnitude and a variation of absolute magnitude with apparent magnitude, there must be some variation of colour index with apparent magnitude even for stars of the same spectral type, but it is not great and for our purposes may be neglected. There is still some uncertainty in the actual value of the mean colour index for each type, and although this uncertainty will enter into our results it does not seriously affect the variation of mean colour index with galactic latitude and apparent magnitude. We have based our calculations on the Harvard colour indices as given on p. 137 of the *Transactions of the I.A.U.*, 4 (1932), and extended to O-type stars, viz.:

Sp.	O	Bo	B5	B8	Ao	A2	A5	Fo
C.I.	−·60	−·42	−·21	−·10	·00	+·08	+·17	+·26
Sp.	F5	Go	G5	Ko	K2	K5	M	
C.I.	+·35	+·57	+·78	+1·03	+1·20	+1·45	+1·67	

TABLE IX

Mean Colour Indices according to Apparent Photographic Magnitude

Mag.		−7·9		8·0–8·9		9·0–9·9		10·0–	
R.A.	Gal. Lat.	C.I.	No.	C.I.	No.	C.I.	No.	C.I.	No.
h h	°								
0–1	−72	·51	47	·64	69	·67	171	·68	358
1–2	−69	·69	45	·60	78	·63	155	·73	311
2–3	−62	·49	43	·64	88	·64	154	·74	341
3–4	−52	·48	55	·59	109	·67	207	78	415
4–5	−42	·40	49	·46	90	·62	284	·66	464
5–6	−31	·37	66	·51	130	·59	308	·69	471
6–7	−21	·25	111	·44	199	·57	451	·64	587
7–8	−12	·14	200	·32	325	·41	701	·51	787
8–9	− 3	·07	311	·19	492	·29	1049	·33	1308
9–10	+ 4	·21	147	·29	295	·32	716	·43	1431
10–11	+10	·31	131	·41	232	·45	546	·55	1321
11–12	+14	·33	101	·45	192	·56	457	·59	1010
12–13	+16	·37	97	·50	152	·51	441	·62	1074
13–14	+15	·27	135	·41	187	·51	428	·61	1217
14–15	+12	·25	119	·38	182	·43	498	·51	995
15–16	+ 6	·27	153	·28	266	·36	687	·41	1785
16–17	− 2	·10	198	·14	285	·21	759	·31	1607
17–18	− 9	·16	172	·24	308	·35	700	·41	1687
18–19	−18	·33	133	·46	212	·47	478	·58	638
19–20	−28	·44	63	·53	130	·59	308	·65	565
20–21	−38	·56	53	·57	99	·63	228	·68	455
21–22	−49	·56	44	·53	89	·65	204	·72	466
22–23	−59	·56	54	·62	84	·66	177	·72	496
23–24	−67	·59	45	·60	65	·66	171	·72	490

Table IX gives the resulting colour indices according to R.A. (or galactic latitude) and apparent magnitude, together with the number of stars. There is a steady increase in the colour index with magnitude and galactic latitude. The colour index, however, is not quite the same for different regions of the same galactic latitude and the minimum is reached a few degrees south of the galactic plane. The actual variation with galactic latitude is shown in fig. 2. For the 1232 stars fainter than 9·5 C.P.D. and of proper motion exceeding 5″ per century the mean colour index is +0·88, and it does not vary appreciably with the galactic latitude.

As has been pointed out by Seares,* the number of stars down to a definite visual magnitude cannot be deduced directly from the number down to a definite photographic magnitude by applying the mean colour index. For this purpose it is important to know the variation of colour index with visual as well as photographic magnitude. From Table III it is possible, with a knowledge of the relation between colour index and spectral type, to form the corresponding table for visual magnitudes. The calculations have been roughly made for the hours of R.A. with the extreme galactic latitudes, and the results are given below, where the colour indices for photographic magnitudes have been added for comparison.

Mag.	Galactic Latitude −61°		Galactic Latitude ± 3°	
	Colour Index for		Colour Index for	
	Visual Magnitudes	Photographic Magnitudes	Visual Magnitudes	Photographic Magnitudes
−7·9	+·72	+·54	+·39	+·11
8·0–8·9	+·76	+·60	+·45	+·21
9·0–9·9	+·81	+·66	+·49	+·28

The colour index is greater for visual than photographic magnitudes, but the difference decreases as the colour index increases, and the relationship between colour index for visual and photographic magnitudes independent of magnitude and galactic latitude is given very closely by

$$\text{C.I. (visual)} = 0{\cdot}28 + 0{\cdot}80 \text{ C.I. (photographic)}.$$

With this formula the two colour indices become equal at +1·40, which is close to the colour index for type K5.

The results given here do not agree well with those given by Seares in *Ap. J.*, **61**, 114 (1925). The variation of colour index varies so greatly with galactic latitude that it does not seem desirable to combine the data of all galactic latitudes together in investigating the change of colour index with magnitude, and *vice versa*.

* *Ap. J.*, **61**, 128, 1925.

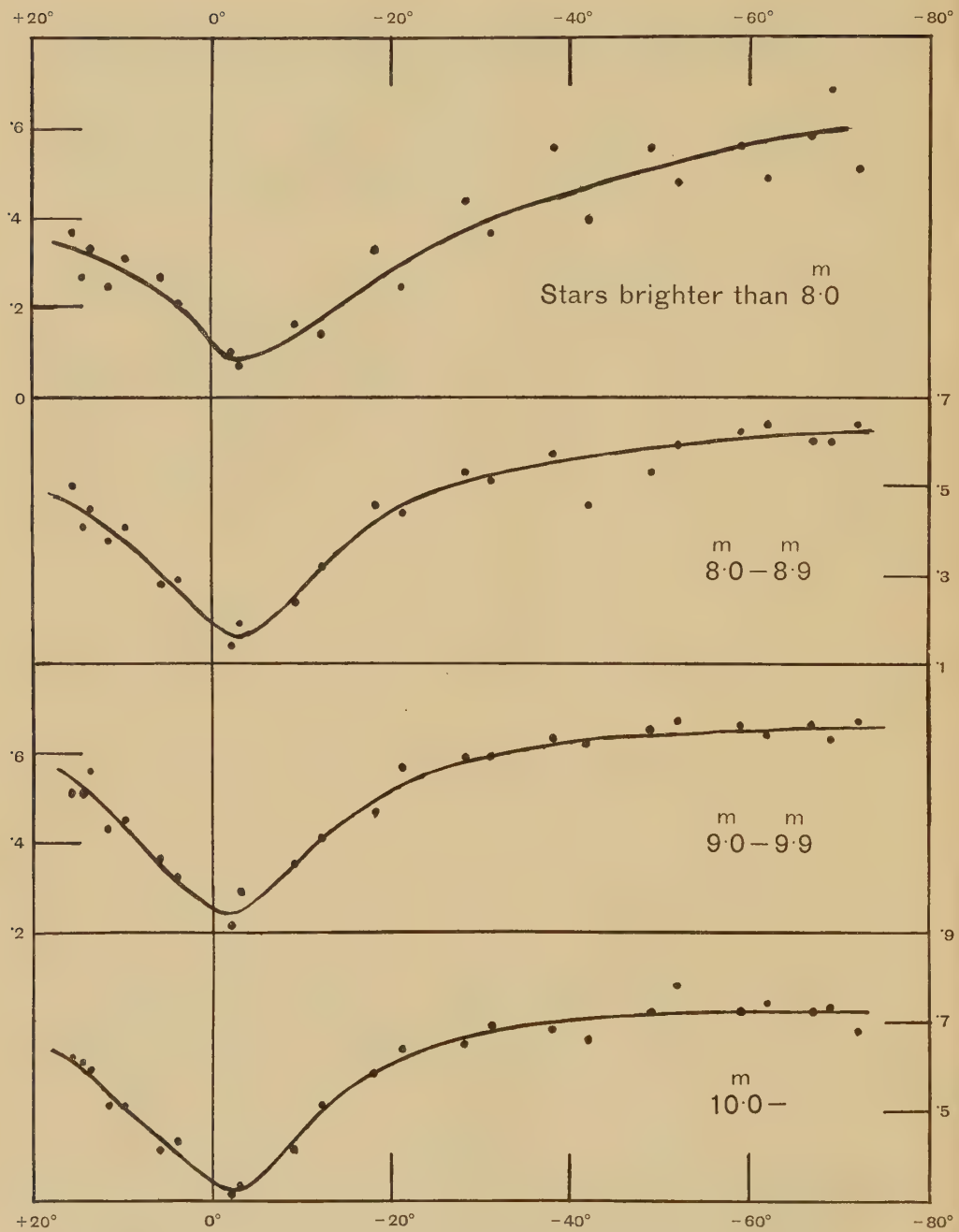

FIG. 2.—*Variation of colour index with apparent photographic magnitude and galactic latitude.*

Mean Parallax.—From an analysis of the proper motions of stars in different spectral ranges and different magnitude ranges the mean parallactic motion, and hence the mean parallax, was derived as follows (Proper Motion of Stars in the Zone Catalogue for 1900, p. xxx) :—

Spec. Type / Mag.	−A3	A5–F5	F8–G5	K–
	″	″	″	″
−7·9	·0054	·0094	·0121	·0073
8·0–8·9	35	68	103	54
9·0–9·9	30	49	77	42
10·2	27	36	42	30

These results were obtained for the whole zone without considering galactic latitude, but, from the agreement of the results when the hours are weighted equally with those when they are weighted according to the number of stars, it appears that these values can be accepted for all galactic latitudes. It should be pointed out that a definite assumption was made in converting the relative proper motions to absolute. The reference stars were of mean photographic magnitude 11·9, and from *Groningen Publications*, **45**, the mean parallactic motion of ″·0092 was adopted. This corresponds to a parallax of ″·0022. When we combine the values of the parallax according to spectral type with the number of stars of each spectral type we obtained the following results for the mean parallax as a function of galactic latitude and apparent photographic magnitude:—

Gal. Lat. / Mag.	−61°	−35°	± 17°	± 10°	± 3°
	″	″	″	″	″
−7·9	·0083	·0079	·0071	·0068	·0065
8·0–8·9	70	64	58	52	47
9·0–9·9	58	54	49	44	41
10·2	46	43	40	37	34

If we extend and interpolate this table to photographic magnitudes 10·0, 11·0 and 12·0, we get the following mean parallaxes in units of ″·0001 :—

Gal. Lat. / Mag.	0°	5°	10°	15°	20°	30°	40°	50°	60°
10·0	35	36	38	40	42	40	45	47	48
11·0	26	27	29	30	31	33	34	35	36
12·0	19	19	20	21	22	24	24	25	26

Proper Motions.—The motions of the stars down to magnitude 9·0 C.P.D. have been analysed. Some of the results have been used in the previous section. Another result is that stars of all spectral types show star-streaming

directed to the same vertex, although there is a range of 10° in the R.A. of the vertex depending on the galactic latitude. A count has been made of the number of stars with proper motions between certain limits. It was considered sufficient to classify the proper motion by the magnitude of the larger component (R.A. or Dec.) and not to combine the two components. The results are being published in detail in a Cape Catalogue, and here we give only a summary in Table X where different ranges of spectral type have been combined. In this table the stars in each spectral range have been classified by magnitude, and a final line shows the stars fainter than 9·5 C.P.D. found to have a proper motion exceeding 5″ per century. This last line is not complete to any definite magnitude, but it shows the variation of large proper motion with spectral type, faint stars of large proper motion not occurring in the earlier types. Of 8395 stars of type Ao or earlier the proper motion exceeds ″·16 for only four stars as follows :—

Z.C. No.	Spec.	Mag.	P.M.	Par.	
			″ ″	″ ″	
19748	B5	2·1	+·118 −·162	+·036 ± ·005	α Gruis
10603	Ao	3·0	−·200 −·015	+·032	γ Centauri
20671	Ao	7·9	+·239 −·871	+·026 ± ·007	Co.D. −42° 16457
13817	Ao	8·9	−·165 −·084	...	Co.D. −44° 10333

The first two of these stars seem to be normal early type stars comparatively near us. The third is faint for an Ao star so near as it is, but if the parallax is accurate it is not so faint as the white dwarfs normally are. Its spectrum should be checked. There are very few other chances of white dwarfs amongst the 38,000 stars brighter than 9·5 C.P.D. in the zone. There are only five stars with a proper motion exceeding 16″ per century of types A2–A7.

The proportion of stars of proper motion exceeding 4″ per century is twice as great for A2–A7 stars as for Ao stars. For types as far as Go the number of stars of large proper motion rapidly increases, and whereas for Ao stars only 2 per cent. have a proper motion exceeding 4″ per century, it reaches 40 per cent. for F8–Go stars. For still later types the number of large proper motions falls off, although it does not tend to vanish as for the early type stars. For the later types also there is a very considerable contribution to the number of large proper motions from the stars fainter than 9·5 C.P.D. The distinction between giants and dwarfs is not clearly drawn in stars of type K, and when stars are selected as here by apparent magnitude it appears that there is a continuous gradation from giants to dwarfs. For M-type stars the division is clearer, and it is tempting to assume that all the stars in the bottom right-hand of the table are dwarfs.

From counts of the number of stars with different proper motions it is easy to deduce the median proper motion. These are given for a rather more extended spectral range in Table XI. This table again shows a close agreement between all the subdivisions of type B. Thereafter there is a

TABLE X

Number of Stars for which the Larger Component of Proper Motion lies between Certain Limits

Unit ″·001 per annum

Spec.	Photographic Magnitude	< 10	10–19	20–39	40–79	80–159	⩾ 160	Total
B–B5	− 7·9	40	106	114	33	1	1	295
	8·0– 8·9	43	59	19	1	...	...	122
	9·0– 9·9	71	76	18	1	1	...	167
	10·0–10·9	90	89	6	...	...	...	185
	11·0–	6	2	1	...	...	...	9
	P.M. stars	...	...	...	...	...	...	...
	Total	250	332	158	35	2	1	778
B8–B9	− 7·9	75	163	163	43	3	...	447
	8·0– 8·9	171	268	120	4	...	...	563
	9·0– 9·9	285	319	72	1	1	...	678
	10·0–10·9	288	334	60	2	...	...	684
	11·0–	22	29	4	...	...	...	55
	P.M. stars	...	...	...	...	...	...	...
	Total	841	1113	419	50	4	...	2427
A0	− 7·9	44	114	134	66	9	2	369
	8·0– 8·9	175	326	214	19	...	1	735
	9·0– 9·9	513	805	346	13	2	...	1679
	10·0–10·9	798	1078	297	14	2	...	2189
	11·0–	100	98	19	...	...	...	217
	P.M. stars	...	...	...	...	1	...	1
	Total	1630	2421	1010	112	14	3	5190
A2–A7	− 7·9	23	72	141	93	25	4	358
	8·0– 8·9	117	189	246	61	3	...	616
	9·0– 9·9	369	641	448	58	3	...	1519
	10·0–10·9	785	1272	606	33	4	...	2700
	11·0–	80	139	48	1	...	...	268
	P.M. stars	...	...	...	1	4	1	6
	Total	1374	2313	1489	247	39	5	5467
F0–F5	− 7·9	18	40	67	98	56	26	305
	8·0– 8·9	66	151	269	199	68	6	759
	9·0– 9·9	201	421	661	275	41	1	1600
	10·0–10·9	563	924	1020	239	32	3	2781
	11·0–	87	127	101	23	3	...	341
	P.M. stars	...	...	...	30	26	8	64
	Total	935	1663	2118	864	226	44	5850

TABLE X—*continued*

Spec.	Photographic Magnitude	< 10	10–19	20–39	40–79	80–159	⩾ 160	Total
F8–G0	– 7·9	4	13	23	23	44	47	154
	8·0– 8·9	10	40	67	128	92	26	363
	9·0– 9·9	77	235	495	403	176	56	1442
	10·0–10·9	310	806	1143	755	212	42	3268
	11·0–	82	151	181	82	15	2	513
	P.M. stars	...	...	7	126	166	24	323
	Total	483	1245	1916	1517	705	197	6063
G5	– 7·9	12	23	28	27	20	15	125
	8·0– 8·9	26	59	86	58	46	24	299
	9·0– 9·9	104	215	246	165	101	51	882
	10·0–10·9	272	469	497	315	133	37	1723
	11·0–	47	85	81	46	11	1	271
	P.M. stars	...	...	4	108	180	32	324
	Total	461	851	942	719	491	160	3624
K0	– 7·9	21	57	97	84	43	17	319
	8·0– 8·9	67	146	215	116	28	8	580
	9·0– 9·9	221	386	452	143	44	28	1274
	10·0–10·9	517	847	665	199	63	27	2318
	11·0–	68	136	89	31	9	2	335
	P.M. stars	...	...	1	78	156	46	281
	Total	894	1572	1519	651	343	128	5107
K2–K7	– 7·9	13	20	19	25	10	6	93
	8·0– 8·9	40	85	82	21	1	2	231
	9·0– 9·9	160	321	270	60	12	7	830
	10·0–10·9	475	681	474	89	19	14	1752
	11·0–	76	112	76	8	1	1	274
	P.M. stars	...	...	...	52	94	64	210
	Total	764	1219	921	255	137	94	3390
M, etc.	– 7·9	2	6	12	9	2	1	32
	8·0– 8·9	13	13	24	5	2	...	57
	9·0– 9·9	29	44	26	11	...	1	111
	10·0–10·9	64	81	47	2	...	2	196
	11·0–	6	20	7	1	...	2	36
	P.M. stars	...	...	...	5	8	10	23
	Total	114	164	116	33	12	16	455

TABLE XI

Median Values of the Larger Component of Proper Motion for Stars of different Spectral Types and Apparent Photographic Magnitude

Spec. \ Mag.	−7·9	8·0–8·9	9·0–9·9	10·0–10·9
	″	″	″	″
B–B3	·020	·013	·012	·010
B5	19	13	11	09
B8	18	14	11	11
B9	19	14	12	11
A0	23	15	14	12
A2	30	18	15	13
A3	35	22	17	15
A5	33	23	17	14
F0	39	24	21	16
F2	43	33	25	18
F5	65	42	28	21
F8	·080	53	33	25
G0	·130	70	40	30
G5	·039	35	30	25
K0	36	26	21	17
K2	34	18	17	16
K5	32	18	17	15
M	·033	·022	·016	·014

progressive change, and by type F0 the motions are nearly doubled except for the faintest group. A definite maximum is reached at type G0. The drop in the motions for type G5 is very considerable. The decline from K0 to M is not large, and for these stars the motions are about a half greater than for those of type B–B9 (rather more for the brightest stars). The median proper motions, however, do not give a proper representation of the distribution of the motions —for example, the K-type stars have median motions not very different from the stars of type A2–A5, but there are many more stars of large proper motion.

The percentage of stars in different ranges of proper motion for stars of all magnitudes (neglecting only the faint proper motion stars, which are shown separately) is given in Table XII. Stars of types A7 and K7 have been omitted as they are not numerous nor representative as regards magnitude.

The Nearest Stars.—In the discussion of star counts it has been found that the increase in number with increasing faintness falls short of the value it would have if we were dealing with a uniform distribution of stars in perfectly transparent space. When we deal with stars belonging to one spectral class we find the rate of increase in the number most nearly to approach the theoretical value for type G0 falling away for stars of both earlier and later types. Taken as a whole, stars of type G0 must therefore be the nearest in space and intrinsically the faintest, a result confirmed by the proper motions. The problem of finding a class of stars for which the increase in number corresponds to uniform star density is an interesting one, for such stars are our nearest neighbours. The number down to magnitude

TABLE XII

Percentage of Stars in Different Ranges of Proper Motion
Unit ″·001

P.M. / Spec.	0–9	10–19	20–39	40–79	80–159	160–	No. of Stars	Per cent. of Faint P.M. Stars
B–B3	31·8	42·9	20·0	5·1	0·2	0·0	466	0·0
B5	32·7	42·3	20·8	3·5	0·3	0·3	312	0·0
B8	36·2	47·0	15·0	1·7	0·1	0·0	928	0·0
B9	33·7	45·2	18·7	2·3	0·2	0·0	1499	0·0
A0	31·4	46·6	19·5	2·2	0·3	0·1	5189	0·0
A2	27·1	43·5	24·9	4·0	0·5	0·0	2807	0·1
A3	22·9	41·7	29·7	4·7	0·8	0·2	1335	0·2
A5	22·9	40·9	29·2	6·0	0·9	0·1	1109	0·1
F0	18·9	33·0	36·6	9·7	1·5	0·2	1811	0·5
F2	16·0	29·2	37·9	13·3	2·9	0·6	1402	0·6
F5	14·3	25·5	35·9	18·4	5·1	0·9	2573	1·8
F8	9·3	25·0	35·0	22·2	6·9	1·6	2377	2·9
G0	7·8	19·3	32·1	25·7	11·1	4·0	3363	7·6
G5	14·0	25·8	28·4	18·5	9·4	3·9	3300	9·8
K0	18·5	32·5	31·4	11·9	3·9	1·7	4826	5·8
K2	23·4	36·6	29·9	7·6	1·6	0·9	1788	4·5
K5	24·7	40·5	27·8	5·0	0·9	1·0	1247	7·7
M	26·4	38·0	26·9	6·5	0·9	1·4	432	5·3

$m+1$ should be 3·98 times the number to magnitude m. As proper motion is the most certain indication of nearness, we confine our attention to stars of large proper motion. Table XIII gives the number of stars down to various magnitude limits for which the proper motion exceeds the limits 0″·126, 0″·200, 0″·317 and 0″·502. These limits are in the ratio of 1 to the square root of 2·512, so that, for example, a star of proper motion greater than 0″·502, if moved to a distance where it would be exactly one magnitude fainter, would have a proper motion exceeding 0″·317 if its linear speed remained unaltered. Consequently if we denote by $N(m, \mu)$ the number of stars brighter than magnitude m and with proper motion greater than μ we would find

$$\frac{N(m+1,\ 0''\cdot126)}{N(m,\ 0''\cdot200)} = \frac{N(m+1,\ 0''\cdot200)}{N(m,\ 0''\cdot317)} = \frac{N(m+1,\ 0''\cdot317)}{N(m,\ 0''\cdot502)} = 3\cdot98$$

if the stars were distributed uniformly through a transparent space extending as far as stars with proper motion 0″·126.

On account of incompleteness amongst the fainter stars the ratio gradually falls off beyond magnitude 11, but for intermediate magnitudes the ratio is reasonably near to the expected value. Amongst the brightest stars the value of the ratio is unexpectedly large, and although the number of stars involved is small the result may be significant. To get the ratio down to the theoretical value we would require an additional three or four naked-eye

TABLE XIII

Number of Stars to Definite Limits of Proper Motion and Apparent Photographic Magnitude

m	$N(m, ''\cdot126)$	$N(m, ''\cdot200)$	$N(m, ''\cdot317)$	$N(m, ''\cdot502)$
5·95	43	23	9	3
6·45	66	31	12	5
6·95	98	49	20	9
7·45	147	75	29	14
7·95	210	99	40	17
8·45	274	125	50	22
8·95	363	150	56	24
9·45	481	196	74	27
9·95	638	261	97	34
10·45	802	318	111	41
10·95	1027	379	122	43
11·45	1265	451	143	51
11·95	1457	508	162	54
12·45	1589	556	176	58
12·95	1691	591	181	59
13·45	1771	615	190	63
13·95	1808	629	197	64

TABLE XIII—*continued*

m	$\frac{N(m+1, ''\cdot126)}{N(m, ''\cdot200)}$	$\frac{N(m+1, ''\cdot200)}{N(m, ''\cdot317)}$	$\frac{N(m+1, ''\cdot317)}{N(m, ''\cdot502)}$
5·95	4·3	5·4	6·7
6·45	4·7	6·2	5·8
6·95	4·3	5·0	4·4
7·45	3·7	4·3	3·6
7·95	3·7	3·8	3·3
8·45	3·85	3·9	3·4
8·95	4·25	4·7	4·0
9·45	4·09	4·3	4·1
9·95	3·93	3·91	3·6
10·45	3·98	4·06	3·5
10·95	3·84	4·16	3·8
11·45	3·54	3·89	3·5
11·95	(3·33)	(3·65)	(3·4)

stars with proper motion exceeding 0″·5 annually, *i.e.* double the actual number. We have not counted the Sun in our list, but this is hardly justified since we are dealing with only about one-fourteenth of the area of the sky. Accidental error in the proper motions cannot have altered the result to any extent as the error is only a small part of the motions. The zero point of

magnitude is not involved, but the scale value is; however, any outstanding error in it cannot be serious.

We now attempt to find the actual distribution in space of the stars of large proper motion. The parallactic motion M is derived from proper motion in arc by the formulæ—

$$\mu_\alpha = M \cos D \sin (\alpha - A),$$
$$\mu_\delta = M \cos D \sin \delta \cos (\alpha - A) - M \sin D \cos \delta,$$

where α, δ are the R.A. and Dec. of the star considered and A, D are the R.A. and the Dec. of the solar apex. We assume from the motion of all the stars in the zone that $A = 273°{\cdot}6$ and $D = +30°{\cdot}8$. For three groups of stars we have solved for M from the motions in R.A. and Dec. separately and jointly —no star has been rejected from any group.

Class of Stars	Mean Parallactic Motion from			No. of Stars
	R.A.	Dec.	R.A. and Dec.	
P.M. > ″·200 Brighter than 10·5	″ ·264	″ ·286	″ ·274	318
P.M. > ″·200 Brighter than 9·0	·290	·264	·279	150
P.M. > ″·502 Brighter than 10·5	·653	·638	·646	41

It is very satisfactory to find in these results that the mean parallactic motion appears to be practically independent of apparent magnitude, and that the motion for the last group of stars is approximately 2·512 times that for the other groups. If we assume that the mean parallax can be derived from the mean parallactic motion by multiplying by a factor 0·243 corresponding to a solar motion of 19·5 km. per sec. we derive ″·0666 as the mean parallax of stars of proper motion greater than ″·200. This value appears larger than we would have expected; also it is well known that large values will result from a selection based on size of proper motion, as stars with a peculiar motion in the direction of the solar antapex will tend to be included (and give too large a parallactic motion), while the stars with a peculiar motion in the opposite direction (which would give the necessary correction for this effect) have been to a large extent excluded because the resultant of the peculiar motion and parallactic motion is too small. However, we may proceed from the derived parallax recognising that if the mean parallax has to be multiplied by a factor x, the resulting star density has to be multiplied by x^3 and the absolute magnitudes have to be corrected by $+5 \log x$.

A uniform distribution of stars with a mean parallax of ″·0666 corresponds to a sphere of radius 22½ parsecs (parallax ″·0444 at the surface). As the zone considered extends from declination $-40°$ to $-52°$ it covers ·0726 of the whole sky, and the volume V of the sphere included to 22½ parsecs is 3465

cubic parsecs. For the purpose of determining the distribution of the stars in space and their absolute magnitudes it is necessary to transform Table XIII into Table XIV, which gives the number of stars within definite ranges of apparent magnitude and definite ranges of distance, it being assumed that the proper motions give the distances. We know that this table may be incomplete beyond magnitude 10·45, and certainly beyond magnitude 11·45. If we write x for $\sqrt{2{\cdot}512}$ we can easily compute that the volume of space considered in the successive columns of Table XIV are $(x^3-1)V$, $\left(1-\frac{1}{x^3}\right)V$, $\left(\frac{1}{x^3}-\frac{1}{x^6}\right)V$, $\frac{1}{x^6}V$. By means of the parallaxes at the inner and outer surfaces of the three shells we can transform the apparent magnitudes into a range of absolute magnitudes. We omit the data from the last column (inner core), for which we can only give an upper limit of brightness to the stars. The first line of Table XIV gives—

20 stars brighter than magnitude 4·2 absolute in a volume $(x^3-1)V$.

14 „ „ „ „ 5·2 „ „ „ $\left(1-\frac{1}{x^3}\right)V$.

6 „ „ „ „ 6·2 „ „ „ $\left(\frac{1}{x^3}-\frac{1}{x^6}\right)V$.

TABLE XIV

Number of Stars of Definite Ranges of Apparent Magnitude within Definite Limits of Parallax

Apparent Photographic Magnitude	Parallax			
	″·0280 −·0444	″·0444 −·0704	″·0704 −·111	> ″·111
Brighter than 5·95	20	14	6	3
5·95– 6·45	15	5	1	2
6·45– 6·95	14	10	4	4
6·95– 7·45	23	17	4	5
7·45– 7·95	39	13	8	3
7·95– 8·45	38	16	5	5
8·45– 8·95	64	19	4	2
8·95– 9·45	72	28	15	3
9·45– 9·95	92	42	16	7
9·95–10·45	107	43	7	7
10·45–10·95	164	50	9	2
10·95–11·45	166	51	13	8
11·45–11·95	135	38	16	3
11·95–12·45	84	34	10	4
12·45–12·95	67	30	4	1
12·95–13·45	56	15	5	4
13·45–13·95	23	7	6	1

The other entries in the three columns contribute stars of different ranges of absolute magnitude as follows :—

Absolute Magnitude	Number of Stars in the Three Shells of Volume 10,300, 2590 and 650 Cubic Parsecs respectively			Deduced Number per 10,000 Cubic Parsecs
3·2– 4·7	15	...	...	14
3·7– 5·2	14	...	...	14
4·2– 5·7	23	5	...	22
4·7– 6·2	39	10	...	38
5·2– 6·7	38	17	1	41
5·7– 7·2	64	13	4	60
6·2– 7·7	72	16	4	68
6·7– 8·2	92	19	8	88
7·2– 8·7	107	28	5	103
7·7– 9·2	164	42	4	155
8·2– 9·7	166	43	15	165
8·7–10·2	...	50	16	203
9·2–10·7	...	51	7	179
9·7–11·2	...	...	9	138
10·2–11·7	...	...	13	199
11·7–12·2	...	...	16	246

It will be seen that there is an overlap of a magnitude in the ranges which each cover, $1\frac{1}{2}$ magnitudes. There are in addition for the outermost shell 19 stars per 10,000 cubic parsecs for which we can only state that they are brighter than absolute magnitude 4·2. Due to incompleteness of data for faint apparent magnitudes and the small volume of space available for faint absolute magnitudes, the data for the end of the table is not very satisfactory, but it should be fairly complete to absolute magnitude 9. We have now to attempt a distribution of the absolute magnitudes through ranges which do not overlap. The first entry indicates 15 stars in the range 3·2 to 4·7 absolute. Now it is clear that all the magnitudes in this range are not equally likely. Those at the brightest end of the range can only come from the brightest stars in the range of apparent magnitude at the outside of the shell, while those with the faintest absolute magnitudes must be the faintest apparent at the inner edge of the shell. If we consider that half of the stars are in the middle half-magnitude and a quarter in each of the two extreme half-magnitudes we cannot be very far wrong. Two sources of error, one the greater number of intrinsically faint stars in a given volume of space and the other the greater volume of space in the outer layers corresponding to a definite change in the reduction from apparent to absolute magnitude, act in opposite directions. The result shows that these two sources of error largely balance one another, as the volume of successive shells, corresponding to a half-magnitude in the reduction to absolute, increases progressively by a factor of nearly 2, and in the range of absolute magnitudes considered there

is roughly a doubling as we proceed from one absolute magnitude to the next fainter.

We thus derive the following number of stars in different ranges of absolute magnitude per 10,000 cubic parsecs and the total number to different limits of magnitude:—

Absolute Magnitude	No.	Total to Limit
Brighter than 4·2	33	33
4·2–4·7	16	49
4·7–5·2	24	73
5·2–5·7	35	108
5·7–6·2	45	153
6·2–6·7	57	210
6·7–7·2	71	281
7·2–7·7	86	367
7·7–8·2	112	479
8·2–8·7	144	623
8·7–9·2	172	795
9·2–9·7	188	983

As the calculation for the last line depends on about 10 faint stars of large proper motion it is very uncertain.

It has already been noted that if our parallaxes require correction by a factor x, the star density has to be multiplied by x^3 and the absolute magnitudes corrected by $5 \log x$—corrections which influence our results in opposite directions.

There are very few determinations with which to compare those results. Eddington, in *Stellar Movements and Structure of the Universe*, p. 43 (1914), estimated from actual parallax determinations that there were 32 stars within 5 parsecs of the Sun, corresponding to 610 in 10,000 cubic parsecs with the general proviso that intrinsically faint stars would be missing from his list. Lundmark, in *Handbuch der Astrophysik*, 5, 529 (1932), from parallax data for stars within 10·53 parsecs, gives results for ranges of absolute magnitude which, reduced to a volume of 10,000 cubic parsecs, become—

Absolute Magnitude	No.	Total to Limit
Brighter than 3·9	33	33
4·0–5·9	73	106
6·0–7·9	65	171
8·0–9·9	90	261

In *A.J.*, 1066 (1937), Miss Jenkins has listed the stars with an observed parallax greater than ″·100. There are 127 stars corresponding to 303 per 10,000 cubic parsecs, but for the stars of largest parallax the number is twice as great, in agreement with Eddington's estimate. Of the known stars nearer

than 5 parsecs only 36 per cent. are brighter than magnitude 10 absolute. The agreement between these results and those of this paper is as close as could be expected.

Density Distribution according to Spectral Type.—In the preceding section we have dealt with the nearer stars without considering spectral type, but we know that such stars include very few stars of early type and that the great majority of the stars are of types F8 to K0. If we could assume a mean absolute magnitude for each spectral type it would be possible from the data in Table VI to find the distribution in space of stars of each spectral type, and according to galactic latitude if we used the data of Table III. For stars of the main sequence we can assume a mean absolute magnitude, but we have seen in our attempts to divide stars into "giants" and "dwarfs" that for all spectral types after the earliest ones a considerable proportion, if not the majority, of the stars did not belong to the main sequence. In Table XV we have attempted to compute the distribution of stars in space (independent of galactic latitude) from the data for stars of magnitude groups 8·0–8·9 and 9·0–9·9. The assumed absolute magnitude for each spectral type is given, the limits of distance and the density per 10,000 cubic parsecs. It will be seen that for different spectral types the density found refers to very different distances. For early type stars we are dealing with distant regions of the galactic system where the density of such stars is much below that in our neighbourhood. The table has been extended as far as type G0, but the

TABLE XV

Density in Space per 10,000 *Cubic Parsecs of Stars of different Spectral Types to G0 calculated from Assumed Absolute Photographic Magnitudes for Stars in the Main Sequence*

Spec.	Assumed Absolute Photographic Magnitude	Stars of App. Mag. 8·0–8·9		Stars of App. Mag. 9·0–9·9	
		Distance in Parsecs	Star Density	Distance in Parsecs	Star Density
O–B2	−2·4	1200–1900	·0002	1900–3000	·0001
B3	−1·8	890–1400	·0005	1400–2200	·0002
B5	−1·1	650–1020	·0026	1020–1600	·0007
B8	−0·1	410– 650	·032	650–1020	·011
B9	+0·3	340– 540	·12	540– 850	·03
A0	+0·6	300– 470	·32	470– 740	·18
A2	+1·1	230– 370	·29	370– 590	·18
A3	+1·3	210– 340	·17	340– 540	·11
A5	+1·8	170– 270	·28	270– 430	·18
F0	+2·9	100– 160	3·1	160– 260	1·45
F2	+3·3	85– 135	3·5	135– 214	1·64
F5	+3·9	65– 102	11	102– 162	7·0
F8	+4·6	48– 74	20	74– 118	18
G0	+5·0	39– 62	34	62– 98	37

results at this stage are becoming meaningless as many of the stars included do not belong to the main sequence for which the absolute magnitude was assumed. Except for the F8 and Go stars, when we are concerned with stars within about 100 parsecs there is a clear falling off of density—either real or due to the presence of distant giant stars in the groups of apparently bright stars. The table suffices to show the great difference in the number of stars of different spectral types. It may be compared with the results given by H. Brück, *Z.S. f. Ap.*, **13**, 289, where the variation with galactic latitude and for stars at greater distances are given.

It is hardly necessary to remark that the material used in this paper is the outcome of work by many members of the staff of the Cape Observatory. The Harvard Observatory, and especially Miss Cannon, have co-operated in the determination of the spectral types. The work of transferring the identification of the faint stars from prints made at the Cape to the spectrum plates at Harvard was partly met by a grant from the Spencer Bequest of the Society.

Summary

The paper discusses the distribution of about 40,000 stars in the zone −40° to −52° with respect to photographic magnitude, spectral type and proper motion. An attempt is made to determine the relative number of giant and dwarf stars, the latter being defined as those near enough to give a constant star density. From the mean colour index for each spectral type and the variation of the number of each spectral type throughout the zone the dependence of mean colour index on galactic latitude and apparent photographic magnitude is deduced. From the mean parallactic motion of groups of stars arranged by spectral type and apparent brightness the mean parallax of such groups is deduced, and hence, as for the colour index, the mean parallax has been calculated as a function of galactic latitude and apparent magnitude. Tables are given showing the connection between spectral type and proper motion arranged by apparent magnitude. From the stars of large proper motion (exceeding 0″·126 per annum) a group of stars in our neighbourhood of uniform star density is found and the star density to definite limits of absolute magnitude is computed. From assumed values of the absolute magnitudes of stars of different spectral types the distribution in space of stars of different spectral type is computed.

AN ANALYSIS OF THE *K* TERM IN THE B-TYPE STARS.

J. S. Plaskett, C.B.E., F.R.S.

The purpose of this paper is to inquire into the nature of a positive residual velocity, the so-called *K* term, which is generally present in solar motion solutions of the high-temperature stars, spectral classes O5–B7, generally called the B-type stars. This *K* term of a magnitude of +4·7 km./sec. first appeared in a solution of the radial velocities of twenty B-type stars for the solar motion by Frost and Adams in 1904. Similar solutions by Campbell in 1910, 1911, and finally in 1928 from increasing numbers of B-type velocities, all gave a *K* term of the same order, while many other solutions before 1930 resulted in values of the *K* term between +4 and +5 km./sec.

Various attempts have been made to explain this high positive residual, appearing particularly in the B-type stars. The principal explanations advanced are: (*a*) downward convection currents in the atmospheres of these high-temperature stars; (*b*) errors in the wave-lengths or in the settings on the diffuse spectral lines used in the measurement of the radial velocities; (*c*) the gravitational displacement to the red of the spectral lines in these massive stars; (*d*) systematic motions outward from the Sun of some of the B-type stars.

The general advance of knowledge along these lines makes it now generally agreed that causes (*a*) and (*b*) can hardly account for more than a few tenths of a kilometre per second. The probable magnitude of the gravitational red-shift has been calculated by Pearce and the writer * (referred to later as PP), in our work on the B-type stars, as varying between +2·6 for O type to +1·0 for B3–B7. In the proportions of the spectral subdivisions present in the sky, the gravitational shift is about +1·3 km./sec., and hence insufficient to account for a *K* term of 4 to 5 km./sec.

There remains then only the last explanation, a systematic motion outward of some of the B-type stars, to account for the remainder of the *K* term. This explanation was first specifically given by the writer † at the 1929 Christmas meeting of the A.A.A.S., in which it was shown that the residuals from the solutions were so preponderatingly positive in the southern sky, between galactic longitudes 210° and 330°, as to indicate some unexplained systematic motion in this region which, when allowed for, would reduce the *K* term approximately to the gravitational shift. These results were provisional only, as the data, the results of PP's six years' observation of O5–B7 stars, north of declination −11° and brighter than $7^{m}\cdot5$, were not yet completed.

* *M.N.*, 94, 691, 1934; *Pub. D.A.O.*, 5, 277, 1936.
† *Science*, **71**, 223, 1930.

The completion of the Victoria Catalogue * of 1010 O5–B7 stars in 1930, and the appearance shortly afterwards of Neubauer's Catalogue † of 213 southern B-type stars, gave for discussion reliable radial velocities of 849 stars between revised spectral classes O5 and B7, classes B8 and B9 being excluded as properly belonging to class A. The earlier solutions were limited generally to the B-type stars brighter than $5^{m}\cdot5$, and the numbers were only about one-third of those available at Victoria, where, consequently, more complete and representative results should be expected.

In the solution of the 849 B-type velocities, terms for the galactic rotation were, for the first time, introduced into the equations, as in these distant stars they are of considerable magnitude, and, being systematic, should be included when solving for the solar motion. As the magnitude of the rotational term increases with the distance, it was deemed advisable to subdivide the 849 stars into four distance groups: 101 brighter and 159 fainter O–B2 stars; 272 brighter and 317 fainter B3–B7 stars. Furthermore, as our earlier work had shown an apparently systematic motion in the southern sky, this was further investigated, and its analogy with Kapteyn's ‡ work on the stream motion of the B-type stars in the same region was at once apparent. The convergent and the stream motion § were redetermined from the more numerous and more accurate proper motions and radial velocities then available. The method and formulæ of Kapteyn were followed, resulting in a stream motion, V_0 of 15·0 km./sec. towards a convergent at $l = 194^{\circ}\cdot2$, $b = -24^{\circ}\cdot3$, with a K term of $+8\cdot3$ km./sec. It was pointed out at the time that the convergent is only about $8^{\circ}\cdot5$ from the solar antapex, with the inference that the stream motion does not greatly differ from the reflex of the solar motion.

Considering the large K term of $+8\cdot3$ km./sec. to be the result of the systematic stream motion, adjusted values of the K term of $+8\cdot3$ km./sec. were removed from the radial velocities of the 132 members of the "stream," and the thus corrected velocities, along with the remaining 717 observed velocities, were solved simultaneously for the K term and the solar motion and for the four values of the rotational terms, corresponding to the four distance groups. The results of this general solution, so far as the K term and solar motion are concerned, are repeated for convenience in the upper half of the last column of Table I, the other four columns, containing the results of the solutions of the four distance groups, each treated singly. The general solution of the 849 B-type velocities, of which 132 were corrected for stream motion, has reduced the K term from its previous high value to $+1\cdot1$ km./sec., in practical agreement with the computed amount $+1\cdot3$ km./sec. of the probable gravitational shift for the stars concerned. Moreover, the high value of the solar velocity of about 21·5 km./sec., obtained in the early solutions of the B-type stars, has been reduced to 19·1 km./sec. in agreement with the mean value of 19·3 km./sec. obtained from several

* *Pub. D.A.O.*, **5**, 99, 1931.
† *L.O.B.*, **15**, 46, 1930.
‡ *Ap. J.*, **40**, 43, 1914.
§ *M.N.*, **94**, 683, 1934; *Pub. D.A.O.*, **5**, 260, 1936.

solutions of 2000 to 4000 stars of all spectral types.* The apparent removal of these two anomalies in the motions of the B-type stars seemed sufficient justification for the claim that the mysterious K term, which had been puzzling astronomers for over thirty years, had been satisfactorily explained.

Unfortunately this claim, so far as it is based on a stream motion among the southern stars, appears to be unfounded. Dr. W. M. Smart † has criticised this procedure on three grounds : (*a*) it is not legitimate to remove the K term of +8·3 km./sec. from the radial velocities of the stream stars before the solution ; (*b*) the method of dividing the K term among the eight groups is incorrect ; (*c*) the so-called stream motion is practically nothing but the reflex of the solar motion among the B-type stars of small peculiar motion.

The first criticism is well founded, as the equation for stream motion $V_0 \cos \lambda = \bar{V}$ takes care of all the motions concerned, and if, as was done, a K term is introduced on the left-hand side, this K term cannot be due to motion, but must arise from some physical cause, as, for example, the gravitational shift. If it can be shown that a gravitational shift of 8·3 km./sec. could arise in these "stream" stars, then its removal would be legitimate. As the probable gravitational shift for the B3–B7 stars, composing nearly 90 per cent. of the "stream" stars, is +1·0 km./sec., the mass and density required for a shift of +8·3 km./sec. would be so improbably large that such a displacement is out of the question.‡ The second criticism of the method of distributing the total amount of the K term of +8·3 km./sec. among the eight groups, though valid, is immaterial, as the final result would be unchanged.

The third criticism that the supposed "stream" motion is nothing but the reflex of the motion of the Sun through the slow-moving B-type stars is perhaps open to argument. It was admitted in the original paper that the convergent was only 8°·5 from the solar antapex, but Dr. Smart's statement that the convergency of these stars is in quite "a different category" from the Taurus stream should be further considered. The members of the southern stream are at 5 times the distance of the Taurus stars, their intrinsic motions are only about one-half as great, so that the relative observational errors of the proper motions are about as 10 to 1. In such case, an average deviation of 15° per star and of 1°·8 for the mean directions of the eight groups does not compare so unfavourably with those of the Taurus stream. Moreover, when the peculiar motion of the B-type stars, from unpublished Victoria observations, is found to be nearly 9 km./sec., in agreement with the Lick value,§ but considerably greater than that of Smart and Green ‖ of 5·8 km./sec., it seems unlikely that a solar velocity only slightly more than twice the random velocity could give the relatively small deviations

* *Pub. D.A.O.*, **5**, 275, 1936.

† *M.N.*, **96**, 568, 1936.

‡ See, however, Trumpler (*Pub. A.S.P.*, **47**, 249, 1935), where Einstein shifts of the bright O-type stars in six open clusters are found to average over 9 km. per second.

§ *Lick Pub.*, **16**, 38, 1928.

‖ *M.N.*, **96**, 572, 1936.

above quoted. It can hardly be doubted, therefore, that these southern stars show a much greater community of motion than could be produced by the motion of the Sun alone.

However, without further discussion of this and the two preceding criticisms, let us examine and analyse the solutions for the K term, solar motion and galactic rotation previously made by PP and repeated here for comparison, and particularly some further solutions by the writer in which the velocities were used as observed without the removal of the K term of +8·3 km./sec. from the "stream" stars in the earlier solutions. Table I contains in the upper half the individual solutions for the four distance groups, and in the last column the values of the K term and solar motion from the general solution of the corrected velocities, while the lower part gives the individual solutions of the four distance groups using the observed velocities, with the weighted means in the last column. In all these solutions the galactic latitude of the apex was assumed as 20°, the normal value, as it is indeterminate in stars so closely concentrated to the galactic plane.

TABLE I

Solutions of 849 O5–B7 *Stars*

Term	Group 1—101** Brighter O–B2	Group 2—159** Fainter O–B2	Group 3—272** Brighter B3–B7	Group 4—317** Fainter B3–B7	General Solution 849**
	Solutions with Correction for Stream Motion				
K	+ 2·41	+ 1·87	+ 2·68	− 0·90	+ 1·13
V_0	17·5	20·6	21·1	17·2	19·1
L_0	1°·2	31°·0	19°·9	19°·1	21°·4
$\bar{r}A$	+ 9·8	+16·7	+ 3·3	+ 4·5	
l_0	325°·9	324°·1	331°·9	308·9	
	Solutions of Observed Velocities—No Corrections				Weighted Mean
K	+ 4·31	+ 3·35	+ 4·63	+ 0·72	+ 2·89
V_0	16·8	22·6	21·7	17·9	20·1
L_0	11°·6	36°·7	29°·2	27°·7	28°·1
$\bar{r}A$	+ 7·9	+15·3	+ 1·9	+ 3·2	
l_0	323°·0	326°·2	276°·3	303·4	

Note.—In this table, V_0 = solar motion ; L_0 = longitude of solar apex ; l_0 = longitude of gravitational centre.

A comparison of these two solutions is of considerable interest and significance. Considering first the solar motion in the early single solutions, the solar velocities range from 17·2 to 21·1, and the longitude of the apex from 1°·2 to 31°·0, a considerable oscillation. The values from the general solution of 849 stars with stream correction are 19·1 km./sec. and 21°·4,

practically identical with various solutions of 2000 to 4000 stars of all spectral types. That this oscillation of the values of the solar motion is not due to removal of the stream motion is shown by the solutions below, in which the velocity ranges from 16·8 to 22·6, a 50 per cent. greater range, while the mean value of the apex 28°·1 is shifted around about 7° beyond its normal value. It seems obvious that much more probable values of the solar motion are obtained when the correction for stream motion, even if wrong in principle, is applied.

A still greater improvement is shown in the rotational terms of the earlier solution, particularly in the third group of the brighter B3–B7 stars. The mean distance of this group, as determined from the mean parallax and the value of $\bar{r}\bar{\pi}$,* is about 200 parsecs, corresponding with the Victoria value of ·0155 for A, to $\bar{r}A$ of +3·1 km./sec. compared with +3·3 for the corrected and +1·9 for the observed velocities. But the situation is much worse than appears from $\bar{r}A$ alone, as the direction to the galactic centre, normally around 325°, is 50° distant at 276°·3, so far that it cannot be considered as galactic rotation in the generally accepted sense. That the observed velocities of this group of 272 bright B3–B7 stars show no galactic rotation is an indication of something abnormal in the motions of this particular group. That the same group when its southern members are corrected for stream motion gives normal values of the solar motions and galactic rotation, points at least to the probable nature of this abnormality.

Finally, considering the K term in the two solutions, the correction for stream motion has reduced the value of K of +2·9 from the solutions of the observed velocities to +1·1, practically agreeing with the computed value of +1·3 km./sec. Although the procedure of removing a K term from the radial velocities of the members of a supposed stream is theoretically wrong, there must be some significance in the fact that this incorrect method gives improved values of the solar motion and galactic rotation, and reduces the K term to the value of the gravitational shift. Obviously, there is need for further analysis of the B-type velocities, particularly those of the brighter B3–B7 stars.

The relations between the K term, solar motion and galactic rotation in the B-type stars will be clarified by further solutions for K term and solar motion only, omitting terms for galactic rotation. This was the procedure adopted in all the early B-type solutions, terms for the galactic rotation being first used by PP about 1930. The results of these simple solutions are given in Table II.

The solution of the observed velocities is given in column 2, while for comparison a similar solution of the velocities corrected for stream motion appears in column 3, and the values of the general solution of the corrected velocities for K term and solar motion are repeated from Table I in column 4. The effect of omitting terms for the galactic rotation in the solutions is obviously to leave the K term practically unchanged. Thus, for the observed velocities, the change is from 2·9 to 3·1, and with stream corrections from 1·1 to 1·4.

* *M.N.*, 94, 698, 1934 ; *Pub. D.A.O.*, 5, 292, 1936.

TABLE II

Solutions without Rotation

Term	Observed Velocities	Corrected Velocities	General Solution
K	+ 3·11	+ 1·40	+ 1·13
V_0	21·7	20·9	19·1
L_0	32°·1	23°·9	21°·4

Although the inclusion of rotational terms has no effect on the value of K, it makes considerable difference in the solar velocity. Thus, the solution of the observed velocities, when rotational terms are included, gives a solar velocity of 20·9, which becomes 21·7 when they are omitted. Similarly, if the stream correction is applied, 19·1 is increased to 20·9. The value of the solar velocity from the early solutions of the B-type stars, where, of course, no rotational terms were used, was on the average of 21·5 km./sec., practically the same as for the 849 stars of 21·7 when no rotational terms were included. On the other hand, Smart and Green * obtained values of the solar velocity of 21·5 km./sec. with rotational terms and 22·4 without, considerably higher than both the early and Victoria values. Smart and Green used the radial velocities of 630 B0–B9 stars, brighter than $6^m.5$, obtained from Schlesinger's 1930 Catalogue. This list is different and considerably less complete than the Victoria data, which contain the O-type but no B8 and B9 stars, generally considered as more properly belonging to the A-type stars. Moreover, there are 267 stars fainter than $6^m.5$ and, hence, entirely absent from the list of Smart and Green. Obviously, the Victoria data are more complete and more representative of the high-temperature stars, and should give more reliable values.

Some additional information in regard to the K term may be obtained on re-examination of its values in the four distance groups of Table I. In the solution of the observed velocities, lower half of the table, K is +4·3 and +4·6, weighted mean +4·6, for the brighter and nearer stars, and +3·4 and +0·7, weighted mean +1·6, about the gravitational shift, for the fainter and more distant stars. It seems undoubted, therefore, that the high value of the K term arises mainly in the brighter and nearer stars, which give values of K identical with those from the early solutions, while the value of K from the fainter, more distant stars is little different from the gravitational shift. Although not shown by these solutions, some of the earlier analyses of the Victoria velocities showed that the O-type stars gave a higher K term than the B-type—to be expected, of course, from the greater mass and larger gravitational shift of these stars.

Returning to the lower half of Table I, the individual solutions of the four distance groups with the observed velocities, it will be noted that the solar velocity ranges between 16·8 and 22·6 km./sec. This unexpectedly

* *M.N.*, 96, 479, 1936.

large range must be due to abnormal distribution or motions in one or more of the groups, and it may be informative to examine what happens to the K term and the rotational terms if a constant solar velocity is assumed in the solutions. While 19 km./sec., the velocity from all spectral types, seems to be suggested, a compromise velocity of 20 km./sec. was adopted, and solutions for the K term and galactic rotation are given in Table III. Owing to the abnormal rotational terms in the brighter B3–B7 stars, additional solutions for this group were made with $V_0 = 19$ and $V_0 = 21$, with results in the last two columns of Table III. However, the differences in the solutions for the three solar velocities are so small that it will be preferable to consider the values for $V_0 = 20$ for all four groups.

TABLE III

Solutions with Adopted Solar Motion

Term	Bright O–B2	Faint O–B2	All O–B2	Bright B3–B7	Faint B3–B7	Bright B3–B7	
						$V_0 = 19$	$V_0 = 21$
K	+3·94	+ 0·36	+ 1·54	+4·53	−0·20	+4·69	+4·37
$\bar{r}A$	+5·9	+17·2	+13·1	+1·4	+3·0	+1·4	+1·5
l_0	325°·4	323°·7	323°·9	31°·1	320°·5	26°·5	35°·3

Considering first the rotational terms in the four distance groups, columns 2, 3, 5, 6, $\bar{r}A$ corresponds approximately to the mean distance of groups 1 and 2, but is only about half the distance value in groups 3 and 4. The directions to the centre, l_0, are practically the same as the standard value of 325° except in group 3, where the deviation of 66° is so great that the brighter B3–B7 stars cannot be said to show any rotational effect whatever when any reasonable solar velocity is assumed. As previously noted, deviation of l_0 of 50°, also quite inadmissible, occurs when the group is solved for solar motion, as well as K term and rotation (Table I). Obviously there must be something abnormal in the velocities or distribution of the brighter B3–B7 stars.

The behaviour of the K term is also interesting, for, as in the former solutions, it is much higher in the brighter and nearer stars, columns 2 and 5, and less than the gravitational shift in the more distant stars, columns 3 and 6. If both bright and faint O–B2 stars are solved together, we have the values of column 4, where the K term of +1·5 km./sec. is, if anything, smaller than the gravitational shift for these stars. As group 4 has $K = -0·2$, the high value of K for the B-type stars must arise mainly in the 272 bright B3–B7 stars. It is of significance to note that of the 132 so-called stream stars, 90 are in the group which shows no rotational effect and which has the highest K term.

Evidently the next stage in the analysis should consist of the examination of the residual velocities, the velocities after removal of the solar motion, of the 20 longitude sub-groups of the brighter B3–B7 stars, and the com-

parison of these velocities with those computed from appropriate values of the rotational terms and the gravitational shift. The residual velocities resulting from the removal of solar velocities of 19, 20, 21 km./sec. towards the standard apex $l = 21°{\cdot}4$, $b = +20°$, were already available from the previous solutions. Of these, the first, where $V_0 = 19$, given in the fifth column of Table IV, is preferred, as this solar velocity corresponds to that obtained from 2000–4000 stars of all spectral types.

If there are no systematic effects, if the random velocities cancel out, and if the K term is not considered at present, then, as the solar motion is already taken care of, the residual velocity of each sub-group should equal the rotational velocity plus the only other known systematic effect, the gravitational shift. The latter has a probable value of +1·0 km./sec. for B3–B7 stars, while $\bar{r}A$ has been taken as +3·3 km./sec., corresponding to the mean distance of the group and l_0 as 325°. Algebraically, this is

$$+3{\cdot}3 \sin 2(\bar{l} - 325°) \overline{\cos^2 b} + 1{\cdot}0 = \bar{\rho}.$$

The left-hand side gives the computed value, C, which should equal the residual velocity, $\bar{\rho}$, if the random motions cancel out and there were no K term.

The successive columns of Table IV are: (1) the longitude group; (2) the number of stars; (3) the mean longitude; (4) the computed velocity;

TABLE IV

Residuals from the Brighter B3–B7 *Stars*

Group	No.	$\bar{l}$	C	$\bar{\rho}$ $V_0 = 19$	$\bar{\rho} - C$ $V_0 = 19$	$\bar{\rho} - C$ $V_0 = 20$	$\bar{\rho} - C$ $V_0 = 21$
		°					
1	6	4·3	+3·68	− ·93	− 4·61	− 3·95	− 3·16
2	10	23·2	+3·50	+ 1·16	− 2·34	− 1·52	− ·71
3	14	38·5	+2·57	+ 1·96	− ·61	+ ·17	+ ·96
4	12	51·8	+1·34	+ 1·80	+ ·46	+ 1·26	+ 1·89
5	9	67·2	0·00	− 1·93	− 1·93	− 1·32	− ·71
6	9	87·6	−1·69	− 3·46	− 1·77	− 1·32	− ·88
7	13	115·5	−1·65	+ 1·29	+ 2·94	+ 2·89	+ 2·83
8	11	132·2	− ·12	+ 1·76	+ 1·88	+ 1·52	+ 1·16
9	14	149·6	+1·47	+ 2·54	+ 1·07	+ ·52	− ·05
10	13	165·8	+3·82	+ 7·99	+ 4·17	+ 3·36	+ 2·57
11	13	183·3	+3·76	+ 3·26	− ·50	− 1·38	− 2·25
12	18	205·2	+3·48	+10·88	+ 7·40	+ 6·51	+ 5·60
13	16	218·5	+2·70	+ 4·11	+ 1·41	+ ·52	− ·35
14	16	235·1	+ ·98	+ 8·31	+ 7·39	+ 6·53	+ 5·74
15	17	249·7	− ·56	+ 7·93	+ 8·49	+ 7·88	+ 7·27
16	20	266·8	−2·10	+11·15	+13·25	+12·88	+12·51
17	23	288·7	−1·77	+ 7·03	+ 8·80	+ 8·81	+ 8·81
18	15	303·9	−1·05	+ 5·93	+ 6·99	+ 7·21	+ 7·44
19	18	319·5	+ ·44	+ 5·08	+ 4·64	+ 5·10	+ 5·56
20	5	341·9	+1·70	− 1·96	− 3·66	− 3·26	− 2·86

(5) the mean residual velocity for $V_0 = 19$; (6) $\bar{\rho} - C$ for $V_0 = 19$; (7) $\bar{\rho} - C$ for $V_0 = 20$; (8) $\bar{\rho} - C$ for $V_0 = 21$. It should be noted again that two-thirds of the stars for which a stream correction was originally made are contained in this distance group and lie within longitude sub-groups 12 to 19, between galactic longitudes 210° and 330°, and that the residuals $\bar{\rho} - C$ for these groups are enclosed by heavy lines.

A glance at column 6, $\bar{\rho} - C$ for $V_0 = 19$, at once gives an explanation for the high K term of +4·7 km./sec. (Table III) in this distance group. The high residuals are concentrated in the longitude sub-groups 12 to 19, containing the 90 stars for which correction for stream motion was made in the original solutions. The weighted mean value of the residuals of the 143 stars in these eight groups is +7·5. The weighted mean value of the residuals of the 90 "stream" stars is +8·7 km./sec. as compared with +8·3 km./sec. for the K term from the "stream" motion originally derived. On the other hand, the weighted mean residual of the remaining sub-groups 1 to 11 inclusive and 20 with no "stream" stars is +0·04 km./sec. That a choice of other solar velocities makes no appreciable difference is shown in columns 7 and 8, the weighted means for 12 to 19 being +7·2 and +6·9 km./sec., and for the remaining sub-groups +0·1 and +0·2 km./sec. for $V_0 = 20$ and 21 km./sec. respectively.

There can be no question then that the high K term of +4·7 km./sec. for the bright B3–B7 stars is due wholly to the high positive velocity, obviously a systematic effect, of the stars in the southern sky between longitudes 210° and 330°, of which the majority belong to the so-called "stream." If this large systematic effect is not a stream, it certainly shows remarkable community of motion and as such should be allowed for if reliable values of the motions are to be obtained.

Although the other three distance groups have not been similarly tested, it is probable they would show a similar but much smaller effect when only few "stream" stars are present. Moreover, the solutions of Table III indicate that the K term for these groups certainly does not exceed the gravitational shift of +1·3 km./sec. Even neglecting these groups, the excess K term of the bright B3–B7 stars $143 \times 7{\cdot}50 \div 849$ or +1·3 km./sec. over the whole group reduces the +2·9 km./sec. (Table I), the weighted mean value of K, from the solutions of the observed velocities of the four distance groups to +1·6 km./sec., within practical distance of the gravitational shift of +1·3 km./sec.

The early statement of PP that the mystery of the K term, which had been puzzling astronomers for over thirty years, was now satisfactorily explained still stands, if instead of an erroneous correction for stream motion we substitute an allowance for the demonstrated excess systematic positive velocity of the bright B3–B7 stars between longitudes 210° and 330°, which reduces the K term to +1·6 km./sec., to practical identity with the gravitational shift of +1·3 km./sec.

Summary.—The principal results of this investigation may be briefly summarized.

(1) A summary of the earlier solutions of the radial velocities of 849

O5–B7 stars by PP, with particular reference to a correction for stream motion, was given. This latter procedure, strongly criticized by Dr. W. M. Smart, is admitted to be in error, and the early solutions and some new ones are reviewed.

(2) A comparison of the early solutions, where corrections for a supposed stream motion were made, with new solutions of the observed velocities, showed conclusively that the early solutions, notwithstanding the wrong procedure followed, gave much more probable values of the solar motion and galactic rotation and reduced the previous high values of the K term to the probable value of the gravitational shift. On the other hand, the new solutions of the observed values gave greater scattering in the individual values of the solar velocity, shifted the apex 7° from the normal position, gave impossible values of the galactic rotation in the bright B3–B7 stars, where it should be definitely present, and gave values of the K term 1·6 km./sec. greater than the probable gravitational shift.

(3) A second group of solutions showed that the introduction of terms for the galactic rotation had no practical effect on the K term, but tended to reduce the high value of the solar velocity of about 21·5 km./sec. of solutions of B-type stars prior to 1930 more nearly into agreement with the average of 19·3 km./sec. obtained from 2000 to 4000 stars of all spectral types.

(4) On account of the wide divergence in the solar velocity ranging from 16·8 to 22·6 km./sec. in the solutions of the observed velocities, new solutions for the K term and galactic rotation, assuming solar velocities of 19, 20, 21 km./sec. to the standard apex, were made. These solutions showed definitely, confirming those of (2), that the high value of K was confined to the brighter and nearer stars and principally arose in the 272 bright B3–B7 stars. While the values of the galactic rotation were approximately those to be expected from the mean distances of the other three groups, the bright B3–B7 stars gave impossible values of l_0 as before.

(5) Further analysis of this group and comparison of its residual velocities, with velocities computed from probable values of the rotation and of the gravitational shift, showed conclusively that the high value of K of +4·7 km./sec. for this group arises wholly in the longitude sub-groups 12 to 19 inclusive, containing 143 southern stars between longitudes 210° and 330°. The weighted mean residual $\bar{p}-C$ from these 8 longitude sub-groups, containing two-thirds of the supposed "stream" stars, is +7·5 km./sec., while from the remaining 12 groups it is +0·04 km./sec. If this large outward systematic motion of these southern stars is not stream motion, it shows certainly a remarkable community of motion and should hence be allowed for if reliable values of the motions are to be obtained. Such an allowance reduces the K term for the whole 849 stars to +1·6 km./sec., sufficiently close to the gravitational shift of +1·3 km./sec. to justify the claim that the causes of the high K term in the early solutions of the B-type stars have been found.

Victoria, B.C.:
April 1938.

THE STABILITY OF CONVECTIVE STARS.

T. G. Cowling, M.A., D.Phil.

1. In 1935 it was suggested by L. Biermann that stars which are convective throughout are necessarily secularly unstable,* or, more correctly, in neutral equilibrium. At the time it did not appear probable that such stars can exist, but recently † Biermann has shown that the hydrogen convection zone in a star may be very extensive, and may, in special circumstances, possibly include the whole star. The temperature gradient is approximately adiabatic right up to the photosphere if conditions favour turbulence, and the ratio of radiation-pressure to gas-pressure is very small (of order 10^{-5}, say).

Biermann's argument is in essence this. In a star in convective equilibrium the temperature T and density ρ are connected by an adiabatic relation similar to the ordinary gas equation

$$T = K\rho^{\gamma-1}; \tag{1}$$

this relation involves an arbitrary constant, like the K in (1), which can only be fixed by some boundary condition. Such a boundary condition is at once forthcoming if the surface-layers are in radiative equilibrium, but if the temperature gradient is adiabatic right up to the surface no such condition would appear to exist. Thus the star possesses an extra degree of freedom, and its equilibrium is accordingly neutral. A similar argument can be used if the star, though not wholly convective, possesses an external part in convective equilibrium.

The argument is, however, incorrect. A star must always radiate out to space as much energy as it generates ; this provides a boundary condition whether the surface-layers are in convective or radiative equilibrium. There will accordingly not be neutral equilibrium ; we show below how to derive the condition of secular stability.

2. Consider, to illustrate the methods, a star in which the ratio γ of specific heats of the material is constant. Radiation-pressure is, by hypothesis, negligible compared with gas-pressure ; we also ignore the stresses due to turbulence, though these are in general not small compared with the gas-pressure near the surface of a convective star. Thus a relation of the form (1) holds up to the surface (*i.e.* up to a region well above the photosphere defined later). The star is a polytrope of index $1/(\gamma-1)$.

We combine (1) with the equation of hydrostatic equilibrium

$$\frac{dp}{dr} = -\frac{Gm\rho}{r^2}$$

---

* *Ast. Nach.*, **257**, 269, 1935. Secular stability is what was termed thermal stability by the author in an earlier paper (*M.N.*, **94**, 768, 1934 : this paper will be denoted by I; also a paper in *M.N.*, **96**, 42, 1935, will be denoted by II).

† *Ast. Nach.*, **264**, 364, 1938.

(m is the mass enclosed by a sphere of radius r concentric with the star), and the gas equation

$$p = \frac{R}{\mu}\rho T. \tag{2}$$

Then we find

$$\frac{dT}{dr} = -\frac{\gamma G m}{(\gamma-1)r^2}\frac{\mu}{R}.$$

If, near the surface, specified by $r = r_1$, $m = M$, the opacity κ is given by *

$$\kappa = \kappa_0 \rho^n / T^s, \tag{3}$$

it follows that the optical depth τ is given by

$$\begin{aligned}\tau &= \int_r^{r_1} \kappa\rho dr = \int_r^{r_1} \kappa_0 \rho^{n+1} T^{-s} dr \\ &= \kappa_0 \frac{R}{\mu}\frac{(\gamma-1)r_1^2}{\gamma G M} K^{\frac{n+1}{\gamma-1}} \int_0^T T^{-s+\frac{n+1}{\gamma-1}} dT \\ &= \kappa_0 \frac{R}{\mu}\frac{(\gamma-1)r_1^2}{\gamma G M} K^{\frac{n+1}{\gamma-1}} Q T^{\frac{1}{Q}} \equiv \left(\frac{T}{T_0}\right)^{\frac{1}{Q}},\end{aligned} \tag{4}$$

say, where

$$\frac{1}{Q} = 1 - s + \frac{n+1}{\gamma-1}. \tag{5}$$

The number Q must be positive; with Kramers's opacity law ($n = 1$, $s = 7/2$) it ranges from $2/7$ to 2 as γ increases from $4/3$ to $5/3$. However, though $n = 1$ is likely to be roughly true, s is probably much smaller than $7/2$ in the surface-layers, on account of the increase of ionisation with temperature. If, for example, $n = 1$, $s = 2$, we find that Q ranges between $1/5$ and $1/2$ as γ increases from $4/3$ to $5/3$.

The light emitted by unit area of the star's surface in directions within an elementary cone of solid angle $d\omega$, whose axis makes an angle θ with the outward radius, is

$$\frac{d\omega}{4\pi}\int_0^\infty acT^4 e^{-\tau\sec\theta} d\tau.$$

Thus the total emission from the whole surface in all directions is L, where

$$L = 4\pi r_1^2 \int_0^\infty \int acT^4 e^{-\tau\sec\theta}\frac{d\omega}{4\pi} d\tau, \tag{6}$$

or, substituting for T in terms of τ from (4), and integrating,

$$\begin{aligned}L &= 2\pi a c r_1^2 T_0^4 \Gamma(1+4Q)\int_0^{\frac{\pi}{2}} \cos^{4Q+1}\theta \sin\theta d\theta \\ &= \pi a c r_1^2 T_0^4 \Gamma(1+4Q)/(1+2Q).\end{aligned}$$

* The indices n and s in (3) will depend on the average behaviour of κ over a range of values of ρ and T, since, because of convection, some fluctuation of ρ and T over the stellar disc will occur.

If T_1 is the effective temperature,

$$L = \pi a c r_1^2 T_1^4. \tag{7}$$

This is accordingly the temperature at an optical depth τ_1, where

$$\tau_1^{4Q} = \Gamma(1+4Q)/(1+2Q). \tag{8}$$

With values of Q less than $1/2$, τ_1 is a number rather less than unity. The level $\tau = \tau_1$ is defined as the photosphere. Thus, by (4), the photosphere is at a level such that

$$K^{\frac{n+1}{\gamma-1}} T_1^{\frac{1}{Q}} r_1^2 / M = A,$$

where A is a known constant. Combining this with (7), we find

$$K^{\frac{n+1}{\gamma-1}} L^{\frac{1}{4Q}} r_1^{2-\frac{1}{2Q}} \Big/ M = A', \tag{9}$$

where A' is a second known constant. But for a polytrope of index $1/(\gamma-1)$,

$$M^{2-\gamma} r_1^{3\gamma-4} / K = B, \tag{10}$$

where B depends only on μ, γ and absolute constants.* Equations (9) and (10) between them fix r_1 and K, and so a unique model with given mass and luminosity can be found. It may be observed in passing that no mass-luminosity law can be predicted for wholly convective stars without a knowledge of the law of generation of energy.

3. Now consider the secular stability of a wholly convective star. It is supposed that the star undergoes an arbitrary small variation which leaves it in mechanical equilibrium, but not in thermal equilibrium; if in re-establishing thermal equilibrium it returns to the original configuration, this is stable.

It may first be observed that if, after the variation, the temperature gradient is not approximately adiabatic, the convective transfer of energy will rapidly cause it to become so; † we may therefore suppose that, after the variation, the temperature gradient is adiabatic. Suppose that, after the variation, instead of (1),

$$T = K(1+\lambda(3\gamma-4))\rho^{\gamma-1}, \tag{11}$$

where λ is small; that is, suppose that as a consequence of the variation the K in (1) is altered in the ratio $1+\lambda(3\gamma-4)$. By (10), this means that the new radius of the model is $r_1(1+\lambda)$; actually a homologous expansion or contraction occurs, such that the linear dimensions of any part of the star are increased in the ratio $1+\lambda$, and the density and temperature are reduced in the ratios $1-3\lambda$ and $1-\lambda$. Thus, by (9), the energy emitted by the star becomes

$$L(1-\lambda[2(4Q-1)+4Q(1+n)(3\gamma-4)/(\gamma-1)]). \tag{12}$$

* This relation is in essence the second of equations (57.3) (Eddington, *Internal Constitution of the Stars*, p. 83).

† The time in which the adiabatic temperature gradient is set up is at most a few years, while the time of return to the original equilibrium configuration is of the order of a million years.

On the other hand, if the rate of generation of energy by the star per unit mass, ϵ, is given by

$$\epsilon = \epsilon_0 \rho^\alpha T^\beta, \tag{13}$$

the effect of the same variation will be to alter the energy generated by the star from L to

$$L(1 - \lambda(3\alpha + \beta)). \tag{14}$$

Take λ as positive, so that the variation undergone by the star is an expansion. If the star now radiates away more energy than it generates, it must cool; because of convection the temperature gradient remains adiabatic during the cooling. Thus λ must decrease, and the star tends to return to its initial state. In this case the star is stable; hence the condition of stability is that (12) exceeds (14), *i.e.* that

$$2(4Q - 1) + 4Q(n+1)(3\gamma - 4)/(\gamma - 1) < 3\alpha + \beta. \tag{15}$$

This condition demands larger values of α and β than the corresponding condition for radiative stars, if γ is appreciably larger than $4/3$. For example, if $\gamma = 5/3$, $n = 1$ and $Q = 1/2$, we find

$$3\alpha + \beta > 8, \tag{16}$$

while for a radiative star in which radiation-pressure is negligible compared with gas-pressure, with Kramers's opacity law,

$$3\alpha + \beta > \tfrac{1}{2}.$$

It accordingly appears probable that the range of values of α and β for which the star is both secularly and vibrationally stable is more limited than for a radiative star.

4. Consider the vibrational stability of a star constructed on the same model. Neglecting the turbulent stresses and the kinetic energy of turbulence, the condition of vibrational stability of a convective star is *

$$\int_0^M \frac{\delta\rho}{\rho}\delta\left[\epsilon - \frac{\partial F}{\partial m}\right] dm < 0, \tag{17}$$

where F is the total outward flux of energy across the sphere enclosing the mass m; $\delta\rho$, $\delta\epsilon$, etc. are the small variations of ρ, ϵ, etc. on this sphere at any instant of the principal radial oscillation of the star. During the oscillation the variation of temperature is nearly adiabatic, even at the surface of the star; for the only factor tending to make it non-adiabatic is the *radiative* transfer of energy, which, by hypothesis, has a much smaller effect on the temperature gradient than convection. Hence, in particular, the phase of δF is that of δr at the surface.

* Equation (41) of II, omitting the terms involving ϵ_2, ϵ_3, F_2 and $C_r \partial p_1/\partial m$, and writing $F = 4\pi r^2(F_1 + F_3)$. In deriving this equation, $\delta\rho/\rho$ is the variation in an adiabatic oscillation, while the other variations are those for the actual (nearly adiabatic) oscillation; in the earlier work we approximated by supposing all the variations to refer to the adiabatic oscillation; here they are all supposed to refer to the actual oscillation.

Suppose that $\gamma > 4/3$, which is necessary for dynamical stability. Then $\delta r/r$, $\delta\rho/\rho$ and $\delta T/T$ all increase steadily in absolute magnitude from centre to boundary. To fix ideas, suppose that $\delta r/r$ is positive; then $\delta\rho/\rho$ and $\delta T/T$ will be negative; also $\delta\rho/\rho + 3\delta r/r < 0$, save at the centre, where the inequality is replaced by equality; and, by (1) and (2),

$$\frac{\delta T}{T} = (\gamma - 1)\frac{\delta\rho}{\rho}, \qquad \frac{\delta p}{p} = \gamma\frac{\delta\rho}{\rho}.$$

When not too close to the boundary (say when the temperature exceeds one-tenth the central temperature) the opacity law may be assumed not to differ widely from that of Kramers. The outward flux of energy F is made up of the radiative flux F_1 and the convective flux F_2; F_1 is not necessarily negligible compared with F_2 even for wholly convective stars.* We have

$$F_1 = -\frac{4\pi cr^2}{\kappa\rho}\frac{\partial p'}{\partial r} = -\frac{16\pi^2 cr^4}{\kappa}\frac{\partial p'}{\partial m},$$

where p' is the radiation-pressure. Thus

$$\delta F_1 = F_1\left\{\frac{4\delta r}{r} - \frac{\delta\kappa}{\kappa} + \frac{\partial\delta p'}{\partial m}\Big/\frac{\partial p'}{\partial m}\right\}.$$

Using equations (8) and (9) of I, this becomes

$$\begin{aligned}\delta F_1 &= F_1\left\{-\frac{\sigma^2 r^2\delta r}{Gm} + \frac{4\pi r^4}{Gm}\frac{\partial\delta p}{\partial m} - \frac{\delta\kappa}{\kappa} + \frac{\partial\delta p'}{\partial m}\Big/\frac{\partial p'}{\partial m}\right\}\\ &= F_1\left\{-\frac{\sigma^2 r^2\delta r}{Gm} - \frac{\partial}{\partial m}\left(\frac{\gamma p\delta\rho}{\rho}\right)\Big/\frac{\partial p}{\partial m} - \frac{\delta\kappa}{\kappa} + \frac{\partial}{\partial m}\left(\frac{4(\gamma-1)p'\delta\rho}{\rho}\right)\Big/\frac{\partial p'}{\partial m}\right\}\\ &= F_1\left\{-\frac{\sigma^2 r^2\delta r}{Gm} - \gamma\frac{\delta\rho}{\rho} - \gamma p\frac{\partial}{\partial m}\left(\frac{\delta\rho}{\rho}\right)\Big/\frac{\partial p}{\partial m} - \frac{\delta\kappa}{\kappa} + 4(\gamma-1)\frac{\delta\rho}{\rho} + \frac{4(\gamma-1)p'}{\partial p'/\partial m}\frac{\partial}{\partial m}\left(\frac{\delta\rho}{\rho}\right)\right\}\end{aligned}$$

($2\pi/\sigma$ is the period of the oscillations). Now, since the temperature gradient is adiabatic,

$$\frac{1}{p'}\frac{\partial p'}{\partial m} = \frac{4(\gamma-1)}{\gamma p}\frac{\partial p}{\partial m}.$$

Thus the third and last terms in the expression for δF_1 cancel out, and so

$$\delta F_1 = F_1\left\{-\frac{\sigma^2 r^2\delta r}{Gm} + (3\gamma - 4)\frac{\delta\rho}{\rho} - \frac{\delta\kappa}{\kappa}\right\}.$$

The first two terms in the bracket are negative; also, with an opacity law similar to Kramers's law, $-\delta\kappa/\kappa$ is also negative. Thus δF_1 is negative when not too near the boundary.

* Actually, of course, F_2 will be small compared with F_1 unless the actual (convective) temperature gradient is considerably less than the radiative gradient required to produce the same total F.

Again, the convective flux F_2 is given by

$$F_2 = -4\pi\rho r^2 lqc_v\left(\frac{\partial T}{\partial r} - \frac{T(\gamma-1)}{\gamma p}\frac{\partial p}{\partial r}\right)$$

$$= -16\pi^2\rho^2 r^4 lqc_v T\left(\frac{1}{T}\frac{\partial T}{\partial m} - \frac{(\gamma-1)}{\gamma p}\frac{\partial p}{\partial m}\right)$$

(*cf.* II, equation (3); l is the "free path" and q the mean velocity of turbulence elements). Thus, using relations given in II (last equation of p. 54 and first and third equations of p. 55), we get

$$\delta F_2 = F_2\left(\frac{2\delta\rho}{\rho} + \frac{4\delta r}{r} + \frac{\delta l}{l} + \frac{\delta q}{q} + \frac{\delta T}{T}\right)$$

$$= F_2\left((\gamma - \tfrac{1}{3})\frac{\delta\rho}{\rho} + \frac{5}{3}\left(\frac{\delta\rho}{\rho} + 3\frac{\delta r}{r}\right)\right),$$

which is also negative.* Thus δF is negative save possibly near the surface.

At the surface, by analogy with (6),

$$F + \delta F = 4\pi(r_1 + \delta r_1)^2 \int_0^\infty\int ac(T+\delta T)^4 e^{-(\tau+\delta\tau)\sec\theta}\frac{d\omega}{4\pi}d(\tau+\delta\tau).$$

Since only a shallow layer contributes to the integral, we can regard $\delta T/T$ and $\delta\tau/\tau$ as constant in it. Thus, integrating as before,

$$F + \delta F = L\left(1 + \frac{\delta r_1}{r_1}\right)^2\left(1 + \frac{\delta T}{T}\right)^4\left(1 + \frac{\delta\tau}{\tau}\right)^{-4Q},$$

whence

$$\delta F = L\left(\frac{2\delta r_1}{r_1} + \frac{4\delta T}{T} - \frac{4Q\delta\tau}{\tau}\right).$$

Now

$$\tau = \int_r^{r_1}\kappa\rho dr = \int_m^M \frac{\kappa dm}{4\pi r^2},$$

and so

$$\delta\tau = \int_m^M\left(\frac{\delta\kappa}{\kappa} - \frac{2\delta r}{r}\right)\frac{\kappa dm}{4\pi r^2}$$

$$= \tau\left(\frac{\delta\kappa}{\kappa} - \frac{2\delta r_1}{r_1}\right)$$

$$= \tau\left((n - s(\gamma-1))\frac{\delta\rho}{\rho} - \frac{2\delta r_1}{r_1}\right),$$

* In calculating δF_2 it is supposed that the variation of temperature is exactly adiabatic. Actually, because F_2 depends on the slight excess of the temperature gradient over the adiabatic, the slight deviations from adiabatic variation produced by the generation of energy and the radiative transfer of heat produce a large variation in F_2. This variation will, however, be one-quarter period out of phase with the radial motion, and so may be neglected, since only the part of δF_2 in phase with the motion affects stability.

since (3) is valid near the boundary. Using this, and simplifying by (5), we find that the boundary value of δF is $(\delta F)_M$, where

$$(\delta F)_M = L\left(2(4Q+1)\frac{\delta r_1}{r_1} + 4Q\gamma\left(\frac{\delta\rho}{\rho}\right)_M\right). \tag{18}$$

Since $\gamma > 4/3$ and $(\delta\rho/\rho)_M < -3\delta r_1/r_1$, $(\delta F)_M$ will be negative if $Q > 1/4$, which is usually true. Thus δF is negative at the surface and in the interior. It does not follow that δF is negative throughout the star, because of the possibility of local variations of the opacity law near the surface; but it may be expected that δF will be negative save in insignificant parts of the star.

Now, using a partial integration,

$$\int_0^M \frac{\delta\rho}{\rho}\frac{\partial\delta F}{\partial m}dm = \left(\frac{\delta\rho}{\rho}\delta F\right)_M - \int_0^M \delta F\frac{\partial}{\partial m}\left(\frac{\delta\rho}{\rho}\right)dm < \left(\frac{\delta\rho}{\rho}\delta F\right)_M,$$

since $\dfrac{\partial}{\partial m}\left(\dfrac{\delta\rho}{\rho}\right)$ is negative over the whole range of m, and δF is negative over most of the range. Thus if (17) is satisfied,

$$\left(\frac{\delta\rho}{\rho}\delta F\right)_M > \int_0^M \frac{\delta\rho}{\rho}\delta\epsilon dm,$$

or, since $\delta\epsilon/\epsilon = (\alpha+\beta(\gamma-1))(\delta\rho/\rho)$, and $(\delta\rho/\rho)^2$ increases steadily with m, we must have

$$\left(\frac{\delta\rho}{\rho}\delta F\right)_M > \left(\frac{\delta\rho}{\rho}\right)_c^2(\alpha+\beta(\gamma-1))\int_0^M \epsilon dm = L\left(\frac{\delta\rho}{\rho}\right)_c^2(\alpha+\beta(\gamma-1)), \tag{19}$$

where a suffix c refers to the centre. This is a necessary, but not sufficient, condition for stability.

5. To apply the condition (19), we need data for the variation of $\delta r/r$ and $\delta\rho/\rho$ with m in the adiabatic oscillation of a convective star. Such data are available only for the limiting case $\gamma = 5/3$, for which $\delta r/r$ and $\delta\rho/\rho$ increase by factors about 1·5 and 2 respectively between centre and boundary.* Thus in this case, using (18), equation (19) becomes

$$\alpha + \tfrac{2}{3}\beta < 2(\tfrac{40}{3}Q - (1+4Q)) = 2(\tfrac{28}{3}Q - 1).$$

If $\alpha = 1$, $Q = \frac{1}{2}$, which are not improbable values, this gives $\beta < 9{\cdot}5$, while from (16) $\beta > 5$. Since (19) is not a sufficient condition of stability, the actual limits of β for stability are likely to be still closer together.

In the limiting case $\gamma = 4/3$, $\delta r/r$ and $\delta\rho/\rho$ do not vary with m, and so (17) and (19) are identical. In this case (19) reduces to

$$\alpha + \tfrac{1}{3}\beta < -\tfrac{2}{3}(1+4Q) + \tfrac{16}{3}Q = \tfrac{2}{3}(4Q-1),$$

while (15) gives exactly the reverse inequality. Thus in this case stability is possible with no value of β.

In general, with values of γ between 4/3 and 5/3, the range of β for

* I, p. 780.

stability may be expected to be less than that for $\gamma = 5/3$. It is clear that the bounds of stability are much closer together than for radiative stars; this is partly because of the change in boundary conditions, but also partly because $\delta r/r$ and $\delta\rho/\rho$ vary much less with m for convective stars than for radiative stars, on account of their greater uniformity of density.

6. This result does not, however, imply that wholly convective stars are unlikely to exist in nature, because of instability. It is possible, as several authors have suggested, that there is a lag between the heating of any element of a star and the consequent increase in generation of energy; this will not affect secular stability, but will make vibrational stability more probable. Moreover, the assumptions on which the above result is based are very special, though a rough calculation indicates that when (1) is replaced by a more general adiabatic law, taking into account variations of ionisation, the range for stability is decidedly less than with $\gamma = 5/3$ in (1), particularly if ionisation has much effect on the specific heat in the surface-layers. A further uncertainty comes from the turbulent stresses, neglected above. An exact determination of their effect demands, amongst other things, a theory of the transport of turbulent kinetic energy, which at present has not been given. However, we may expect the boundary conditions to be in any case roughly similar to those given above.

The boundary conditions for a star in which the outer layers alone are in convective equilibrium resemble those for a completely convective star. The convective outer layers affect the radius of the star, and the mass-luminosity relation, in much the same way as outer layers in radiative equilibrium with an opacity law different to that valid in the interior.

The boundary conditions cease to resemble those given above when there is a surface-layer in which radiation dominates convection, whose optical depth is at least of order unity. For a star wholly convective save for such a surface-layer, if (1) holds in the interior and (3) in the surface-layers, the condition of secular stability is

$$3\alpha + \beta > s - 3n$$

as for a wholly radiative star.

Summary.—It is shown how to determine boundary conditions for a star which is in convective equilibrium up to the photosphere: these boundary conditions determine its radius. Conditions of secular and vibrational stability are found for a special model: these are jointly satisfied only when the law of generation of energy lies in a rather restricted range.

Dundee:
1938 *April* 20.

ON THE ORIGIN OF THE PLANETS.

Raymond A. Lyttleton, M.A., Ph.D.

Introduction.—The hypothesis that the Sun was formerly one component of a binary star system has been considered by the writer in a previous paper * with a view to resolving certain dynamical difficulties of the theory of the origin of the planets. When this idea was put forward the main problem seemed to be the removal of the companion of the Sun, and it was to this matter that chief attention was given. It has, however, been shown by Luyten and Hill in a recent paper † that the energy necessary to disrupt such a binary system is only a small fraction of the energy required to remove a mass comparable with that of the planets from the surface of a star similar to the Sun. For, in order to satisfy angular momentum requirements, the companion of the Sun must have been at a distance from the Sun of order 4000 solar radii. So that the exhaustion of energy per unit mass of the surface material of the companion must have been about 4000 times the amount per unit mass of the binary system. Accordingly, the removal of sufficient material to form the planets from the surfaces of the companion and an intruding star requires considerably more energy than the mere disruption of the binary.

Luyten and Hill consider the case when the companion and intruder have masses equal to that of the Sun, and in these circumstances come to the conclusion that no portion of a suitable filament may have less than the escape velocity relative to the Sun. Moreover, it is shown that the situation is not improved if the intruder is less massive than the companion. The problem can at best be discussed only by means of rough approximations, but in the cases considered the arguments advanced, although not taking into account one of the main features of the problem, show it to be improbable that the solar system was generated by an encounter of stars whose masses are in the above categories.

The only remaining case is that in which the intruder is more massive than the companion. For reasons not stated Luyten and Hill have not discussed this possibility, and it is the purpose of the present notice to inquire whether the theory can be developed from this hypothesis.

1. It is proposed to consider first two unequal stars which undergo an encounter so close as to result in the removal of a small quantity of material from the surface of at least one of them. The mechanism of this removal need not be specified at present. If the assumption is made that the various parts of this material have velocities distributed more or less uniformly between the velocities of the two stars just after the collision, it is clear that the end portions of the material may be unable to escape from the stars, while an intermediate portion of material may escape both stars. It is this

* *M.N.*, **96**, 559, 1936. † *Ap. J.*, **86**, 470, 1937.

intermediate material the theory requires to form the primitive planets, and hence some indication of its velocity must be of extreme importance.

Suppose that two stars M_1 and M_2 are separating with parabolic velocity, and consider the motion of a small particle of negligible mass moving between them, the whole motion being regarded as taking place in one line.

The relative velocity of M_1 and M_2 when at a distance r apart is given by

$$\dot{r}^2 = 2(M_1+M_2)/r,$$

so that

$$r = \sqrt[3]{\tfrac{9}{2}(M_1+M_2)t^2} = Rt^{2/3}$$

if $t=0$ when $r=0$, and $2R^3 = 9(M_1+M_2)$. (The motion may be regarded as having begun when $t>0$.) If the small particle is at a distance d from G, the centre of mass of M_1 and M_2, its motion is given by

$$\ddot{d} = -\frac{M_1}{(r_1+d)^2} + \frac{M_2}{(r_2-d)^2},$$

where

$$r_1 : r_2 : r = M_2 : M_1 : M_1+M_2 = m_2 : m_1 : 1.$$

This equation has a solution $d = Dt^{2/3}$ if

$$\frac{2}{9}D = \frac{M_1}{(m_2R+D)^2} - \frac{M_2}{(m_1R-D)^2}.$$

In order to solve this equation M_1+M_2 may be taken as the unit of mass, so that

$$D(m_2R+D)^2(m_1R-D)^2 + m_2R^3(m_2R+D)^2 - m_1R^3(m_1R-D)^2 = 0.$$

Suppose $m_2 > m_1$; the equation has only one root between $-m_2R$ and m_1R, and further this root lies between $-m_2R$ and 0, *i.e.* the particle is between G and M_1, the smaller star. Accordingly, the particle can have a motion given by $d = Dt^{2/3}$ such that its distances from the two stars remain in a constant ratio. Hence for a series of particles of negligible mass moving at the start with velocities linearly distributed between those of the two stars, there is one particle which has both the appropriate velocity and appropriate position for subsequent escape from both stars.

If, for example, $M_2 = 4M_1$, the root of the above equation is approximately $D = -0{\cdot}44R$. The position of the particle divides the distance between the two stars in the ratio 0·36 : 0·64, the point being nearer the smaller star. Moreover, the neutral point of the gravitational field between these two stars divides their distance in the ratio 0·33 : 0·66, and it appears that in this case the particle which can escape is always moving near this neutral point.

The actual case differs somewhat from this ideal example. The mass of the planetary material, although only a small fraction of the mass of the stars, cannot be neglected in considering the motion; this material will lie somewhere between the two stars and retard them in their escape, this being the energy requirement to which Luyten and Hill have drawn attention.

It should perhaps be stressed that the motion of the planetary material is conditioned almost entirely by the colliding stars until these have separated again to such a distance that the attraction of the Sun on the planets becomes at least comparable with that of the parent stars. It will be seen later that this period is of the order of 10 years. Also the planetary material would not remain directly between the two stars, but instead would tend to lie on the concave side of their subsequent parabolic orbit, though this point is probably unimportant. The previous considerations indicate that the material escaping from both the colliding stars would have velocity nearer the velocity of the smaller star, and would also be situated nearer to it. Also some indication of this velocity could be derived for any particular ratio of the masses in a manner similar to that given above.

2. *The Removal of Material by a Collision.*—It has been pointed out by Jeffreys * that an explanation of the rotations of the planets demands a bodily collision between the two stars, and this form of the encounter is adopted here.

Imagine a series of encounters to take place between two stars, the relative velocity always being made sufficient to permit their subsequent escape from each other, while the closest distance between the centres is continually diminished as the series is described. At a certain stage the encounter will become of the nature of a collision, and a small quantity of matter will find itself distributed in the region between the two stars just after the collision is finished. Clearly, portions of this matter will return to one or other of the two stars, but there must be some intermediate material which will not be recaptured by either star. Presumably by adjusting the depth of the collision the mass of this intermediate material may be increased until it becomes comparable with that of the planets. The quantity of matter disturbed from the surfaces of the stars, but unable to escape, will likewise be increased, but it is not obvious how much matter will be involved in this way. At the present stage suppose a mass $0{\cdot}003\odot$ to be assigned to the material escaping both stars, and assume in addition twice this mass to be disturbed but unable to escape completely, thus making a total mass $0{\cdot}009\odot$. If this material has velocity distributed uniformly between those of the two stars, the kinetic energy of a mass $0{\cdot}006\odot$ unable to escape will be equal to that of a mass $0{\cdot}002\odot$ endowed with the escape velocity. Hence energy will be required comparable with that necessary to remove a mass $0{\cdot}005\odot$ from the surface of a star. For the purposes of numerical calculation it is fair to assume that the potential energy near the surface of either of the stars is similar to the value at the surface of the Sun, so that the necessary velocity for escape may be taken as 620 km. per sec. Accordingly, if the Sun is taken as unit mass and the velocity measured in kilometres per sec., the energy required to remove $0{\cdot}005\odot$ is 961 units.

3. *An Encounter with a Binary Star.*—Suppose the Sun M_0 to have a companion M_1 moving in an orbit of major axis $2a$, and that a third star M_2 is projected at an infinite distance with velocity V relative to the centre of mass of the binary system. Then the total orbital energy of the stars is given by

* *M.N.*, 89, 636, 1929.

$$-\frac{M_0M_1}{2a}+\frac{1}{2}\cdot\frac{(M_0+M_1)M_2}{M_0+M_1+M_2}V^2,$$

the velocity of the centre of mass of the whole system being ignored.

As a numerical example suppose $M_0=\odot=1$ while $M_1=2$ and $M_2=8$, with $a=18$ astronomical units. The first term is the energy of the binary system and represents a deficiency of 50 units, which, as Luyten and Hill have remarked, is very small compared with the 961 units required to remove the planetary material.

The encounter can be illustrated to some extent by means of a vector diagram similar to that used in previous discussions, but in addition it appears that the change of velocity of the Sun must be included, and it is first necessary to discuss how this may be done before proceeding to the diagram.

The star M_2 will approach the binary system and, if it is to collide with M_1, then for a certain period of time the motion of M_1 and M_2 relative to their mass-centre G will be conditioned almost entirely by their own attractions and may be regarded as hyperbolic. During this stage their action on the Sun M_0 may be approximated to by considering it to be the same as that produced by the combined mass M_1+M_2 acting at G. Accordingly, the relative motion of M_0 and G, during the encounter of M_1 and M_2, may be regarded as approximately hyperbolic about the centre of mass of the whole system.

Again, the relative velocity of M_1 and M_2 is reduced by the effects of the collision, and hence their hyperbolic motion is described more slowly after the impact than before it. It happens, nevertheless, that the relative velocity of M_1 and M_2, which is reversed in general direction by the encounter, can be turned through only a small angle; but this feature of the encounter is unimportant, and the difficulties which might appear to arise from it are offset by the change in velocity and position of M_0 during the 10 years or so that the planets are controlled by the colliding stars.

Now the energy required for the complete removal of the planetary material from M_1 and M_2 must come entirely from that possessed by these stars just before the collision. Hence if U_1 and U_2 are their relative velocities at the beginning and end respectively of the hyperbolic motion, it is necessary that

$$\frac{1}{2}\cdot\frac{M_1M_2}{M_1+M_2}(U_1^2-U_2^2)>1000,$$

the distance M_1M_2 being supposed the same at these two times. With the adopted units and $M_2=4M_1=8\odot$, this becomes

$$U_1^2-U_2^2>1250(<50^2-35^2).$$

Hence the requirements of the collision would be met if the beginning and end velocities of the hyperbolic approach were respectively 50 km. per sec. and 35 km. per sec. With these values of the velocities an estimate can now be obtained of the angle through which the velocity is turned, and its value is about 10°.

Luyten and Hill have pointed out that the primitive planets will remain closer to M_1 and M_2 than to M_0 for a period of the order of 10 years. This fact makes it clear that the change in the velocity of M_0 during this time cannot be neglected. How near the centre of mass of M_1 and M_2 passes to M_0 can scarcely be stated with accuracy, but it seems improbable that it would be of an order of magnitude different from the size of the original orbit of M_0 and M_1. If the relative velocity of M_0 and G before the encounter be taken as about 35 km. per sec., and the shortest distance between M_0 and G as of order 10 astronomical units, the eccentricity of their hyperbolic motion is about 1·13, so that the angle between the asymptotes is about 60°. Accordingly, the velocity of M_0 relative to G will be turned through a large angle while M_1 and M_2 are undergoing their encounter. This may be seen otherwise ; for if the star M_2 were absent, the Sun would describe a considerable part of its orbit about M_1 during, say, 10 years, thereby changing the magnitude and direction of its velocity. The presence of a more massive star M_2 near to M_1 will cause the change of motion of the Sun M_0 to proceed more rapidly.

The hyperbolic approach of M_1 and M_2 may be regarded as beginning and ending when their distance apart attains successively some value comparable with the original extent of the binary star. There is no reason to expect that the velocity of the Sun relative to G will be the same as these two times.

4. The motion, which need not be regarded as taking place in one plane, can now be described by means of a vector diagram (fig. 1). $M_1GM_2 = 50$ km. per sec. represents the relative velocity of M_1 and M_2 at the beginning, and $M_1'GM_2' = 35$ km. per sec. its value at the end of their hyperbolic motion. At this latter stage the planetary material will have velocity vector GP, where P is in the neighbourhood of the point of trisection of $M_1'M_2'$ nearer to M_1'. Meanwhile GM_0, the velocity vector of M_0 relative to G, will have rotated about the mass-centre of the whole system, and it is clear that the capture of the planetary material by M_0 depends on the end of the velocity vector of M_0 being brought near to the region P. The relative velocity of 50 km. per sec. at 18 astronomical units' separation of M_1 and M_2 implies a velocity at infinity of about 37 km. per sec. for M_2 relative to the binary star, and this is not an exceptional stellar velocity.

The decrease of velocity of M_0 which fig. 1 shows indicates that its distance from G has changed, so that the escape of M_0 and M_1 from each other presents no difficulty. As the distances apart of the stars further increase the velocities diminish to their final values, and thus the ends of the velocity vectors would approach somewhat nearer to G, their directions and ratios changing but little.

These features of the motion may equally well be shown by means of an actual space diagram of the motions of the stars and planetary material. Fig. 2 gives a general indication of the motion relative to G (the centre of mass of M_1 and M_2). The stars M_1 and M_2 are at first approaching G, at which point they swing round each other and recede in practically the same directions from whence they came. This encounter between

M_1 and M_2 cannot be regarded as beginning until M_1 is no longer much affected by M_0, so that the Sun itself will be little affected by M_1 but mainly by M_2 during the encounter of M_1 and M_2. The orbit of M_0 about G will clearly be only approximately hyperbolic, and the figure shows how M_0 can come to move near the planetary material and also have a similar

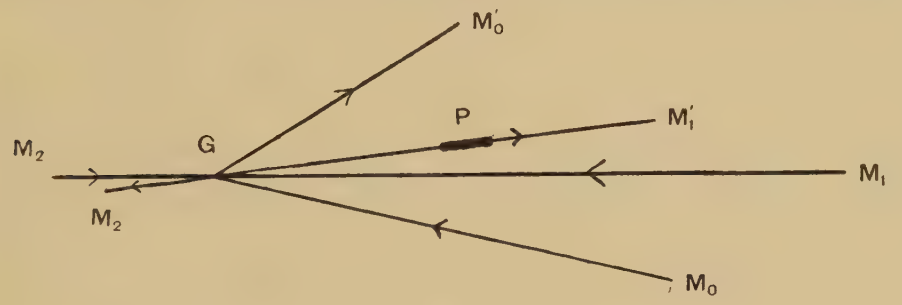

FIG. 1.

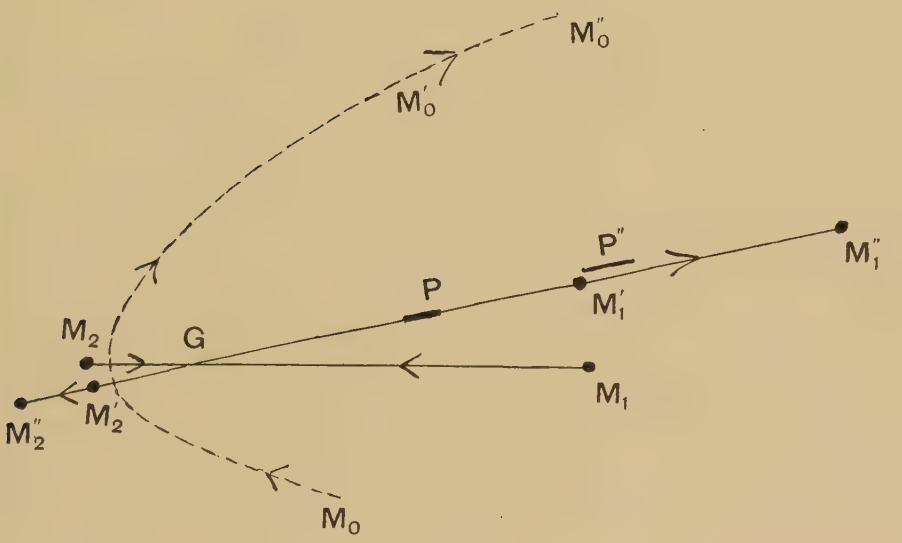

FIG. 2.

velocity. The primitive planets will continue to occupy a region near that point of trisection of $M_1'M_2'$ nearer M_1'. The points M_0'', M_1'', M_2'' and the region P'' denote a later position of the stars and the planetary material.

Further, the possible positions of the end P of the planetary velocities will be restricted to a small region near P in the diagram, and hence if a number of primitive planets were so formed their velocities would probably be in the same general direction round the Sun.

It therefore appears that the formation of a planetary system comparable with the solar system requires a more specialised type of encounter than the earlier investigations by the writer seemed to show. The restrictions on the encounter, considered herein, supply no argument, however, against the hypothesis as a basis for the theory. This point, which applies to any

form of encounter hypothesis, has been stressed by Eddington and Jeffreys.* In demonstration of the principle it may perhaps be remarked that if the double-star hypothesis were shown to be unsatisfactory, the encounter theory could still be saved by invoking a collision between two stars occurring in the neighbourhood of a third star. But the present discussion indicates that the binary hypothesis can still be used as a basis of a theory, and accordingly forms a more plausible starting-point than a triple encounter.

In this paper the amount of material disturbed from the surfaces of the stars has been taken as $0{\cdot}009\odot$, and the energy necessary for its removal as the solar value of M/R, to agree closely with the value adopted by Hill and Luyten. Any reduction of these quantities clearly facilitates the formation of a planetary system. Now for the brighter component of Capella, for example, the value of M/R is only about one-third of that for the Sun ; also since the total mass of the planets is less than $0{\cdot}0015\odot$, an amount $0{\cdot}003\odot$ might suffice for an estimate of the original material. The corresponding energy to be supplied by the intruding star is now only about 250 units instead of the 1250 which has been considered here, and a reduction of the mass and velocity of the third star is permissible.

Any material not immediately forming any portion of a primitive planet may eventually be swept into the Sun, or, as has been suggested by H. N. Russell,† may be capable of being reabsorbed by the planets.

5. Some mention of the resisting medium is also relevant here. It has not yet been shown that any agency apart from purely gravitational action is necessary to account for the existing small eccentricities of the planetary orbits. E. W. Brown has expressed himself on this subject,‡ and explains that predictions, both past and future, of the planetary orbits cannot be made for intervals in excess of 10^8 years. For such intervals the eccentricities and inclinations may undergo fluctuations large enough to permit of close encounters of the planets with each other, which event would greatly reduce the interval over which subsequent predictions could be made. But in so far as the future is concerned statistical evidence seems to show that the orbits tend to become more and more circular, and this tendency appears to be borne out by reference to those satellite systems which can be compared with the planetary system. Thus the eccentricities of the orbits of Jupiter's four great satellites are exceedingly small, while, measured in terms of the number of revolutions, this system must be much more advanced than the planetary system. On the other hand, large eccentricities and inclinations may have existed in the past and may have been reduced by dynamical action alone.

Accordingly the present degree of circularity of the planetary orbits may be of purely dynamical origin or ascribable to the dissipative effects of a

* Eddington, *I.C.S.* (Camb. Univ. Press, 1930), p. 313 ; Jeffreys, *The Earth* (Camb. Univ. Press, 1929), p. 316 ; H. N. Russell, *The Solar System and Its Origin* (Macmillan, 1935), p. 122.

† H. N. Russell, *loc. cit.*, p. 109.

‡ For references see Brown and Shook, *Planetary Theory* (Camb. Univ. Press, 1933), pp. 248 and 249.

resisting medium, or to both of these causes. An amount $0{\cdot}002\odot$ for the mass of the captured material is sufficient to provide a resisting medium; for, as Jeffreys has explained, it is not necessary for the medium to have a mass as large as the mass of the planets.

6. *The Aggregation of the Filament.*—It seems fairly generally agreed that a stream of matter would find itself spread out ribbon-like between the two stars just after their collision. If planets are to be formed, this material must be capable of collecting some part of itself into a number of masses, though that such an aggregation can take place has never been conclusively shown. However, if such a process can occur there seems no reason to suppose that it would be delayed until the colliding stars are again at any great distance from each other and the filament greatly extended. The velocity of any portion of the material may be estimated in terms of its position by the assumption of a linear distribution, but the material itself does not remain uniformly distributed between the stars. Again, the region in which a planet must move if it is to escape from both stars may be only a small fraction of the space between them, but it is not essential to suppose that the filament would aggregate into a large number of planets ranging right from one star to the other.

The temperature of the material of the initial filament must have been of the order of a million degrees at least, and it is not here suggested that the masses of the primitive planets were other than comparable with the total mass of the major planets. There appears to be no indication that small bodies could have been formed at this stage.

The temperature of the material of the filament sets a lower limit to the mass of the planets, and the subsequent escape of the parent stars from each other sets an upper limit. The mass of the great planets of the solar system conforms fairly well to the range imposed by these conditions.

Summary.—In considering the binary hypothesis of the origin of the solar system three factors are more important than the mere disruption of the binary star. Luyten and Hill have drawn attention to the energy required to remove material from the surface of a star. But in addition it turns out that any material which escaped after a collision would have a velocity nearer to that of the smaller of the stars involved, and furthermore the change in the velocity of the Sun must be taken into account. The first contingency requires energy to be supplied by the intruding star and is thus a restriction on the encounter; but the second and third factors enable the planets to have small velocity relative to the Sun under suitable initial conditions. It appears that the encounter is most likely to be effective when the mass of the third star is greater than that of the companion of the Sun. Nothing approaching exactness can be attained in discussing the motion, but it seems entirely possible for the binary hypothesis to give a satisfactory basis for a theory.

St. John's College,
Cambridge:
1937 *December* 31.

MOLECULAR CARBON IN THE SOLAR SPECTRUM.

M. G. Adam.

(Communicated by the Director of the University Observatory, Oxford)

Introduction.—The application of band line theory to the molecular Fraunhofer lines should furnish valuable information about the physical condition of the solar atmosphere. Unfortunately, such investigations are seriously hampered by the general faintness of band lines and by their blending with atomic lines. Two determinations of the solar temperature from band line intensities have hitherto been made, the first by Birge * from the CN bands giving 4300° K, and the other by Richardson † from the C_2 bands giving 5700° K. Both investigations were, however, based on visual estimates of intensity, and by no means established beyond doubt that the molecular lines were showing a distribution of intensity corresponding to thermodynamic equilibrium. The object of the present paper is to identify and determine absolute intensities for a group of molecular lines. Three bands suggest themselves as suitable for measurement: the CN band at λ 3883 A., the CH band at λ 4300 A. approx. and the λ 5165 C_2 band. Of these bands the carbon band is the faintest, and consists chiefly of lines of Rowland Intensity (R.I.) -2 and -3, but as it appears in a region of the spectrum comparatively free from atomic lines, it has been selected for the present absolute intensity determinations.

The Swan bands are emitted as a result of a transition of the molecule between the two electronic configurations,‡

B $^3\Pi_{even}$ 2·39 volts $1s\sigma^2 2p\sigma^2 2s\sigma^2 3p\sigma 2p\pi^3 3d\sigma^2$,

A $^3\Pi_{odd}$ 0 (ground state) $1s\sigma^2 2p\sigma^2 2s\sigma^2 3p\sigma^2 3p\pi^3 3d\sigma$,

in both of which states the four unpaired electrons give a spin quantum number Σ of 1. An electronic change alone from the upper to the ground state would correspond to the emission of a line in the region λ 5160 A., but the changes in the vibrational energy of the nuclei which accompany the electronic jump give rise to the familiar series of vibrational bands which extend from $\lambda\lambda$ 4370–6700 A. Fig. 1, based on Jevons ‡ (p. 58), shows the two electronic states with the associated vibrational levels of each. Any change of the vibrational quantum number v may take place during the electronic transition, and the relative position in the spectrum of the resulting bands depends on the vibrational level spacings in each

* *A.J.*, 55; 273, 1922.

† *A.J.*, 73, 216, 1931. Also a preliminary account of measured absolute intensity determinations in the G band (*Trans. Int. Ast. Union*, 4, 55, 1932; *Mount Wilson Reports*, 1929–30, p. 193).

‡ Jevons, *Report on Band Spectra of Diatomic Molecules*, p. 112, 1932.

state. It will be seen from fig. 1 that for the Swan bands the interval between any two given successive levels are almost equal in both states, so that the vibrational bands corresponding to the same change in vibrational quantum number Δv occur close together. The vertical lines in fig. 1 show the

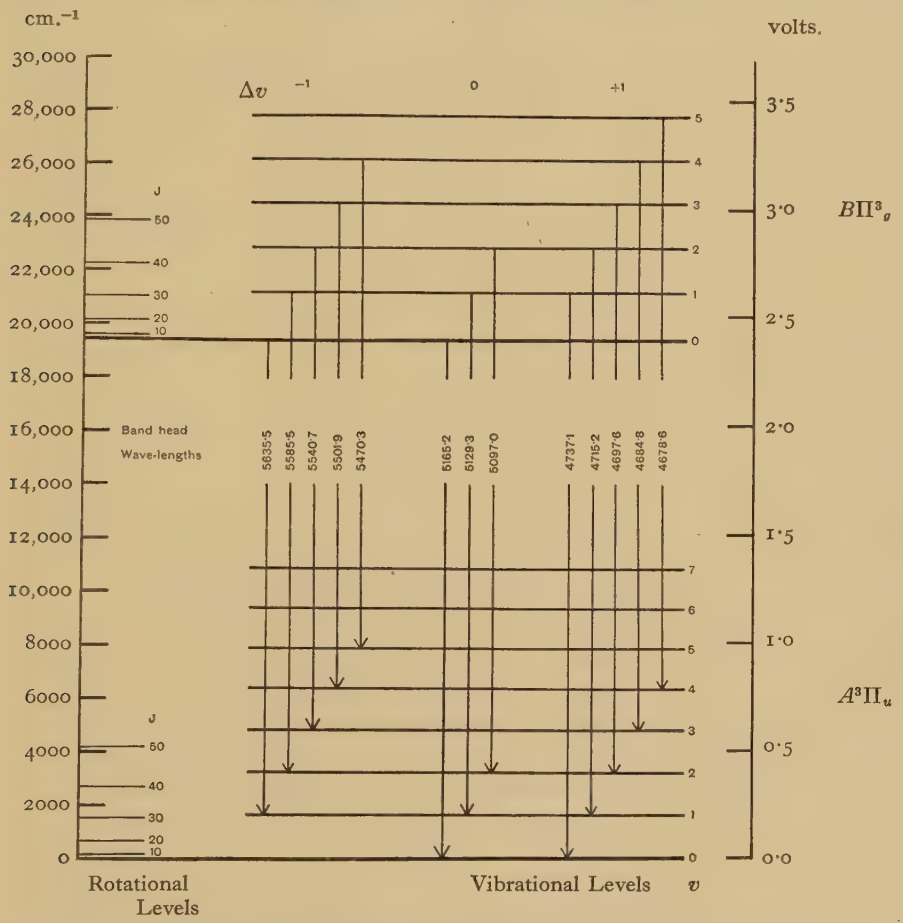

FIG. 1.—*Electronic and Vibrational Energy Levels of the Carbon Molecule for the Swan Band System.*

transitions corresponding to $\Delta v = -1, 0, +1$, with the wave-lengths of the heads of the resulting bands. In the λλ 5070–5160 A. region we find the sequence corresponding to $\Delta v = 0$, the (0, 0) band with head at λ 5165·2 A., (1, 1) at λ 5129·3 A. and (2, 2) at λ 5097·0 A.

We must now consider the fine structure of each of the vibrational bands produced by the rotational energy changes accompanying the changes in vibrational energy. The rotational energy levels for the $v = 0$ vibrational levels are shown on the left of fig. 1. In each vibrational band we should expect to find P, Q and R branches corresponding to changes in the rotational quantum number J of +1, 0 and −1 respectively. Since $\Sigma = 1$, each J value corresponds to a triplet of energy levels $^3\Pi_0$, $^3\Pi_1$, $^3\Pi_2$, and each of the P, Q

and R branches should therefore show a multiplet structure. Fig. 2 shows the triplet rotational levels for $J = n$ and $n+1$ in any vibrational level of the $^3\Pi_g$ and $^3\Pi_u$ states, and transitions which are observed to take place between these levels. The strongest branches of the multiplet are P_1, P_2, P_3, R_1, R_2, R_3, in which the change in the angular momentum quantum

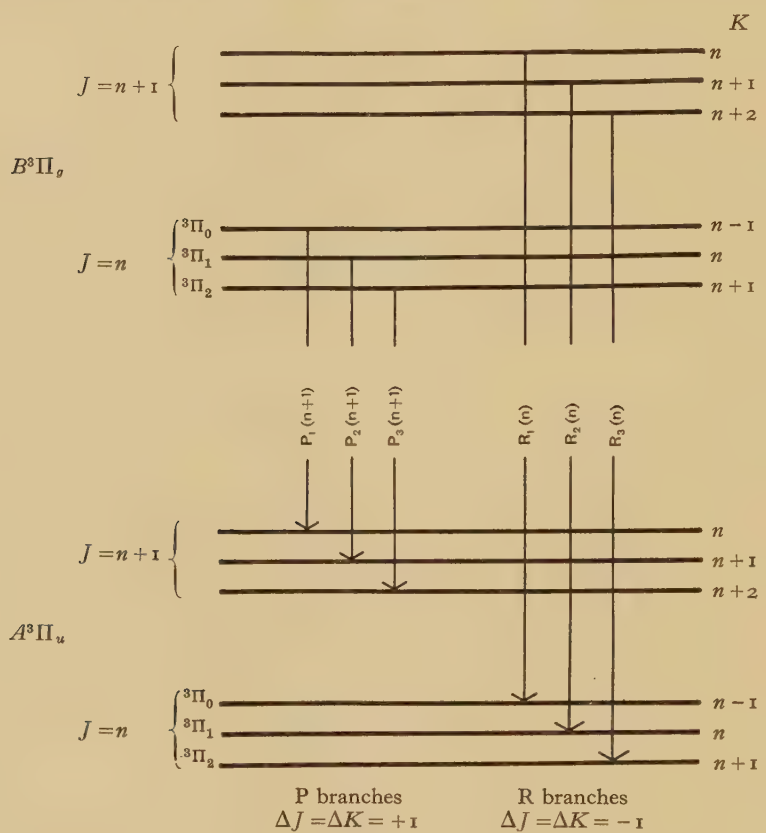

FIG. 2.—*Rotational Transitions for the Swan Bands.*

number K, exclusive of spin, is the same as the change in J. No Q branches are observed for the Swan bands, although they are allowed by the selection rules; their intensity, predicted by Hönl and London's theory, is zero for the Q_1 branch and very small for the Q_2 and Q_3 branches.

J value assignments have been made in the Swan bands by Johnson * and Shea; † the two are in agreement for the P lines, but Johnson's J value for the R lines must be decreased by 1. As Shea illustrates, the separation of the triplet members of the P and R branches is never very great, and decreases with increasing J number. Thus for the R branches the red R_1 and violet R_3 branches (Johnson's terminology) are separated by 1·415 A. at $J = 4$, while for $J = 39$ the R_2 and R_3 branches are no longer separated, and are only distant 0·136 A. from R_1 (39). For the P branches the separa-

* *Phil. Trans.*, **226**, 157, 1927. † *Phys. Rev.*, **30**, 825, 1927.

tions are even smaller, and the P_2 and P_3 branches were only observed separately by Johnson in the tube and not in the arc. At $J = 42$ we have P_1 and P_{23} (coincident P_2 and P_3) with a wave-length difference of only 0·108 A., and from $J = 66$ approx. Johnson gives only a single P branch line.

From this brief survey of the carbon bands and band branches which we should expect to find in the λ 5100 A. region, we may now attempt to identify the carbon lines appearing in the solar spectrum. Section 1 of the paper describes the method by which wave-lengths and equivalent widths were obtained for all lines fainter than R.I. +1 in the region $\lambda\lambda$ 5070–5160 A., and the method by which those due to carbon were selected from amongst these. In Section 2 the absolute intensity variation amongst the identified lines is considered, from which excitation temperatures are obtained at centre and limb.

Section 1. Identification of Carbon Lines

As the present problem is to identify the faint molecular lines as well as to measure their absolute intensities, wave-lengths and central intensities were determined for all measurable unblended lines of R.I. < 1 in the wave-length region available ($\lambda\lambda$ 5070–5160 A.). As described in an earlier paper,* the final values were based on measurements of microphotometer tracings from three different plates each with centre and limb spectra. Only sharp peaks were selected for measurement on each tracing, which were apparently unaffected by the presence of stronger lines, and for each of these the position and height of the peak and continuous background height were measured. Wave-lengths were obtained from the x co-ordinate using the position of stronger lines in the region (maximum R.I. +5), for which the wave-lengths at the centre of the disc are given in the Revision of Rowland's Table. True absorption lines were distinguished from chance peaks on the tracings due to silver grain, by retaining as lines only those peaks which were measured on at least two of the three plates, and for which the measured wave-lengths on the different plates all lay within an interval not > ·05 A. With this criterion the presence of 169 lines was established at the centre of the disc and 157 at the limb (mean $\cos\theta = 0{\cdot}3$), all of R.I. 0, −1, −2 and −3. The wave-length adopted for these lines was the mean of the measurements from the three plates.

Absolute central intensities were determined for all the peaks selected on each tracing, from the measured height of the peak and of the continuous background, and wedge characteristic curves obtained for each plate at $\lambda\lambda$ 5082, 5114 and 5136 A. approx. The mean of the central intensities for each peak adopted as a line was then converted into equivalent width, from the empirical relation between central intensity and equivalent width obtained from profile measurements of stronger lines (R.I. +5 to −2) given in the earlier paper.†

The first step in identification is to eliminate from these measured lines those already known to be atomic in origin. This was done by a comparison with the Revision of Rowland's Table, and all the measured lines within

* *M.N.*, 98, 112, 1937. † *M.N.*, 98, 119, 1937, fig. 2.

·05 A. of a Rowland atomic line were removed (48 lines at the centre and 40 at the limb). The wave-lengths of the remaining lines, among which we must seek those due to carbon, are given in columns 1 (centre) and 3 (limb, cos θ 0·3) of Table I below,* followed in columns 2 and 4 by the equivalent widths. Columns 5 and 6 are given for comparison with the present measurements; they give the wave-lengths and intensity estimates of Rowland lines which are within ·05 A. of the present lines, and which are either unidentified or attributed to carbon by Rowland.

Since in this investigation we are not concerned with assigning each of the measured solar lines to its appropriate source, but only in selecting from among all the lines those definitely due to carbon, it is not absolutely essential to consider all the possible carriers which might be producing faint, as yet unidentified lines in this region. The fact, however, that we ignore all other sources means that our carbon identifications must be made with extreme caution. The laboratory wave-length measurements for carbon show that over 350 molecular lines occur between λλ 5070–5160 A., a line density which on Russell and Bowen's calculations † would give about forty chance coincidences with the 120 lines available for identification (identifying lines not > ·05 A. from carbon lines).

The method adopted for identification has been in the first place to consider only the strongest of the carbon lines appearing in the laboratory spectrum, since, unless a convincing proportion of these are identified, there is small hope that identifications of fainter lines will not be chance coincidences. For thermodynamic equilibrium at 6000° K the ratio of the intensities of the (0, 0) and (1, 1) bands as a whole is approx. 3 : 2, and accordingly only lines of the (0, 0) band have been considered. The omission of the (1, 1) and (2, 2) bands reduces the number of carbon lines to 230 approx. from λλ 5070–5160 A. Secondly, we have made a selection of these laboratory carbon lines in just the same way as the observed lines appearing in columns 1 and 3 of Table I were selected. To do this we must in effect artificially superpose the solar spectrum on the (0, 0) band spectrum and eliminate all the carbon lines, which are then seen to be obscured by atomic Fraunhofer lines; the remaining molecular lines will then be those which we can fairly expect to find in the list of observed solar lines. The lines

* It is of interest to compare the wave-lengths in Table I at centre and limb. For the 69 lines in common, the arithmetic mean of the differences $\lambda_c - \lambda_L$ is +·0047 A., with a standard deviation of the mean of ± ·0026 A. This is probably a consequence of limb effect (St. John, *A.J.*, **67**, 195, 1928; McCrea and Mitra, *Observatory*, **42**, 379, 1934). Suppose λ' and L' are the laboratory wave-lengths of a faint and strong line, $\Delta\lambda'$ and $\Delta L'$ the decrease in wave-length due to radial motion outwards in the Sun's atmosphere, and λ and L the wave-lengths now adopted in the solar spectrum. At the centre true wave-lengths were adopted for the strong lines, and therefore $\lambda_c = \lambda' - \Delta\lambda'$. At the limb, however, for L_L we have taken the shorter L_c instead of the true L', and therefore λ_L based on the value adopted for L_L is given by $\lambda' - \Delta L'$. Therefore $\lambda_c - \lambda_L = \Delta L' - \Delta\lambda'$. The positive residual therefore indicates that the limb effect is greater for strong than for faint lines, and the observed value corresponds to a radial velocity of ·28 km./sec. approx. for strong lines relative to faint ones.

† *A.J.*, **69**, 196, 1929.

TABLE I

Observed Wave-lengths and Equivalent Widths of Non-atomic Faint Lines in the Solar Spectrum from λλ 5070–5160 A. and the Strongest Lines of the Swan Spectrum

CENTRE		LIMB		ROWLAND		JOHNSON		
λ in A.	E.W. in A.	λ	E.W. in A.	λ	Int.	λ	Arc Int.	Identification
5073·480	·0096	·454	·0165	·464	−1	·453	9	R_{23} (41)
5073						·578	4	R_1 (41)
5074		·752	·0115	·751	−2			
5074		·354	·0080	·347	−2			
5075						·389	1	P_1 (68)
5076						·626	7	R_{23} (40)
5076						·762	4	R_1 (40)
5077·428	·0093	·423	·0118	·388	−2			
5078·100	·0050	·111	·0080	·071	−2			
5078						·346	1	P_{23} (67)
5078		·443	·0078			·431	0	P_1 (67)
5080						·085	6	R_1 (39)
5081·798	·0078	·764	·0092	·768	−2	·756	1	P_{23} (66)
5081		·861	·0140	·845	−2			
5082		·075	·0051	·058	−3			
5083						·006	5	R_3 (38)
5083						·051	5	R_2 (38)
5083						·169	5	R_1 (38)
5084·561	·0101	·557	·0150	·563	−2			
5084·688	·0071	·736	·0095	·705	−2	·688	2	P_{23} (65)
5084						·809	0	P_1 (65)
5085·707	·0051			·685	−2			
5086		·272	·0180	·251	−1	·234	9	R_{23} (37)
5086·296	·0147							
5086						·386	5	R_1 (37)
5086·646	·0105	·607	·0120	·623	−3			
5087		·781	·0048					
5087						·994	2	P_{23} (64)
5089·202	·0133					·178	5	R_3 (36)
5089		·209	·0198	·217	−2	·236	5	R_2 (36)
5089						·350	5	R_1 (36)
5089		·430	·0105					
5089		·470	·0070					
5090·200	·0084			·221	−2			
5090						·932	0	P_1 (63)
5091		·280	·0083	·307	−3			
5091·362	·0075							

Note to Table I.—The lines λλ 5127·875 and 5147·068 A. are now identified by King * as due to *Fe*II. λ 5128·494 is identified by C. E. Moore † as due to vanadium.

* *A.J.*, 87, 109, 1938.

† *A Multiplet Table of Astrophysical Interest*, 1933.

TABLE I—*continued*

CENTRE		LIMB		ROWLAND		JOHNSON		
λ in A.	E.W. in A.	λ	E.W. in A.	λ	Int.	λ	Arc Int.	Identification
5091·761	·0096	·739	·0120	·726	−2			
5092·323	·0168	·314	·0179	·313	−1	·292	8	R_{23} (35)
5092						·444	5	R_1 (35)
5092·527	·0220	·516	·0130	·495	−3			
5093·712	·0070			·688	−3			
5094		·029	·0133	·029	−2	·002	3	P_{23} (62)
5094·053	·0119					·095	0	P_1 (62)
5095						·134	5	R_3 (34)
5095·209	·0115	·183	·0159	·178	−1	·194	5	R_2 (34)
5095		·289	·0146					
5095·357	·0102			·342	−1	·311	6	R_1 (34)
5095·867	·0107	·858	·0119	·861	−2			
5096		·076	·0060	·045	−3			
5096·551	·0050			·592	−3			
5098·140	·0133	·142	·0185	·132	−1	·133	(6)	R_{23} (33)
5098						·284	(3)	R_1 (33)
5099						·774	4	P_{23} (60)
5099						·877	1	P_1 (60)
5100·276	·0030	·281	·0055	·244	−3			
5100·669	·0147	·654	·0136	·658	−1			
5100·885	·0115			·859	−2	·857	(3)	R_3 (32)
5100		·937	·0126	·939	−2	·929	(3)	R_2 (32)
5101·517	·0026	·491	·0069	·486	−2			
5101·809	·0040			·825	−3			
5102·217	·0030			·241	−3			
5102·447	·0092			·430	−2	·422	4	P_{23} (59)
5102		·473	·0144					
5102						·526	0	P_1 (59)
5103·357	·0022	·390	·0056	·398	−2			
5103						·717	(3)	R_3 (31)
5103·762	·0070	·752	·0105	·741	−2	·761	(3)	R_2 (31)
5103						·901	(3)	R_1 (31)
5104·450	·0292	·431	·0272	·441	0			
5104		·904	·0044	·898	−2			
5105						·342	4	P_{23} (58)
5105						·434	1	P_1 (58)
5105·930	·0019							
5106		·399	·0138	·388	−3	·350	(2)	R_3 (30)
5106·478	·0112	·458	·0132	·455	−2	·432	(2)	R_2 (30)
5106						·536	(2)	R_1 (30)
5106		·591	·0123	·605	−2			
5106		·834	·0048	·879	−3			
5106		·926	·0046					
5107						·872	5	P_{23} (57)
5107·903	·0082	·930	·0118	·889	−2			
5107						·972	1	P_1 (57)
5108		·618	·0049	·638	−3			

TABLE I—*continued*

CENTRE		LIMB		ROWLAND		JOHNSON		
λ in A.	E.W. in A.	λ	E.W. in A.	λ	Int.	λ	Arc Int.	Identification
5109						·089	(2)	R_3 (29)
5109·160	·0048	·134	·0091	·124	−2	·143	(2)	R_2 (29)
5109						·294	(2)	R_1 (29)
5110		·026	·0068	·021	−3			
5110						·665	3	P_{23} (56)
5111		·097	·0068					
5111·392	·0050	·348	·0102	·372	−2			
5111·641	·0097	·634	·0125	·635	−2	·606	(2)	R_3 (28)
5111						·703	(2)	R_2 (28)
5111·855	·0087	·804	·0098	·882	−2	·833	(2)	R_1 (28)
5113						·196	0	P_1 (55)
5114						·190	(2)	R_3 (27)
5114·310	·0166	·254	·0139	·264	−2	·283	(2)	R_2 (27)
5114						·438	(2)	R_1 (27)
5114·968	·0031							
5115						·856	1	P_1 (54)
5116·610	·0098					·638	(2)	R_3 (26)
5116		·686	·0160	·682	−3	·732	(2)	R_2 (26)
5116						·876	(2)	R_1 (26)
5118		·092	·0125	·074	−3	·062	3	P_{23} (53)
5118						·241	3	P_1 (53)
5118·411	·0027			·362	−3			
5118·832	·0039	·809	·0068	·820	−2			
5119·230	·0126			·201	−3	·199	(2)	R_2 (25)
5119·392	·0050	·354	·0078	·388	−2	·364	(2)	R_1 (25)
5119·642	·0037			·653	−3			
5119		·877	·0063					
5119·936	·0051			·917	−3			
5120·648	·0072	·643	·0123	·635	−2	·617	5	P_{23} (52)
5120						·707	1	P_1 (52)
5121						·424	(1)	R_3 (24)
5122·336	·0047			·313	−3			
5122						·852	1	P_1 (51)
5123						·865	(1)	R_2 (23)
5124·058	·0119			·051	−2	·038	(1)	R_1 (23)
5124·622	·0173	·614	·0170	·617	−1			
5125		·527	·0089	·477	−3			
5125·626	·0072							
5125						·961	(1)	R_3 (22)
5126						·028	...	P_{23} (25)
5126						·069	(1)	R_2 (22)
5126		·601	·0066					
5126		·993	·0073	·019	−3			
5127·875	·0079			·884	−3			
5128·115	·0152	·112	·0174	·083	−2			
5128						·175	(1)	R_3 (21)

TABLE I—*continued*

CENTRE		LIMB		ROWLAND		JOHNSON		
λ in A.	E.W. in A.	λ	E.W. in A.	λ	Int.	λ	Arc Int.	Identification
5128						·294	(1)	R_2 (21)
5128·494	·0082	·474	·0089	·493	−2	·476	(1)	**R_1 (21)**
5129						·582	6	P_{23} (48)
5130						·255	(1)	R_3 (20)
5131						·573	5	P_{23} (47)
5131						·675	2	P_1 (47)
5132·144	·0055			·171	−3			
5132						·481	(1)	R_2 (19)
5132·672	·0242	·690	·0200	·676	−1	·681	(1)	**R_1 (19)**
5133·151	·0052			·197	−2			
5134·073	·0090							
5134·329	·0086	·270	·0088	·338	−3	·300	(1)	R_3 (18)
5134						·472	(1)	R_2 (18)
5134·549	·0128			·530	−2			
5134·590	·0117	·589	·0139					
5134·651	·0105			·682	−3	·654	(1)	**R_1 (18)**
5134		·945	·0037					
5135·206	·0047	·163	·0057	·188	−3			
5135·555	·0072	·564	·0091	·585	−2	·561	5	P_{23} (45)
5135·590	·0084	·606	·0099					
5135·668	·0071	·672	·0083	·713	−2	·672	2	P_1 (45)
5135		·812	·0049					
5136·260	·0098	·233	·0130	·276	−2	·256	(1)	**R_3 (17)**
5136		·292	·0108					
5136·453	·0063	·463	·0088	·458	−3	·426	(1)	**R_2 (17)**
5136		·526	·0073					
5136						·640	(1)	R_1 (17)
5136·794	·0130			·802	−2			
5137						·566	7	P_{23} (44)
5137						·672	3	P_1 (44)
5137·944	·0048			·963	−3			
5138·127	·0059	·134	·0049	·112	−3	·094	(0)	**R_3 (16)**
5138·309	·0070	·330	·0095	·351	−3	·296	(0)	**R_2 (16)**
5138		·372	·0101					
5138·540	·0086			·523	−3	·493	(0)	**R_1 (16)**
5138·714	·0120	·704	·0098	·723	−2			
5139						·911	(0)	R_3 (15)
5139·995	·0072							
5140·166	·0078			·169	−3	·122	(0)	**R_2 (15)**
5140		·191	·0073					
5140·362	·0048	·395	·0050	·386	−3	·363	(0)	**R_1 (15)**
5140		·574	·0049					
5140·814	·0135	·817	·0156	·825	−1			
5141·190	·0115	·221	·0138	·219	−2	·187	8	**P_{23} (42)**
5141·246	·0086							
5141·311	·0084	·305	·0100	·330	−3	·295	3	P_1 (42)

TABLE I—*continued*

CENTRE		LIMB		ROWLAND		JOHNSON		
λ in A.	E.W. in A.	λ	E.W. in A.	λ	Int.	λ	Arc Int.	Identification
5141						·626	(0)	R_3 (14)
5141						·877	(0)	R_2 (14)
5142·092	·0022	·122	·0099	·112	−3	·092	(0)	**R_1 (14)**
5143·297	·0070	·309	·0061	·344	−2	·307	(0)	**R_3 (13)**
5143		·384	·0060					
5143·608	·0096			·597	−2	·578	(0)	**R_2 (13)**
5143·727	·0205	·731	·0253	·734	−1			
5143						·846	(0)	R_1 (13)
5144		·022	·0048	·036	−3			
5144		·083	·0048					
5144·375	·0041	·333	·0057	·376	−2			
5144·574	·0140	·572	·0190	·591	−2	·551	8	**P_{23} (40)**
5144						·899	(0)	R_3 (12)
5145						·210	(0)	R_2 (12)
5145·771	·0043	·735	·0057	·740	−3			
5146·116	·0293					·069	7	**P_{23} (39)**
5146		·123	·0280	·124	−1			
5146						·183	3	P_1 (39)
5147·064	·0141	·075	·0116	·106	−2	·090	(0)	R_1 (11)
5147·119	·0149	·126	·0101					
5147·715	·0100	·703	·0149	·704	−2	·673	8	**P_{23} (38)**
5147						·792	3	P_1 (38)
5147						·902	(0)	R_3 (10)
5148·549	·0065	·633	·0105			·583	(0)	R_1 (10)
5148·840	·0103	·842	·0108	·846	−2			
5149						·186	3	P_1 (37)
5149						·303	...	R_3 (9)
5149·516	·0047	·517	·0055	·518	−3			
5149·849	·0055							
5150						·113	...	R_1 (9)
5150		·167	·0165					
5150·195	·0149	·216	·0181	·196	−1			
5150·373	·0071			·358	−3			
5150·582	·0113			·569	−2	·532	8	**P_{23} (36)**
5150						·625	...	R_3 (8)
5150						·645	4	P_1 (36)
5151						·143	...	R_2 (8)
5151·457	·0043	·488	·0042	·461	−3	·495	...	R_1 (8)
5151						·812	7	P_{23} (35)
5152						·482	...	R_2 (7)
5152·817	·0031							
5152·952	·0033			·962	−2	·933	...	R_1 (7)
5153						·049	...	R_3 (6)
5153						·143	8	P_{23} (34)
5153·757	·0061					·748	...	R_2 (6)
5154						·148	...	R_3 (5)

TABLE I—*continued*

CENTRE		LIMB		ROWLAND		JOHNSON		
λ in A.	E.W. in A.	λ	E.W. in A.	λ	Int.	λ	Arc Int.	Identification
5154						·204	...	R_1 (6)
5154						·302	6	P_{23} (33)
5154·379	·0201			·338	−3			
5154·422	·0205	·398	·0238	·412	−2	·419	4	P_1 (33)
5154·694	·0041							
5154						·969	...	R_2 (5)
5155·544	·0110			·527	−2	·496	8	**P_{23} (32)**
5155						·563	...	R_1 (5)
5155						·627	4	P_1 (32)
5156		·577	·0215	·561	−3	·537	6	**P_{23} (31)**
5156·644	·0223	·638	·0243	·656	−1	·658	4	**P_1 (31)**
5156						·758	...	R_1 (4)
5156		·944	·0060	·996	−3			
5157·073	·0056							
5157						·141	...	R_2 (3)
5157·211	·0101	·213	·0092	·209	−2			
5157·459	·0041							
5157·644	·0122	·642	·0172	·616	−2	·601	8	**P_{23} (30)**
5157·732	·0114	·732	·0138	·748	−2	·728	4	**P_1 (30)**
5158·219	·0029					·175	...	R_2 (2)
5158·531	·0117	·515	·0151	·534	−2	·504	6	**P_{23} (29)**
5158·609	·0101	·594	·0156			·637	4	**P_1 (29)**
5158·682	·0081	·695	·0088	·665	−3			
5159		·450	·0148	·467	−2	·435	8	**P_{23} (28)**
5159·513	·0070							
5159		·528	·0121			·568	5	**P_1 (28)**
5159·623	·0087	·622	·0121	·609	−3			

omitted from the laboratory wave-lengths were those within ·05 of a Rowland atomic line, or within the equivalent width as given by Allen * for a line stronger than equivalent width ·05 A. This amounts to assuming a triangular profile with zero central intensity for the stronger lines, and must mean that more laboratory lines are included than would in measuring the tracings have been regarded as unaffected by stronger lines. This selection results in the 150 carbon lines of the (0, 0) band given in column 7 of Table I.

Since, as we have demonstrated, wave-length coincidence with a laboratory line is insufficient evidence for identifying a solar line as due to carbon, it is important to have some guide to the intensity variation we should expect to find among the carbon lines. Johnson gives estimated intensities on a scale 0–10 for carbon lines in the tube and in the arc spectra. From the variation of intensity within the band he deduces that the tube intensities correspond to a temperature of 760° K approx. and the arc intensities

* *Mem. Commonwealth Solar Obs.*, 5, 22, 1934.

to 7300° K approx. It is therefore obvious that only the arc intensities are at all relevant to the solar carbon lines, and Johnson's estimated arc intensity is therefore given in column 8 of Table I. Unfortunately, Johnson did not give complete intensity estimates, and intensities on the same scale, given in brackets, have had to be deduced for most of the R lines. These were obtained by assuming a symmetrical variation of intensity about the maximum which Johnson considers to be at J = 38. His estimated intensities show such a wide scatter, that those deduced can only be regarded as a very rough guide to the probable intensity of a line.

The last column of Table I gives the assignments of the carbon lines according to Johnson. Those in heavy type show where one of the solar lines is identified with a carbon line. No lines have been identified as carbon which are outside of ·05 A. of the laboratory wave-length, but agreement in wave-length has been by no means the only criterion. The estimated intensities have also been considered, and especially the appearance of successive lines of a series without large unaccountable gaps. Thus the lines coincident with P_1 (67), P_{23} (66), P_{23} (62), P_1 (62), etc. at the beginning of Table I have not been identified as carbon, since the appearance of the P branch here is fairly sporadic, and P_1 lines of greater predicted intensity do not appear. As we should expect, the strongest lines of the (0, 0) band are the combined P and the combined R lines, and these comprise the majority of the identified lines. The measured solar wave-lengths show that the R_2 and R_3 lines have been measured as a single peak after they have been given as resolved by Johnson (in such cases the R_2 and R_3 lines are shown bracketed in column 9, and the unresolved solar lines are subsequently denoted by $R_{2,3}$). The dispersion of Johnson's plates was 1·3 A./mm. as compared with the present value of 1·16 A./mm. We may attribute the non-resolution of the lines in the present instance to the greater width and extreme faintness of the solar absorption lines compared with the fine emission lines in the laboratory spectrum.

The combined R_2 and R_3 lines are identified consistently from J = 41 to J = 26, with the exception of R_{23} (40) and R_{23} (38). (There is an *Fe* (4) line at λ 5083·347 which might account for the non-measurement of $R_{2,3}$ (38).) The single resolved R_2 and R_3 lines are identified from J = 17 to J = 13 with R_3 (15), R_2 (14) and R_3 (14 absent) (the latter pair are probably not measured on account of *Fe* (3) 5141·748). The disappearance of the R_2 and R_3 lines from $R_{2,3}$ (26) to R_2 (17), R_3 (17), is probably due to the fact that as these close branches gradually separate with decreasing J number to appear finally as single lines, they will give a broadened "hump" on the tracing rather than one of the definite sharp peaks which would be selected for measurement. The single R_1 lines are identified from J = 25 to J = 14, with only a single gap at R_1 (17). Of the P branch lines, P_{23} lines are identified from J = 42 to J = 28 (the limit of the plates), but with P_{23} (35), P_{23} (34) and P_{23} (33) missing; the continuity of the identifications on either side of this unexplained gap is considered sufficient justification for their being made. Single P_1 lines appear from J = 31 to the limit of the measure-

ments J = 28. It is obvious that only the strongest lines of the (0, 0) band appear in the solar spectrum, and that lines of the (1, 1) and (2, 2) bands may therefore be neglected. Of the identified (0, 0) band lines only 5—$R_{2,3}$ (36), $R_{2,3}$ (28), $R_{2,3}$ (27), R_1 (25) and R_1 (23)—have a (1, 1) line within ·05 A.; the fact that these lines are not abnormally strong justifies our neglecting the (1, 1) band and so *a fortiori* the (2, 2) band.

Section 2. Temperature Determination from the Observed Intensity Distribution

The population n of any rotational energy level of a molecule is given by

$$n = Cge^{-E_r/kT},$$

where g is the statistical weight of the state, C is a constant over a small frequency range, and E_r is the rotational energy. The strength of a line arising from this level depends upon this population, and the transition probability to the final level. The total number N of transitions made per second is

$$N = Cie^{-E_r/kT},$$

where i is the "intensity factor," and includes the weight of the state and the transition probability. i factors have been determined by Hönl and London, and for the $\Pi - \Pi$ band now observed are given below.* J is the larger of J′ (upper level) and J″ (lower level), and Ω is the total electronic angular momentum along the internuclear axis; for the R_1, P_1 branches $\Omega = 0$ (anti-parallel spin), for the R_2, P_2 branches $\Omega = 1$ (no spin), and for the

Branch	i	Sub-branch	i
P (J)	$\frac{(J^2-\Omega^2)}{J}$	P_1	J
		P_2	$J-\frac{1}{J}$
		P_3	$J-\frac{4}{J}$
R (J)	$\frac{(J+1)^2-\Omega^2}{J+1}$	R_1	$J+1$
		R_2	$(J+1)-\frac{1}{(J+1)}$
		R_3	$(J+1)-\frac{4}{(J+1)}$

R_3, P_3 branches $\Omega = 2$ (parallel spin). E_r, the rotational energy of the initial state, is given by $hcB_vJ(J+1)$ ergs, where B_v depends upon the moment of

* Jevons, *Report on Band Spectra of Diatomic Molecules*, p. 134.

inertia of the molecule and the given vibrational level. The observed intensity of a rotational line (or its equivalent width W) is therefore

$$W = f\left(Cie^{\frac{-hcB_v J(J+1)}{kT}}\right). \quad (1)$$

If we assume that for these very faint lines the equivalent width is directly proportional to the number of transitions made per second, *i.e.* the faint lines are on the linear part of the curve of growth, we may determine T by choosing it so that the curve

$$W = Cie^{\frac{-hcB_v J(J+1)}{kT}} \quad (2)$$

gives a fit with the observed intensity distribution.

In column 1 of Table II are given all the carbon identifications made from Table I. It will be seen that the identified lines fall into two distinct classes: the *coincident* P_{23} and R_{23} lines for which a single wavelength is given by Johnson, and the single P_1, R_1, R_2, R_3 lines. Since we cannot predict how the equivalent width of two coincident lines will be related to their separate equivalent widths, we cannot combine the coincident double lines with the single lines to make a unique determination of temperature from all the identified lines. In subsequent calculations we must therefore treat these two classes of lines quite separately. The solar unresolved double lines $R_{2,3}$, shown bracketed together in Table I, for which a single or a double peak was almost an accident of observation, obviously cannot be used in calculations either as a distinct class of lines, or combined with the single or with the coincident double lines.

Columns 2 and 3 of Table II contain the equivalent widths at centre and limb respectively for all the identified lines. (The limb equivalent width given for $R_{2,3}$ (30), for which two separate peaks were measured, is the mean of the two.) The abnormally great equivalent widths measured for R_1 (19), P_{23} (39) and P_1 (31) show that these molecular lines must be coincident with some unidentified atomic Fraunhofer line, and they are omitted from further considerations. Column 4 gives the factor $J(J+1)$ for the single and coincident double lines (for the R lines in all calculations Johnson's J number has been reduced by 1 in agreement with Shea's later J value assignments). The i factors given in the last column are obtained from the expressions given above; for the coincident P_{23}, R_{23} lines the sum of the i factors of the two separate components is given.

Fig. 3 shows the relation between equivalent width and J number for the two classes of identified lines. The lines not used as being too strong are shown enclosed in square brackets. It will be seen that, as a whole, the points show the familiar variation in intensity with J number corresponding to thermal equilibrium; in view of the two distinct classes of lines we are observing, it is surprising that the intensities of the coincident double lines are so comparable with the single line intensities. (The intermediate unresolved $R_{2,3}$ lines, not shown in fig. 3, do not show a wild scatter from this general intensity variation.) Considering the two classes of lines

TABLE II

Identified Carbon Lines

Identification (Johnson)	CENTRE. E.W. in A.	LIMB. E.W. in A.	$J(J+1) \times 10^{-3}$ (True J)	i
R_{23} (41)	·0096	·0165	1·640	81·9
R_{23} (37)		·0180	1·332	73·9
$R_{2,3}$ (36)	·0133	·0198		
R_{23} (35)	·0168	·0179	1·190	69·9
$R_{2,3}$ (34)	·0115	·0159		
R_{23} (33)	·0133	·0185	1·056	65·8
$R_{2,3}$ (32)	·0115	·0126		
$R_{2,3}$ (31)	·0070	·0105		
$R_{2,3}$ (30)	·0112	·0135		
$R_{2,3}$ (29)	·0048	·0091		
$R_{2,3}$ (28)	·0097	·0125		
$R_{2,3}$ (27)	·0166	·0139		
$R_{2,3}$ (26)	·0098	·0160		
R_1 (25)	·0050	·0078	0·600	25·0
R_1 (23)	·0119		0·506	23·0
R_1 (19)	·0242	·0200	Too strong.	
R_1 (18)	·0105		0·306	18·0
R_3 (17)	·0098	·0130	0·272	16·8
R_2 (17)	·0063	·0088	0·272	16·9
R_3 (16)	·0059	·0049	0·240	15·7
R_2 (16)	·0070	·0095	0·240	15·9
R_1 (16)	·0086		0·240	16·0
R_2 (15)	·0078		0·210	14·9
R_1 (15)	·0048	·0050	0·210	15·0
P_{23} (42)	·0115	·0138	1·806	83·9
R_1 (14)	·0022	·0099	0·182	14·0
R_3 (13)	·0070	·0061	0·156	12·7
R_2 (13)	·0096		0·156	12·9
P_{23} (40)	·0140	·0190	1·640	79·9
P_{23} (39)	·0293		Too strong.	
P_{23} (38)	·0100	·0149	1·482	75·9
P_{23} (36)	·0113		1·332	71·9
P_{23} (32)	·0110		1·056	63·8
P_{23} (31)		·0215	0·992	61·8
P_1 (31)	·0223	·0243	Too strong.	
P_{23} (30)	·0122	·0172	0·930	59·8
P_1 (30)	·0114	·0138	0·930	30·0
P_{23} (29)	·0117	·0151	0·870	57·8
P_1 (29)	·0101	·0156	0·870	29·0
P_{23} (28)		·0148	0·812	55·8
P_1 (28)		·0121	0·812	28·0

separately, there is, as we might expect on account of their greater faintness, a great scatter among the single lines (open circles in fig. 3), and as further they are largely concentrated over a small range in J value, they are not suitable for exact determinations of temperature. We now proceed to

examine in greater detail the intensity variation in the coincident double lines (filled circles in fig. 3).

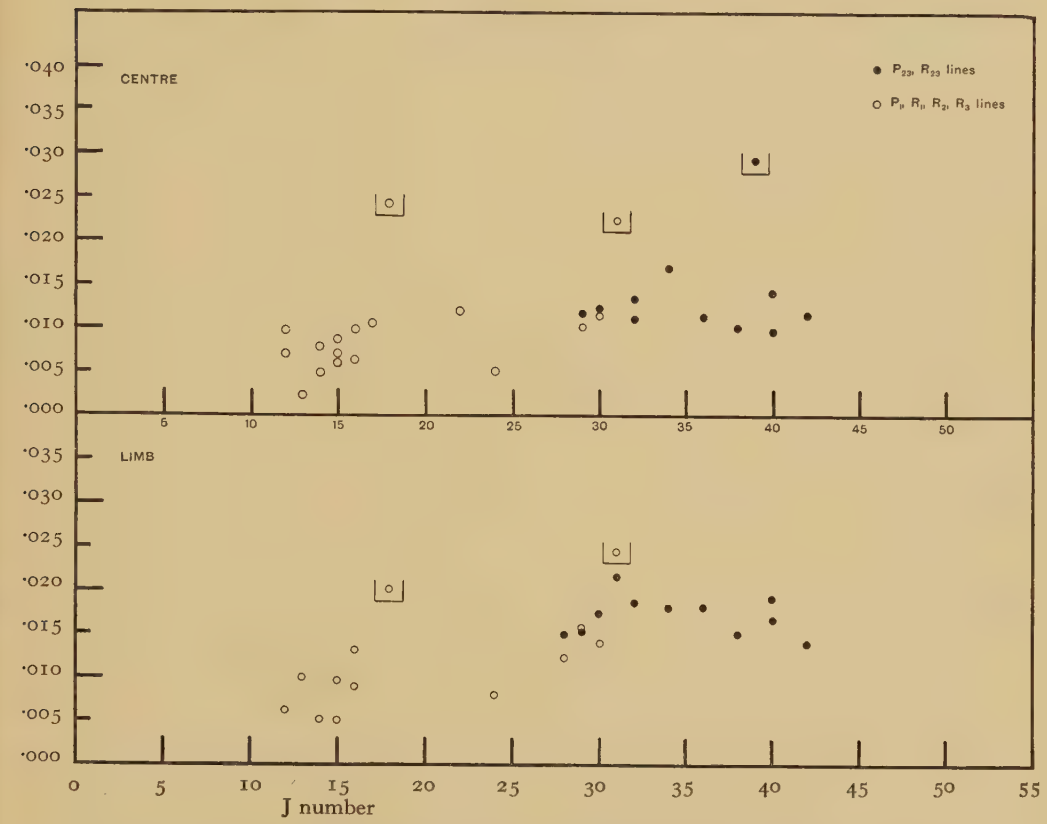

FIG. 3.—*Variation of Equivalent Width with Rotational Quantum Number (J) for the Single and Coincident Double Lines.*

Temperatures are best obtained from the observed intensity distribution by writing (2) in the form :

$$\log_{10}\left(\frac{W}{i}\right) = k - \frac{hcB_v J(J+1)}{2{\cdot}3kT}. \qquad (3)$$

If then we plot $\log\left(\frac{W}{i}\right)$ (ordinates) against $J(J+1)$ (abscissæ), we should obtain a straight line the slope of which gives $-\frac{hcB_v}{2{\cdot}3kT}$, and the intercept on the y axis will be proportional to the abundance of carbon. Fig. 4 shows the observed values of $\log\left(\frac{W}{i}\right)$ plotted against $J(J+1)$ for the coincident double lines at centre and limb. It will be seen that the points define a straight line with fair precision, showing that there is a thermal distribution of intensity along the band. A least squares solution was made to determine

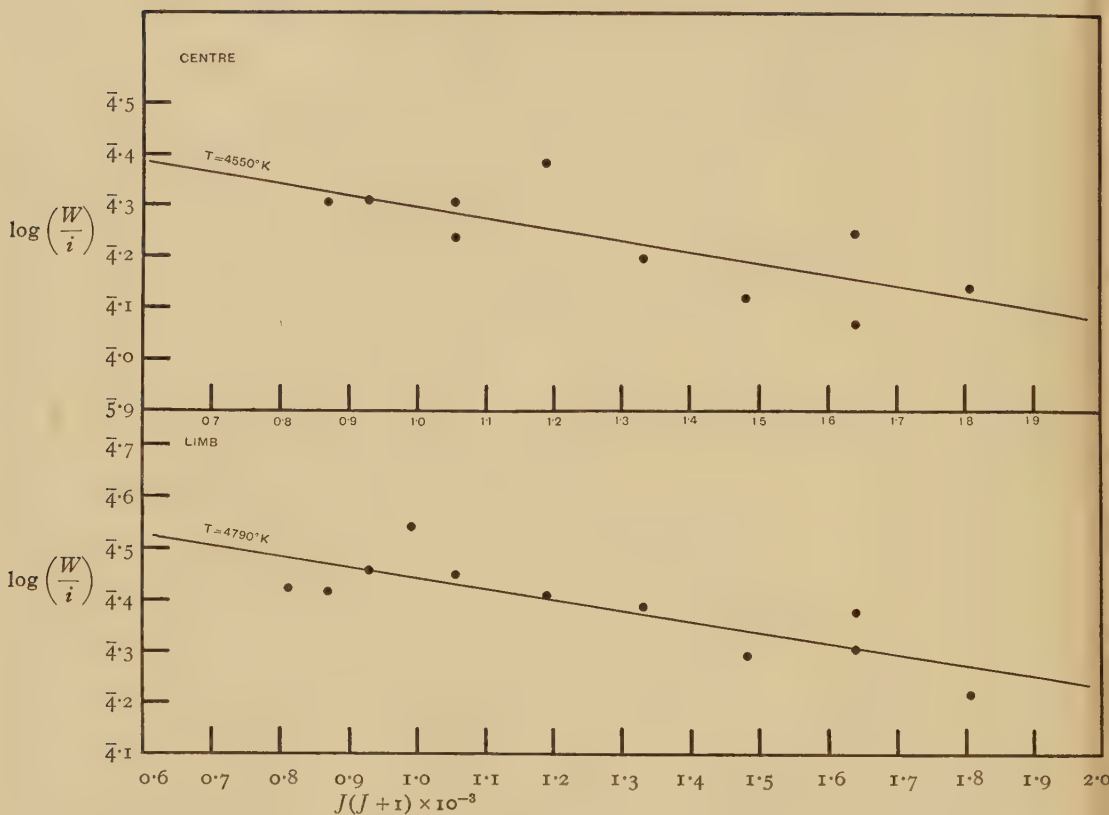

FIG. 4.—*Relation between* $\log\left(\frac{W}{i}\right)$ *and* $J(J+1)$ *for the Coincident Double Lines.*

the line given by the points with the results and standard errors given below, where m is the slope of the line and c is the intercept on the y axis :

Lines Used		No.	$m \times 10^3$	c	T
P_{23}, R_{23}	Centre	10	$-\cdot2218 \pm \cdot0716$	$\bar{4}\cdot5188 \pm \cdot0960$	4550° K {3400° K, 6700° K}
	Limb	11	$-\cdot2107 \pm \cdot0492$	$\bar{4}\cdot6519 \pm \cdot0636$	4790° K {3900° K, 6300° K}

T in the last column is derived from $-\frac{B_v hc}{2{\cdot}3km}$; substituting $B_v = 1{\cdot}63$ cm.$^{-1}$ for the (0, 0) band in absorption * then gives $T = -\frac{1{\cdot}01}{m}$. This value of T is followed by the limiting values corresponding to the standard error in m.

The striking features of these excitation temperatures are first their lowness compared with the effective temperature (5740° K), and secondly that

* Jevons, *Report on Band Spectra of Diatomic Molecules*, p. 282.

the limb temperature is higher than the centre temperature. We may point out that the temperatures have been derived by assuming that f in equation (1) was a linear function of N—a usual assumption for very faint lines where Doppler effect is largely responsible for the broadening.* If we make our calculations using Allen's curve of growth,† the variation in the equivalent

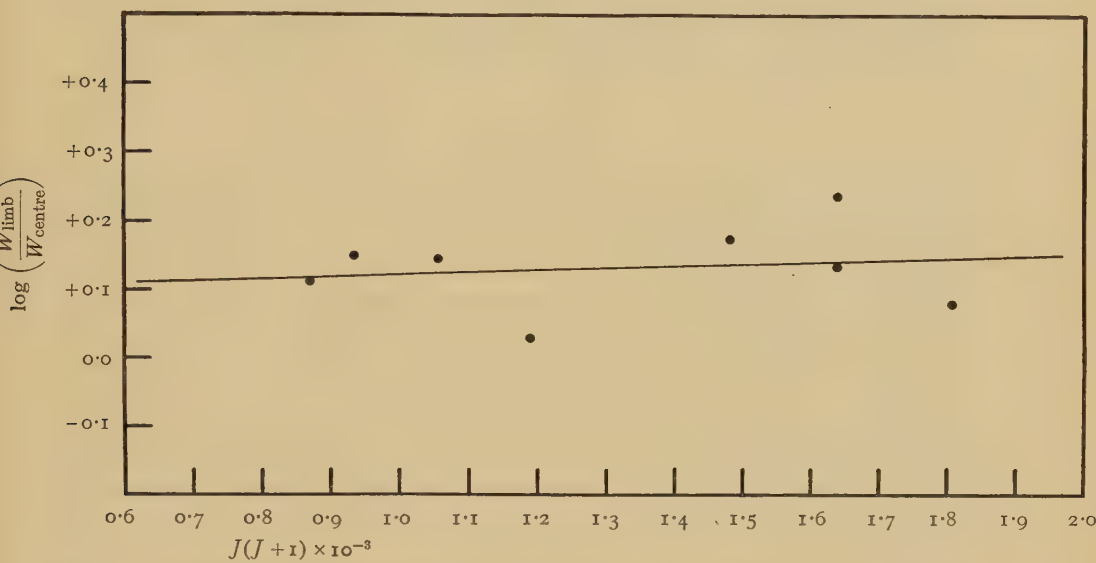

FIG. 5.—*Strengthening of Molecular Lines to the Limb as a function of $J(J+1)$ for the Coincident Double Lines.*

width of the lines is so slight that the temperatures obtained are very little changed and are in fact slightly lower than those given. The low value of the excitation temperature of the Sun is in agreement with the excitation temperatures recently obtained by King,‡ and by Menzel, Baker and Goldberg,§ and with the original temperature estimated by Birge ‖ from the CN bands.

By comparing lines which have been measured at both centre and limb we have an alternative method, which is independent of the theoretical i factors, of investigating the second anomaly, the equivalence of the centre and limb temperatures. Assuming again that we are on the linear part of the curve of growth, if we determine the ration W_L/W_c and plot the logarithm of this ratio against $J(J+1)$, we should obtain a straight line the slope of which gives $-1{\cdot}01\left(\frac{1}{T_L}-\frac{1}{T_c}\right)$. Fig. 5 shows the graph of $\log (W_L/W_c)$ against $J(J+1)$ for the eight coincident double lines in common to centre and limb, and a least squares solution gives the straight line shown

* Minnaert, *Observatory*, 57, 133, 1934.
† *Mem. Commonwealth Solar Obs.*, 5, 27, 1934, for *Ca*, λ 5000.
‡ *A.J.*, 87, 40, 1938.
§ *A.J.*, 87, 81, 1938.
‖ *A.J.*, 55, 273, 1922.

for which $m = +\cdot0304 \pm \cdot0691$ and $c = \cdot0911 \pm \cdot0946$.* The positive slope indicates that the limb temperature is if anything higher than the centre temperature, confirming the previous result.

These absolute intensity measurements therefore establish that the Swan band lines do show a thermal distribution of intensity; the temperature to which this distribution corresponds is, however, surprisingly low, and, moreover, within the errors of measurement, there is no difference between the centre and limb temperatures.

Summary

1. Wave-lengths and equivalent widths are obtained for all measurable unblended lines of R.I. 0, −1, −2 and −3 in the region λλ 5070–5160 A. of the solar spectrum at centre and limb; in Table I are listed all those attributed to carbon or otherwise unidentified.

2. By a comparison with the laboratory carbon spectrum, 37 Swan band lines are identified in the centre spectra and 33 in the limb.

3. The molecular lines are shown to have a thermal distribution of intensity.

4. From the intensity variation excitation temperatures of 4550° K at the centre and 4790° K at the limb are obtained. The comparatively high limb temperature is confirmed by an alternative method of calculation from the observed intensities.

I am deeply indebted to Professor H. H. Plaskett, not only for suggesting the investigation and providing the observational material, but also for his unfailing help throughout the course of the work.

University Observatory, Oxford:
1938 *May* 6.

* The strengthening of the molecular lines as a whole to the limb has already been considered (*M.N.*, 98, 135, 1937).

THE CONSTANTS OF THE STAR-STREAMS FROM THE PHOTOGRAPHIC PROPER MOTIONS OF 1775 STARS.

W. M. Smart and T. R. Tannahill, M.A., B.Sc.

1. In an earlier paper * by one of us, with a similar title (we shall refer to this paper as Paper I), an analysis was made of the photographic proper motions of 3029 stars. The earlier plates, on which the determination of proper motions was based, were mainly parallax plates, dating from the years 1900–1906, taken with the Sheepshanks (Coudé) equatorial of Cambridge Observatory; the plates required for the later epoch were photographed through the glass with the same instrument. The material of the present paper is derived from the measurement of similar Cambridge plates of 21 regions, and we have to express our indebtedness to Sir Arthur Eddington for the opportunity to discuss the measures. We are also indebted to Mr. H. E. Green, who was responsible for making most of the measures by the film-to-film method and for deriving relative proper motions.

2. As in Paper I, the conversion of relative proper motions into absolute proper motions in a single region was effected by means of the parallactic motions of the regional B.D. stars as derived from Kapteyn's values of the mean secular parallaxes of stars of known apparent magnitude; for this purpose the position of the solar apex was assumed to be: R.A. 270°, dec. +34°.

In Paper I it was concluded that the average probable error of the centennial proper motions, taken over the regions concerned, was $\pm 0''{\cdot}4$ in each co-ordinate. In a recent investigation † of the Cambridge proper motions of Paper I, Stenquist has inferred an unaccountable and rapid increase of the probable errors for stars beyond a certain distance (about 15/32 of the side of a plate) from the centre of each region, and in his subsequent discussion he has omitted such stars as are beyond this distance; the rejection of these stars accounts for about 13 per cent. of the whole. For the remaining stars he concludes that, numerically, the true average probable error is not likely to exceed $0''{\cdot}3$. In the present investigation we have rejected stars with images in the corners of the plates, roughly in accordance with Stenquist's procedure. With intervals rather longer on the average than those in Paper I, it may be expected that the average probable errors in the two investigations are pretty much alike.

3. Neighbouring groups have been combined together whenever practicable, and in this way ten groups were formed as shown in Table I. The

* W. M. Smart, *M.N.*, 87, 122, 1926.
† *Upsala Medd.*, No. 72, p. 63, 1937.

interval between the two epochs is given for each region in column 3, and the number of stars in column 4. The next two columns give the co-ordinates of the centre of the group obtained by weighting the co-ordinates of each constituent region according to the number of stars concerned. In one or two regions a few proper motions which were derived from fewer comparisons than usual have been accorded half-weight, and the seventh column

TABLE I

Group	Regions	Interval	No. of Stars	R.A.	Dec.	Reduced No. of Stars	Gal. Lat.	Weight
		y		h m	° ′		°	
I	β Cas	22·0	121	0 3·9	58 36	113	− 3	1
II	Eros 63	25·1	56					
	Eros 70	25·1	36	2 11·4	52 14	218	− 7	2
	Eros 85	25·0	126					
III	Lal 15565	25·0	78					
	Lal 17050	25·0	92	8 19·4	15 35	173	+29	2
	ϵ Hyd	23·0	33					
IV	11 Leo Min	25·0	40	9 29·7	36 16	40	+49	½
V	γ Ser	18·0	34					
	Lal 32390	21·7	40	17 17·8	23 30	152	+28	1
	μ Her	25·0	78					
VI	6 Cyg	21·6	132	19 9·5	49 39	131	+16	1
VII	17 Cyg	20·2	164	19 49·6	29 15	276	0	2
	Lal 38383	18·9	112					
VIII	61 Cyg	24·8	47	21 5·6	25 8	133	−16	1
	WB_2 97	20·9	87					
IX	ϵ Cep	20·8	194					
	η Cep	18·4	75	21 49·5	59 40	333	+ 4	3
	ξ Cep	24·8	96					
X	Lal 44541	18·8	80	23 10·1	28 38	134	−29	1
	85 Peg	18·8	54					

contains the reduced number of stars on which the subsequent analysis depends. The penultimate column shows the galactic latitude of the centre of each group, and the last column gives the weight accorded to each group in forming the normal equations of the later analysis.

4. Table II gives the smoothed distribution of proper motions in sectors $\theta - 5°$ to $\theta + 5°$, where θ is the position angle in the first column; this distribution has been obtained by taking the means of the counts in three consecutive 10° sectors. The resulting frequency-curves were analysed by Eddington's method into two constituent drift-curves.

We denote by hV_1 and hV_2 the projections on the tangent plane, for a given group of regions, of the drift-velocities relative to the Sun, θ_1 and θ_2 the position angles of the axes of the drift-curves, N_1 and N_2 the numbers of stars belonging to the drifts in each group. Then the polar equation

of a theoretical frequency-curve is, from Paper I,

where

$$\rho = r_1 + r_2,$$
$$r_1 = 0{\cdot}04923 N_1 \phi(hV_1,\ \theta - \theta_1),$$
$$r_2 = 0{\cdot}04923 N_2 \phi(hV_2,\ \theta - \theta_2),$$

in which ϕ is the function tabulated in Paper I, pp. 128, 129. The analysis of each group of regions gives the values of hV_1, hV_2; θ_1, θ_2; N_1, N_2, which are considered to fit best the observed frequency-curves.

TABLE II

Distribution of Proper Motions in Position Angle

Position Angle	I	II	III	IV	V	VI	VII	VIII	IX	X
°										
10	1·0	0·8	2·3	0·6	1·2	4·3	7·3	1·7	5·7	1·0
20	1·0	1·0	2·0	0·0	2·4	4·8	6·5	1·0	6·7	1·0
30	2·0	1·0	2·2	0·0	3·0	5·0	7·1	2·7	9·7	2·0
40	2·0	0·2	2·2	0·0	3·6	4·3	9·6	3·0	13·2	2·7
50	3·7	0·8	2·0	0·0	2·8	5·5	14·2	5·0	16·3	4·0
60	3·0	1·3	3·2	0·0	3·3	5·0	14·8	5·8	16·8	5·7
70	4·7	1·7	3·5	0·0	3·4	4·3	13·2	6·5	18·2	8·0
80	4·0	2·2	3·5	0·4	4·0	3·0	11·1	7·7	17·0	11·0
90	5·3	6·7	4·0	1·2	3·3	1·7	10·0	8·2	17·0	9·3
100	7·5	13·5	5·0	1·4	2·8	1·5	10·2	8·7	15·2	8·8
110	9·5	24·2	6·0	1·2	2·2	1·2	11·2	8·0	15·8	7·5
120	9·7	27·5	7·1	0·6	1·8	1·8	10·9	6·7	13·8	10·3
130	8·2	27·5	7·5	0·4	2·2	3·2	10·4	5·2	13·5	8·2
140	5·8	20·0	8·3	0·6	2·3	3·7	8·9	2·7	9·7	6·8
150	6·7	15·3	6·3	1·0	2·6	5·5	8·0	2·0	10·0	4·0
160	4·3	12·3	7·7	2·4	5·1	5·0	9·4	3·0	8·8	4·0
170	4·7	9·5	7·7	2·7	7·7	6·7	13·2	6·0	12·0	2·7
180	2·7	10·0	10·5	2·2	9·5	5·3	14·7	6·3	12·8	3·0
190	3·0	7·3	9·7	1·6	8·6	7·0	12·5	6·0	12·5	2·7
200	2·5	8·0	9·3	1·0	7·4	6·7	8·4	3·7	12·0	2·2
210	3·3	4·8	7·3	1·4	5·5	6·0	7·3	2·8	10·7	2·8
220	3·3	4·7	5·7	2·4	4·5	4·0	7·9	2·7	9·5	3·3
230	3·2	3·0	5·2	2·5	5·8	3·0	5·6	3·3	6·5	3·8
240	2·3	3·0	4·8	3·5	6·4	3·3	3·6	3·8	4·5	2·5
250	1·3	2·3	4·7	2·9	5·8	2·7	1·7	3·0	4·5	2·0
260	1·3	3·0	4·5	3·7	3·4	2·3	1·9	2·3	5·0	2·0
270	1·3	2·3	6·0	2·4	3·8	2·0	1·3	2·3	4·7	2·0
280	1·5	1·7	5·5	1·2	4·2	2·0	0·6	2·8	3·3	2·3
290	1·3	0·3	4·8	0·0	5·0	2·3	1·7	3·3	3·2	2·0
300	0·7	0·3	2·5	0·4	4·3	1·7	3·4	2·3	2·3	1·7
310	0·5	0·7	2·8	0·4	4·6	2·3	5·0	1·2	2·8	1·0
320	0·0	0·7	2·3	0·4	4·3	2·0	5·0	0·0	1·7	0·7
330	0·3	0·7	1·8	0·0	3·8	4·0	4·1	0·3	3·5	0·3
340	0·3	0·3	1·2	0·0	4·5	3·0	4·0	0·7	3·8	0·7
350	0·7	0·0	2·0	0·6	3·4	2·5	4·4	1·3	5·2	1·0
360	0·3	0·0	2·0	0·6	3·2	2·3	6·7	1·0	5·2	1·0

Table III contains the results.

TABLE III

Analysis of the Drift-curves

Group	hV_1	θ_1	N_1	hV_2	θ_2	N_2
		°			°	
I	1·2	115	75	0·7	210	38
II	1·7	125	160	1·1	190	58
III	0·8	240	57	0·6	150	116
IV	1·5	250	20	1·0	170	20
V	0·4	310	81	1·0	180	71
VI	1·1	35	46	0·7	185	85
VII	0·9	60	150	1·0	180	126
VIII	1·2	95	60	0·5	200	73
IX	0·95	70	173	0·7	185	160
X	1·2	100	87	0·5	210	47

TABLE IV

Residuals (Theoretical Frequency-curve—Observed Frequency-curve)

Position Angle	I	II	III	IV	V	VI	VII	VIII	IX	X
°										
10	−0·6	−0·5	−0·8	−0·6	+1·8	0·0	−0·7	−0·5	+0·3	+0·1
20	−0·4	−0·7	−0·5	+0·1	+0·3	+0·3	+1·9	+0·4	+1·2	+0·4
30	−1·2	−0·7	−0·5	+0·1	−0·6	+0·5	+3·4	−0·9	+0·6	−0·2
40	−0·9	+0·2	−0·3	+0·1	−1·5	+1·3	+2·8	−0·5	−0·4	−0·2
50	−2·1	−0·1	+0·2	+0·1	−0·8	−0·2	−0·4	−1·6	−0·9	−0·4
60	−0·7	+0·1	−0·7	+0·1	−1·5	−0·4	−0·4	−1·2	+0·4	−0·7
70	−1·2	+0·9	−0·5	+0·1	−1·6	−0·6	+0·9	−0·6	0·0	−1·0
80	+0·9	+2·7	+0·1	−0·2	−2·2	+0·1	+1·9	−0·3	+0·8	−2·1
90	+1·4	+2·3	+0·3	−1·0	−1·4	+1·0	+1·5	0·0	−0·5	+1·3
100	+0·7	+1·6	+0·1	−1·1	−0·7	+1·1	−0·2	−0·3	−0·4	+2·3
110	−0·3	−2·3	−0·1	−0·7	+0·2	+1·5	−2·2	−0·1	−2·7	+3·1
120	−0·3	−0·8	−0·3	+0·1	+1·2	+1·2	−2·5	+0·1	−2·0	−1·0
130	+0·4	−0·3	+0·1	+0·5	+1·6	+0·3	−1·9	+0·7	−2·4	−0·6
140	+1·5	+3·4	−0·1	+0·6	+2·5	+0·4	+0·3	+2·5	+1·4	−0·9
150	−0·8	+2·3	+2·1	+0·4	+3·3	−0·6	+2·2	+2·6	+1·5	+0·7
160	+0·5	+0·5	+0·9	−0·7	+2·0	+0·5	+1·8	+1·4	+3·4	−0·1
170	−0·7	+0·4	+0·8	−0·9	+0·3	−0·6	−1·1	−1·6	+0·8	+0·7
180	+1·0	−1·5	−2·3	−0·5	−1·2	+1·1	−2·4	−1·8	+0·1	+0·3
190	+0·5	+0·2	−1·8	+0·1	−0·4	−0·6	−0·8	−1·5	+0·2	+0·5
200	+0·8	−1·3	−1·5	+0·7	+0·1	−0·6	+2·1	+0·8	+0·1	+0·9
210	−0·1	+0·8	+0·3	+0·3	+1·1	−0·5	+1·6	+1·6	+0·2	+0·2
220	−0·3	−0·4	+1·8	−0·5	+1·2	+0·8	−0·8	+1·4	−0·1	−0·4
230	−0·4	+0·2	+2·1	−0·2	−0·8	+1·0	0·0	+0·5	+1·4	−1·0
240	+0·2	−0·6	+2·1	−0·9	−1·9	0·0	+0·7	−0·4	+2·0	+0·1
250	+0·7	−0·7	+1·8	−0·2	−1·6	−0·1	+1·6	0·0	+0·8	+0·2
260	+0·4	−1·9	+1·3	−1·2	+0·7	−0·2	+0·7	+0·3	−0·7	0·0
270	+0·1	−1·5	−1·0	−0·5	+0·3	−0·3	+0·8	0·0	−1·1	−0·3
280	−0·4	−1·1	−1·3	+0·1	+0·2	−0·5	+1·3	−0·9	−0·3	−0·8
290	−0·2	+0·1	−1·3	+0·9	−0·6	−1·1	0·0	−1·6	−0·5	−0·7
300	+0·1	0·0	+0·3	+0·2	+0·1	−0·5	−1·8	−0·8	+0·2	−0·6
310	+0·1	−0·4	−0·5	0·0	−0·1	−1·0	−3·3	+0·1	−0·5	0·0
320	+0·5	−0·5	−0·3	−0·2	0·0	−0·6	−3·1	+1·1	+0·7	+0·3
330	+0·2	−0·5	−0·1	+0·1	+0·4	−2·4	−1·7	+0·7	−0·9	+0·6
340	+0·2	−0·1	+0·4	+0·1	−0·5	−1·1	−1·1	+0·4	−0·8	+0·1
350	−0·2	+0·2	−0·6	−0·6	+0·2	+0·1	−0·6	−0·3	−1·6	−0·1
360	+0·1	+0·2	−0·6	−0·6	+0·1	+1·0	−1·7	+0·1	−0·6	−0·1

Table IV exhibits the residuals representing the difference between the theoretical distribution derived from the data of Table III and the observed frequency distribution as given by Table II. On the whole the agreement between the theoretical and the observed distributions may be regarded as satisfactory, especially when the comparatively small number of stars per group of regions is remembered; in Paper I the average number of stars per group of regions was almost 380, whereas in the present investigation the average number is only 170. Group IX, with a total of 333 stars, gives a fit between theory and observation comparable in accuracy with the groups in Paper I (diagrams, pp. 130–132), and this is by far the most satisfactory group of the present paper. We can apply a rough criterion to the groups as follows. Taking the sums, S, of the residuals (without regard to sign) in Table IV we find the mean residual, ρ, for the 36 sectors, arbitrarily reducing the number of stars per region to 100. The results are in Table V. As might have been expected Group IV, with its exceptionally

Table V

Mean Residual per Sector per 100 Stars

Group	I	II	III	IV	V	VI	VII	VIII	IX	X
S	21·2	32·0	29·8	15·3	35·0	24·1	52·2	29·6	32·5	23·0
ρ	0·52	0·41	0·48	1·06	0·64	0·51	0·53	0·62	0·27	0·48

small number (40) of stars, is distinctly the least satisfactory from the point of view here considered.

5. *The Drift-constants.*—We now determine the drift-constants, using the results in Table III. Let X, Y, Z denote the linear components of the space-velocity of a drift relative to the Sun and with reference to the usual equatorial system of co-ordinates. Then for each group and for each drift we have the following equations of conditions :—

$$X \sin \alpha - Y \cos \alpha = -hV \sin \theta,$$
$$X \cos \alpha \sin \delta + Y \sin \alpha \sin \delta - Z \cos \delta = -hV \cos \theta.$$

On the right-hand sides of these equations, hV and θ are respectively the projected drift-velocity and the position angle of the drift-axis, as given in Table III. Least-square solutions * are, in terms of the theoretical unit $1/h$, as follows :—

	Drift I	Drift II
X	$+0.090 \pm 0.044$	$+0.100 \pm 0.054$
Y	$+1.306 \pm 0.045$	-0.213 ± 0.055
Z	-0.289 ± 0.051	-0.877 ± 0.062

The right ascension, A, and the declination, D, of the drift-apices are found from

$$\tan A = Y/X; \qquad \tan D = Z/(X^2 + Y^2)^{\frac{1}{2}}$$

and the drift-velocities, hW, from

$$(hW)^2 = X^2 + Y^2 + Z^2.$$

* The subsequent calculations were carried out using an additional place of decimals.

The results are :

	Drift I	Drift II
R.A. of apex	86°·0 ± 2°·5	295°·2 ± 11°·4
Dec. of apex	−12°·5 ± 2°·6	−74°·8 ± 4°·1
hW	1·337 ± 0·046	0·908 ± 0·062

The corresponding results from Paper I are as follows :—

	Drift I	Drift II
R.A. of apex	88°·4 ± 1°·5	289°·0 ± 7°·0
Dec. of apex	−11°·8 ± 1°·4	−73°·3 ± 1°·9
hW	1·497 ± 0·025	0·975 ± 0·037

Having derived the positions of the apices we can now calculate for any region the position angle of the axis of symmetry of each drift. These calculated values are given in columns 2 and 6 of Table VI and compared

TABLE VI

The Calculated and Observed Values of the Position Angles of the Drifts

Group	Drift I				Drift II			
	Cal.	Obs.	Cal. −Obs.	β_1	Cal.	Obs.	Cal. −Obs.	β_2
	°	°	°	°	°	°	°	°
I	101	115	−14	14	202	210	− 8	5
II	127	125	+ 2	2	205	190	+15	9
III	236	240	− 4	3	177	150	+27	23
IV	239	250	−11	10	169	170	− 1	1
V	330	310	+20	4	171	180	− 9	9
VI	33	35	− 2	1	178	185	− 7	6
VII	67	60	+ 7	4	182	180	+ 2	2
VIII	85	95	−10	7	186	200	−14	14
IX	71	70	+ 1	1	192	185	+ 7	5
X	97	100	− 3	3	193	210	−17	16

with the observed position angles (reproduced from Table III). In addition we have given, in columns 5 and 9, the angular distances, β, of the apices from the great circles defined by the observed values of the position angles ; the appropriate formula is

$$\sin \beta = \sin \lambda \sin (\theta_c - \theta_0),$$

where λ is the angular distance of a group from the apex, θ_c and θ_0 are the calculated and observed values of the position angles of the drift-axes. Except for an occasional group it is sufficient to use a modified form of the above formula, viz. :

$$\beta = (\theta_c - \theta_0) \sin \lambda.$$

In a similar way we can compare the observed values of the projected drift-velocities, hV, as given in Table III, with the values calculated from the positions of the apices and the values of the space-velocities, hW, of the drifts. We have, for any group and for each drift,

$$hV(\text{calculated}) = hW \sin \lambda.$$

The results of the comparison are shown in Table VII. There are several large discrepancies, not wholly unexpected, however, in view of the relative numerical poverty of the observational material.

TABLE VII

The Calculated and Observed Values of the Projected Drift-velocities

Group	Drift I			Drift II		
	λ_1	hV_1		λ_2	hV_2	
		Cal.	Obs.		Cal.	Obs.
	°			°		
I	98·1	1·32	1·2	140·2	0·58	0·7
II	79·2	1·32	1·7	141·7	0·57	1·1
III	47·6	0·99	0·8	120·5	0·78	0·6
IV	72·2	1·27	1·5	139·2	0·59	1·0
V	167·4	0·29	0·4	101·0	0·89	1·0
VI	138·9	0·88	1·1	124·6	0·75	0·7
VII	146·5	0·74	0·9	104·1	0·88	1·0
VIII	131·0	1·01	1·2	100·9	0·89	0·5
IX	115·0	1·29	0·95	136·2	0·63	0·7
X	103·3	1·30	1·2	108·8	0·86	0·5

6. *The Vertex of Star-streaming.*—Denoting by (ξ, η, ζ) the linear components of the space-velocity of Drift I relative to Drift II we have, from the numerical results in the previous section,

$$\xi \equiv X_1 - X_2 = -0{\cdot}010 \pm 0{\cdot}070$$
$$\eta \equiv Y_1 - Y_2 = +1{\cdot}519 \pm 0{\cdot}071$$
$$\zeta \equiv Z_1 - Z_2 = +0{\cdot}587 \pm 0{\cdot}080.$$

From these values we derive :

$$\text{R.A. of vertex} = 90^\circ{\cdot}4 \pm 4^\circ{\cdot}0$$
$$\text{Dec. ,,} = +21^\circ{\cdot}1 \pm 2^\circ{\cdot}8.$$

In galactic co-ordinates this position is :

$$\text{Long. of vertex} = 157^\circ \quad \text{or} \quad 337^\circ$$
$$\text{Lat. ,,} = +1^\circ{\cdot}4 \quad \text{or} \quad -1^\circ{\cdot}4.$$

The vertex thus lies close to the galactic equator and about 10° from the direction generally assigned to the galactic centre.

The space-velocity of one stream relative to the other is 1·63 in terms of the theoretical unit, $1/h$.

The results of Paper I, given for comparison, are :

$$\text{Long. of vertex} = 158^\circ{\cdot}5$$
$$\text{Lat. ,,} = +2^\circ{\cdot}4$$
$$\text{Relative speed} = 1{\cdot}84.$$

7. *The Solar Apex.*—According to the analysis, 909 stars belong to Drift I and 794 to Drift II. The solar motion with respect to the effective total of stars is found to be directed towards the position :

R.A. (of solar apex) = 261°·1
Dec. (,, ,,) = +42°·5.

The solar speed, in terms of the theoretical unit, is 0·821. It is to be remarked that this position of the solar apex is not quite an independent determination, since the calculation of the correction from relative to absolute proper motions by way of the parallactic motions of the regional B.D. stars involved an assumption as to the position of the solar apex.

The results of Paper I are :

R.A. of solar apex = 273°·2
Dec. ,, ,, = +43°·6
Solar speed = 0·881.

8. *Summary.*—The photographic proper motions of 1775 stars determined from Cambridge plates have been analysed according to the two-streams theory by Eddington's method. The drift-constants have been derived and the principal results are :

Position of vertex, in galactic co-ordinates : (337°, −1°·4).
Position of solar apex, in equatorial co-ordinates : (261°·1, +42°·5).

University Observatory,
Glasgow, W. 2 :
1938 *May 2.*

NOTE ON THE MINIMUM INTEGRAL IN THE THEORY OF INTERNAL CONSTITUTION OF STARS.

W. Gleissberg.

(Communicated by Professor E. A. Milne)

In a previous paper * I have proved a theorem which states that any configuration satisfying the equations of mechanical and radiative equilibrium—and no other configuration—gives a minimum value to the integral

$$I=\int_0^{M_1}[Q_1^2+Q_2^2-(a_1p_g+a_2p_r)]dM(r) \qquad (1)$$

in comparison with all neighbouring configurations having the same radius, the same central and boundary values of p_g and p_r, and the same functions $M(r)$ and $k\bar{\epsilon}$ as the equilibrium configuration. Here, p_g is the gas pressure, p_r the radiation pressure, $M(r)$ the mass enclosed in a sphere of radius r around the centre of the configuration, M_1 the total mass, while Q_1, Q_2, a_1, a_2 are defined by

$$\left.\begin{aligned} Q_1&=\frac{r^2}{\sqrt{c}}\left(\frac{dp_g}{dM(r)}+\frac{dp_r}{dM(r)}\right), \qquad Q_2=\frac{\sqrt{G}r^2}{\sqrt{k\bar{\epsilon}}}\cdot\frac{dp_r}{dM(r)},\\ a_1&=\frac{G}{2\pi c}, \qquad a_2=\frac{G}{\pi c}, \end{aligned}\right\} \qquad (2)$$

where k denotes the absorption coefficient, $4\pi\bar{\epsilon}$ the mean amount of energy produced within the mass $M(r)$ in one second by unit mass, G the constant of gravitation and c the velocity of light.†

Although it is known from the above theorem that the value of the integral I at any equilibrium configuration is a minimum, the theorem states nothing about the amount of this minimum value itself. But if we assume that the mean value $\bar{\rho}$ of density ρ, inside r, decreases outward and that the product $k\bar{\epsilon}\bar{\rho}$ also decreases outward—this assumption making allowance for a certain increase of $k\bar{\epsilon}$—an upper and a lower limit of the value of the "minimum integral" I at any equilibrium configuration can be found. If we set

$$P=p_g+p_r, \qquad (3)$$

---

* *M.N.*, 98, 164, 1937.

† The above definitions of Q_1, Q_2, a_1, a_2 are somewhat different from those used in my previous paper; but, with the new definitions, the theorem stating that the value of the integral I is a minimum under the mentioned conditions can be proved in entirely the same manner as with the former definitions. I have altered these definitions so that the integral I contains no more terms of different physical dimensions. I am indebted to Dr. H. Jeffreys and Professor E. A. Milne for calling my attention to the necessity of such an alteration.

these limits are given by the following theorem which I shall prove in this paper:—

Theorem.—If I_e denotes the value of the minimum integral I at any equilibrium configuration in which the functions $\bar{\rho}$ and $k\bar{\epsilon}\bar{\rho}$ both decrease outward, then

$$\frac{G}{5c}\left(\frac{4}{3\pi^2}\right)^{\frac{1}{3}}\bar{\rho}_1^{\frac{4}{3}}M_1^{\frac{5}{3}}\left[G+\frac{(k\bar{\epsilon})_1}{c}\right]-\frac{GM_1}{2\pi c}[P_c+(p_r)_c] < I_e$$
$$< \frac{G}{5c}\left(\frac{4}{3\pi^2}\right)^{\frac{1}{3}}\rho_c^{\frac{4}{3}}M_1^{\frac{5}{3}}\left[G+\frac{(k\bar{\epsilon})_c}{c}\right]-\frac{GM_1}{2\pi c}[P_c+(p_r)_c], \quad (4)$$

where the values marked with the indices c and 1 relate to the centre and to the boundary respectively.

To prove this theorem I make use of the following:—

Auxiliary Theorem.—In any equilibrium configuration in which $\bar{\rho}$ and $k\bar{\epsilon}\bar{\rho}$ each decrease outward, the function

$$f=p_r+\frac{1}{2c}(\tfrac{4}{3}\pi)^{\frac{1}{3}}\bar{\rho}^{\frac{4}{3}}M^{\frac{2}{3}}(r)k\bar{\epsilon}$$

decreases outward and the function

$$f'=p_r+\frac{1}{2c}(\tfrac{4}{3}\pi)^{\frac{1}{3}}\rho_c^{\frac{4}{3}}M^{\frac{2}{3}}(r)(k\bar{\epsilon})_c$$

increases outward.

Proof of the Auxiliary Theorem.—Using the equation of radiative equilibrium

$$\frac{dp_r}{dr}=-\frac{\rho M(r)k\bar{\epsilon}}{cr^2},$$

we have

$$\frac{df}{dr}=-\frac{\rho M(r)k\bar{\epsilon}}{cr^2}+\frac{1}{2c}(\tfrac{4}{3}\pi)^{\frac{1}{3}}\left[\tfrac{4}{3}\bar{\rho}^{\frac{1}{3}}M^{\frac{2}{3}}(r)k\bar{\epsilon}\frac{d\bar{\rho}}{dr}+\tfrac{2}{3}\bar{\rho}^{\frac{4}{3}}M^{-\frac{1}{3}}(r)k\bar{\epsilon}\frac{dM(r)}{dr}+\bar{\rho}^{\frac{4}{3}}M^{\frac{2}{3}}(r)\frac{d(k\bar{\epsilon})}{dr}\right],$$

or

$$\frac{df}{dr}=-\frac{\rho M(r)k\bar{\epsilon}}{cr^2}+\frac{1}{2c}(\tfrac{4}{3}\pi)^{\frac{1}{3}}\left[\tfrac{1}{3}\bar{\rho}^{\frac{1}{3}}M^{\frac{2}{3}}(r)k\bar{\epsilon}\frac{d\bar{\rho}}{dr}+\bar{\rho}^{\frac{1}{3}}M^{\frac{2}{3}}(r)\frac{d(k\bar{\epsilon}\bar{\rho})}{dr}+\tfrac{2}{3}\bar{\rho}^{\frac{4}{3}}M^{-\frac{1}{3}}(r)k\bar{\epsilon}\frac{dM(r)}{dr}\right].$$

According to the assumption that $\bar{\rho}$ and $k\bar{\epsilon}\bar{\rho}$ decrease outward, the first two terms within the brackets are negative; hence, the omission of these two terms will augment the right member of the above equation. Now, using

$$\frac{dM(r)}{dr}=4\pi r^2\rho, \quad (5)$$

we get

$$\frac{df}{dr} < -\frac{\rho M(r)k\bar{\epsilon}}{cr^2}+\frac{1}{c}(\tfrac{4}{3}\pi)^{\frac{1}{3}}\bar{\rho}^{\frac{1}{3}}M^{-\frac{1}{3}}(r)k\bar{\epsilon}r^2\rho.$$

But by definition

$$M(r)=\tfrac{4}{3}\pi r^3\bar{\rho}. \quad (6)$$

Introducing this into the above inequality, we get $\frac{df}{dr} < 0$, which proves the first part of the auxiliary theorem.

On the other hand, we have

$$\frac{df'}{dr} = -\frac{\rho M(r) k\bar{\epsilon}}{cr^2} + \frac{1}{3c}(\tfrac{4}{3}\pi)^{\frac{1}{3}}\rho_c^{\frac{4}{3}}(k\bar{\epsilon})_c M^{-\frac{1}{3}}(r)\frac{dM(r)}{dr}.$$

Using (5) and (6), we obtain

$$\frac{df'}{dr} = \frac{4\pi}{3c}\rho r[(k\bar{\epsilon})_c \rho_c^{\frac{4}{3}}\bar{\rho}^{-\frac{1}{3}} - k\bar{\epsilon}\bar{\rho}].$$

Since $\bar{\rho}$ and $k\bar{\epsilon}\bar{\rho}$ are assumed to be decreasing functions of r, we have

$$\bar{\rho} < \rho_c, \qquad k\bar{\epsilon}\bar{\rho} < (k\bar{\epsilon})_c\rho_c. \tag{7}$$

Hence, by substituting ρ_c for $\bar{\rho}$ and $(k\bar{\epsilon})_c\rho_c$ for $k\bar{\epsilon}\bar{\rho}$, the right member of the above equation will be diminished; and thus $\frac{df'}{dr} > 0$, which proves the second part of the auxiliary theorem.

From this theorem we deduce the inequalities

$$f \leqq f_c, \qquad f_c' \leqq f', \tag{8}$$

where again the index c denotes the central value. Since $M_c(r) = 0$, we have, from the definitions of the functions f and f',

$$f_c = f_c' = (p_r)_c.$$

Thus, the inequalities (8) reduce to

$$\frac{1}{2c}(\tfrac{4}{3}\pi)^{\frac{1}{3}}\bar{\rho}^{\frac{4}{3}}M^{\frac{2}{3}}(r)k\bar{\epsilon} \leqq (p_r)_c - p_r \leqq \frac{1}{2c}(\tfrac{4}{3}\pi)^{\frac{1}{3}}\rho_c^{\frac{4}{3}}M^{\frac{2}{3}}(r)(k\bar{\epsilon})_c, \tag{9}$$

which is similar to the following inequality proved by Chandrasekhar * only on the assumption that $\bar{\rho}$ decreases outward:

$$\frac{G}{2}(\tfrac{4}{3}\pi)^{\frac{1}{3}}\bar{\rho}^{\frac{4}{3}}M^{\frac{2}{3}}(r) \leqq P_c - P \leqq \frac{G}{2}(\tfrac{4}{3}\pi)^{\frac{1}{3}}\rho_c^{\frac{4}{3}}M^{\frac{2}{3}}(r). \tag{10}$$

Now we can pass on to the

Proof of the Theorem.—By introducing $dr = \frac{dM(r)}{4\pi r^2\rho}$ into the conditions of mechanical and radiative equilibrium,

$$\frac{dp_g}{dr} + \frac{dp_r}{dr} = -\frac{GM(r)\rho}{r^2},$$

$$\frac{dp_r}{dr} = -\frac{M(r)\rho k\bar{\epsilon}}{cr^2},$$

---

* *M.N.*, 96, 644, 1936. The first part of this inequality has been proved earlier by Milne, *M.N.*, 96, 179, 1936.

we obtain the following equations :—

$$\frac{dp_g}{dM(r)}+\frac{dp_r}{dM(r)}=-\frac{G}{4\pi}\frac{M(r)}{r^4},$$

$$\frac{dp_r}{dM(r)}=-\frac{1}{4\pi c}\frac{M(r)k\bar{\epsilon}}{r^4}.$$

Introducing these into (2) we have for any equilibrium configuration :

$$Q_1=-\frac{G}{4\pi\sqrt{c}}\frac{M(r)}{r^2},\qquad Q_2=-\frac{\sqrt{G}}{4\pi c}\frac{M(r)\sqrt{k\bar{\epsilon}}}{r^2};$$

using (2) and (3) we get

$$a_1p_g+a_2p_r=\frac{G}{2\pi c}(P+p_r).$$

Therefore it follows from (1) that the value I_e of the minimum integral I at any equilibrium configuration is given by

$$I_e=\frac{G}{2\pi c}\int_0^{M_1}\left(\frac{G}{8\pi}\cdot\frac{M^2(r)}{r^4}-P+\frac{1}{8\pi c}\cdot\frac{M^2(r)k\bar{\epsilon}}{r^4}-p_r\right)dM(r). \tag{11}$$

From Chandrasekhar's inequality (10) we have

$$\frac{G}{2}(\tfrac{4}{3}\pi)^{\frac{1}{3}}\bar{\rho}^{\frac{4}{3}}M^{\frac{2}{3}}(r)-P_c\leqq -P\leqq\frac{G}{2}(\tfrac{4}{3}\pi)^{\frac{1}{3}}\rho_c^{\frac{4}{3}}M^{\frac{2}{3}}(r)-P_c,$$

and

$$\frac{G}{2}(\tfrac{4}{3}\pi)^{\frac{1}{3}}\bar{\rho}^{\frac{4}{3}}M^{\frac{2}{3}}(r)-P_c+\frac{G}{8\pi}\cdot\frac{M^2(r)}{r^4}\leq\frac{G}{8\pi}\cdot\frac{M^2(r)}{r^4}-P$$

$$\leqq\frac{G}{2}(\tfrac{4}{3}\pi)^{\frac{1}{3}}\rho_c^{\frac{4}{3}}M^{\frac{2}{3}}(r)-P_c+\frac{G}{8\pi}\cdot\frac{M^2(r)}{r^4}.$$

Since

$$r=(\tfrac{4}{3}\pi)^{-\frac{1}{3}}\bar{\rho}^{-\frac{1}{3}}M^{\frac{1}{3}}(r), \tag{12}$$

the above inequality becomes

$$\frac{2G}{3}(\tfrac{4}{3}\pi)^{\frac{1}{3}}\bar{\rho}^{\frac{4}{3}}M^{\frac{2}{3}}(r)-P_c\leqq\frac{G}{8\pi}\cdot\frac{M^2(r)}{r^4}-P\leq\frac{G}{2}(\tfrac{4}{3}\pi)^{\frac{1}{3}}M^{\frac{2}{3}}(r)[\rho_c^{\frac{4}{3}}+\tfrac{1}{3}\bar{\rho}^{\frac{4}{3}}]-P_c.$$

Since $\bar{\rho}$ is assumed to decrease outward, we have the inequality

$$\bar{\rho}_1<\bar{\rho}, \tag{13}$$

where again $\bar{\rho}_1$ denotes the boundary value of $\bar{\rho}$, *i.e.* the mean density of the whole configuration. Therefore, if we substitute ρ_c for $\bar{\rho}$ in the right member of the above inequality, that member will be augmented, and if we substitute $\bar{\rho}_1$ for $\bar{\rho}$ in the left member, that member will be diminished. The inequality will then read :

$$\frac{2G}{3}(\tfrac{4}{3}\pi)^{\frac{1}{3}}\bar{\rho}_1^{\frac{4}{3}}M^{\frac{2}{3}}(r)-P_c<\frac{G}{8\pi}\cdot\frac{M^2(r)}{r^4}-P<\frac{2G}{3}(\tfrac{4}{3}\pi)^{\frac{1}{3}}\rho_c^{\frac{4}{3}}M^{\frac{2}{3}}(r)-P_c. \tag{14}$$

On the other hand, the inequality (9) yields

$$\frac{1}{2c}(\tfrac{4}{3}\pi)^{\frac{1}{3}}\bar{\rho}^{\frac{4}{3}}M^{\frac{2}{3}}(r)k\bar{\epsilon}-(p_r)_c+\frac{1}{8\pi c}\cdot\frac{M^2(r)k\bar{\epsilon}}{r^4}\leqq\frac{1}{8\pi c}\cdot\frac{M^2(r)k\bar{\epsilon}}{r^4}-p_r$$

$$\leqq\frac{1}{2c}(\tfrac{4}{3}\pi)^{\frac{1}{3}}\rho_c^{\frac{4}{3}}M^{\frac{2}{3}}(r)(k\bar{\epsilon})_c-(p_r)_c+\frac{1}{8\pi c}\cdot\frac{M^2(r)k\bar{\epsilon}}{r^4}.$$

Using (12) we get

$$\frac{2}{3c}(\tfrac{4}{3}\pi)^{\frac{1}{3}}\bar{\rho}^{\frac{1}{3}}M^{\frac{2}{3}}(r)\bar{\rho}k\bar{\epsilon}-(p_r)_c\leqq\frac{1}{8\pi c}\cdot\frac{M^2(r)k\bar{\epsilon}}{r^4}-p_r$$

$$\leqq\frac{1}{2c}(\tfrac{4}{3}\pi)^{\frac{1}{3}}M^{\frac{2}{3}}(r)[\rho_c^{\frac{4}{3}}(k\bar{\epsilon})_c+\tfrac{1}{3}\bar{\rho}^{\frac{1}{3}}\bar{\rho}k\bar{\epsilon}]-(p_r)_c. \quad (15)$$

Since we have assumed that $k\bar{\epsilon}\bar{\rho}$ decreases outward, we have

$$\bar{\rho}_1(k\bar{\epsilon})_1<\bar{\rho}k\bar{\epsilon}, \quad (16)$$

where again the index 1 denotes the value at the boundary of the configuration. According to the inequalities (7), (13) and (16), we diminish the left-hand side of (15) if we substitute in it $\bar{\rho}_1$ for $\bar{\rho}$ and $\bar{\rho}_1(k\bar{\epsilon})_1$ for $\bar{\rho}k\bar{\epsilon}$, and we augment the right-hand side of (15) if we substitute in it ρ_c for $\bar{\rho}$ and $\rho_c(k\bar{\epsilon})_c$ for $\bar{\rho}k\bar{\epsilon}$. These substitutions being made, we get

$$\frac{2}{3c}(\tfrac{4}{3}\pi)^{\frac{1}{3}}\bar{\rho}_1^{\frac{4}{3}}M^{\frac{2}{3}}(r)(k\bar{\epsilon})_1-(p_r)_c<\frac{1}{8\pi c}\cdot\frac{M^2(r)k\bar{\epsilon}}{r^4}-p_r$$

$$<\frac{2}{3c}(\tfrac{4}{3}\pi)^{\frac{1}{3}}\rho_c^{\frac{4}{3}}M^{\frac{2}{3}}(r)(k\bar{\epsilon})_c-(p_r)_c. \quad (17)$$

Adding (17) to (14) and integrating over $M(r)$ from 0 to M_1 and by using (11) we obtain the inequality (4). Hence the theorem has been proved.

Summary.—After having proved, in a previous paper, that at any equilibrium configuration—and at no other configuration—the value of the integral I as given by (1) is a minimum in comparison with certain neighbouring configurations, I have proved in the present paper that, if the mean density $\bar{\rho}$ and the product of $\bar{\rho}$ by the absorption coefficient k and by the mean rate $\bar{\epsilon}$ of generation of energy both decrease outward, this minimum value I_e satisfies the inequality (4).

University Observatory,
Istanbul (Turkey) :
1938 *March.*

ON THE EXISTENCE OF STELLAR SYSTEMS IN A QUASI-STEADY STATE OF MOTION.

Bertil Lindblad.

1. We consider a typical stellar system composed of a great number of free particles of widely different individual masses attracting each other according to Newton's law. We introduce cylindrical co-ordinates R, θ, z with the centre of gravity as origin and the invariable plane as the plane $z=0$. The linear velocities in the R, θ, z directions are denoted by Π, Θ, Z. We then introduce as new variables the quantities I_1, I_2, Z_0, defined as follows:—

$$I_1=\Pi^2+\Theta^2+Z^2-2V, \qquad I_2=R\Theta, \qquad Z_0^2=Z^2-2[V(R,z)-V(R,0)]. \quad (1)$$

The intersection of the surfaces

$$I_1=\text{const.}, \qquad I_2=\text{const.}, \qquad Z_0^2=\text{const.} \quad (2)$$

is a three-dimensional surface to which the instantaneous motion of the particles will adhere more or less closely. In a previous paper * the author has demonstrated how the general process of mixing of matter along the instantaneous three-dimensional surfaces (2) may produce a quasi-steady state of motion in which the frequency to be expected *a priori* in a phase-element $RdRd\theta dzd\Pi d\Theta dZ$ for the stars of mass m may be written

$$f_m(I_1, I_2, Z_0^2). \quad (3)$$

In a state preceding the quasi-steady state the quantity $f_m(I_1, I_2, Z_0^2)$ may be defined as the average frequency per unit phase-volume along the surface (2). Integrating (3) with respect to Π, Θ, Z, with due attention to the velocity limit expressed by the condition $I_1 \leqslant 0$, and multiplying by m, we find the space-density ρ_m. Adding together, we get the total density

$$\rho_* = \Sigma\rho_m.$$

By Poisson's equation we then find the corresponding potential V_*. The quasi-steady state is defined as a state of motion in which V_* converges towards the actual potential V of the system. The aim of the present work is to give a more formal proof of the existence of the steady state (3). We do not consider here, however, to what extent the actual systems in nature—for instance, our own stellar system—have actually approached to such a state. This question has been discussed at length in the paper cited, as well as in a later one † in which the local conditions around the Sun have been more closely analysed.

* *Stockholms Observatoriums Annaler*, **12**, No. 4, p. 7, 1936.

† *M.N.*, **97**, 15, 1936.

2. We consider first the case when Z_0^2 does not enter into the function (3), so that the frequency function for particles of mass m may be written

$$f_m(I_1, I_2). \tag{4}$$

This is a special case of a theorem first given by Poincaré,* and is the form proposed by Jeans.† In an ellipsoidal distribution on this model the axes of the velocity ellipsoid along the R and z directions are equal. In Eddington's ‡ general analysis of the existence of steady ellipsoidal stellar systems we have therefore $a=b$, so that the special condition for the potential function (p. 46) vanishes. In fact, G. L. Clark § has shown that the equations of Eddington's special condition express the condition for the existence of those integrals of the motion which enter into the frequency function. In the present case I_1 is an integral as soon as V is stationary, and I_2 is an integral if V has rotational symmetry. The only condition remaining is therefore Poisson's equation,

$$\nabla_2 V = -4\pi G\rho.$$

In this case the density ρ_m for the stars of mass m may be written

$$\rho_m = m\phi_m(R, V)$$

and

$$\rho = \sum_m m\phi_m(R, V) = \bar{m}\phi(R, V), \tag{5}$$

where we let $\bar{m}$ represent the mean value of the mass of a particle when all $\phi_m = 1$. The function ϕ is finite and positive for finite values of V, and further, $\frac{\partial\rho}{\partial V} > 0$. This is evident when we consider that in the "characteristic diagram" the limits of integration in I_1 and I_2 increase with V.

3. We may write for a particle in an arbitrary system

$$I_1 = H^2 + \Theta^2 - 2V,$$

and further let an angle ψ define the direction of the vector H in the Π, Z-plane. For the element of phase-volume we may then put

$$RdRdzd\theta d\psi HdHd\Theta,$$

or, introducing I_1 and I_2 as independent variables instead of H and Θ,

$$dRdzd\theta d\psi dI_1 dI_2. \tag{6}$$

In the motion of a particle in any system we have

$$\frac{DI_1}{Dt} = -2\frac{\partial V}{\partial t}, \qquad \frac{DI_2}{Dt} = \frac{\partial V}{\partial \theta}. \tag{7}$$

For the stars which at a certain moment are situated in a given interval of

* *Leçons sur les hypothèses cosmogoniques*, p. 100, 1911.
† *M.N.*, **76**, 70, 1915 ; *Astronomy and Cosmogony*, p. 364, 1929.
‡ *M.N.*, **76**, 37, 1915.
§ *M.N.*, **97**, 182, 1937.

space defined by ΔR, $\Delta\theta$, Δz, we may therefore keep I_1 and I_2 constant by changing artificially H and Θ, so that

$$\frac{\partial H^2}{\partial t} = 2\frac{\partial V}{\partial t} - \frac{\partial \Theta^2}{\partial t}, \qquad R\frac{\partial \Theta}{\partial t} = -\frac{\partial V}{\partial \theta}. \tag{8}$$

In the case when $H = 0$ we may apply, instead of the correction to H, a small displacement of the particles in z according to the equation

$$2\frac{\partial V}{\partial z}\frac{\partial z}{\partial t} = -2\frac{\partial V}{\partial t} + \frac{\partial \Theta^2}{\partial t}, \tag{8a}$$

or, if $\frac{\partial V}{\partial z} = 0$, a displacement in R. In this case we obtain for I_1 and I_2 constant the equation

$$\left(\frac{\partial V}{\partial R} + \frac{\Theta^2}{R}\right)\frac{\partial R}{\partial t} = -\frac{\partial V}{\partial t} - \frac{\Theta}{R}\frac{\partial V}{\partial \theta}. \tag{8b}$$

This equation fails only for $\frac{\partial V}{\partial R} + \frac{\Theta^2}{R} = 0$, which means that the particles follow momentarily circular orbits. If we start from symmetry of rotation, as will presently be described, these particles, though we have to admit changes in their I_1 and I_2 values, will give no contribution to $\frac{\partial V}{\partial t}$ if, by adjusting Θ, we let them continue to follow circular orbits of constant R. As long as the matter in the state $H = 0$ with $\frac{\partial V}{\partial z} \neq 0$ or $\frac{\partial V}{\partial R} + \frac{\Theta^2}{R} \neq 0$ may be assumed to form an infinitesimal part of the entire mass of the system, the direct influence of displacements according to (8*a*) or (8*b*) on $\frac{\partial V}{\partial t}$ will be small. Considering the phase-space defined by R, z, θ, ψ, I_1, I_2, where θ and ψ only vary between 0 and 2π, we find that the phase-volume (6) will be constant in the motion, and it will evidently not be affected by the transformation (8) for $H > 0$. We may now arrange a steady artificial interchange of the stars of given m between phase-elements of equal size on different parts of the intersection surface $I_1 = \text{const.}$, $I_2 = \text{const.}$, and let $\frac{\partial V}{\partial t}$ in (8) include the change of V due to this process as well. Starting from the state at a certain moment in the natural motion, we arrange first, however, a uniform distribution in θ for the particles of mass m in a given interval $dRdzd\psi dI_1 dI_2$. In this process it may be necessary to allow certain shifts in I_1, forming first a spatial distribution of rotational symmetry for given R, z, ψ, I_2, and arranging afterwards, when V has symmetry of rotation, a random distribution in θ for each value of I_1 as well. After rotational symmetry has been attained, the interchange of particles of mass m between phase-elements of given values of I_1 and I_2 may proceed simultaneously with the natural motion. By spreading the particles of $H = 0$ and of $\frac{\partial V}{\partial z}$ or $\left(\frac{\partial V}{\partial R} + \frac{\Theta^2}{R}\right)$ differing from

zero uniformly over all the phase-elements of the corresponding values of I_1 and I_2, we may counteract the steady production of such particles by (8) when $\frac{\partial V}{\partial t} < 0$, and keep the number of such particles small. After a uniform distribution of the particles of $H > 0$ over the I_1, I_2 surfaces has been attained, we distribute slowly the remaining particles of $H = 0$, which we may keep artificially in the state $H = 0$ at constant R and z without disturbing $\frac{\partial V}{\partial t}$, over the corresponding I_1, I_2 surfaces in such a manner that $\frac{\partial V}{\partial t}$ remains infinitely small. Any given system containing a great number of material particles may in this way be arranged, steadily satisfying Poisson's equation, into a state with on the average even frequency along the surfaces $I_1 = \text{const.}$, $I_2 = \text{const.}$, and thus into a steady distribution of the type $f_m(I_1, I_2)$.

Moreover, starting from a given equilibrium $f_m(I_1, I_2)$ of rotational symmetry, so that $\frac{\partial V}{\partial \theta} = 0$, we may increase slowly the frequency for any I_1, I_2, and by (8) steadily counteract the corresponding change in V so that I_1 and I_2 remain constant for all particles. In this way a given equilibrium form may be steadily modified. If we start from a known equilibrium of small mass, *e.g.* a spherical system or a ring-shaped system of particles in circular motion, corresponding to a certain frequency distribution in I_1 and I_2 (*cf.* the function V_1 below), we may change the system successively into the equilibrium form of a greater total mass.

4. It is evident that the results just obtained suffice to demonstrate the very general existence of a steady state of the kind in question. In what follows, however, we shall approach the problem analytically, in order to try to find new properties of its solutions. We then turn our attention first to the case of spherical symmetry. We assume in this case that I_2 disappears in $f(I_1, I_2)$ and form in analogy with (5) the density $\rho = \bar{m}\phi(V)$. Defining a constant λ by

$$\lambda = G\bar{m}, \tag{9}$$

we have then Poisson's equation, if r is the distance from the centre, in the form

$$\frac{d^2V}{dr^2} + \frac{2}{r}\frac{dV}{dr} = -4\pi\lambda\phi(V). \tag{10}$$

We have $\phi(V)$ and $\phi'(V) \geqslant 0$. On account of the condition $I_1 \leqslant 0$ we must have $\phi(V) = 0$ for $V < 0$. In the actual systems occurring in nature we must expect a rapid decrease of ϕ when V decreases towards $V = 0$, and therefore limit ourselves here to such systems where we may put $\phi = 0$ for $V < V_0 < 0$. For great r we may then assume

$$V = \frac{C}{r}. \tag{11}$$

We assume that V attains the value V_0 at $r = r_0$, and thus have

$$V_0 = \frac{C}{r_0}; \qquad \left(\frac{dV}{dr}\right)_0 = -\frac{C}{r_0^2}. \tag{12}$$

With these initial values for $r = r_0$ we integrate (10) from r_0 down to the small radius $r = \epsilon$, and assume for the small sphere with $r < \epsilon$ a constant value of ϕ equal to $\phi(V(\epsilon))$. We then compute the total mass M as a function of C. For sufficiently small values of C we have $M = 0$, $\frac{dM}{dC} = 0$. For greater values of C we may write

$$M = F(C)C^3, \tag{13}$$

where $F(C)$ changes slowly with C, if $\phi(V)$ does not change very rapidly with V. There will then be one, and only one, value of C for which $C = GM$. In this case we have everywhere $\frac{dV}{dr} = -G\frac{M_i}{r^2}$, where M_i is the mass interior to r, and letting ϵ decrease towards zero we have the solution of our problem. It may easily be shown that for given $\phi(V)$ and V_0 but with varying λ we have $M^2\lambda = \text{const.}$

5. We approach now our general problem. Let the function $\phi(R, V)$ in (5) be prescribed on the basis of the given functions $f_m(I_1, I_2)$ for the different mass-classes of the particles. The function ϕ may be called the generating function. Keeping the mass-ratio of the different kinds of particles constant, we assume now a proportional increase in the absolute values of the masses, which gives a steady increase of λ. We assume the potential V to be generated partly by the system which is governed by ϕ and λ, and partly by an auxiliary system which does not depend explicitly on ϕ and λ and which gives a potential function V_1. We introduce

$$\psi(R, V) = \frac{\partial \phi}{\partial V}, \tag{14}$$

and assume ψ to be continuous, finite and positive for all values of R and for finite values of V. We assume further that ϕ and ψ decrease rapidly to 0 for small V, so that we may put $\phi = 0$, $\psi = 0$ for $V < V_0$. For a finite system we may therefore assume a finite volume Ω in space outside of which we may put $\phi = 0$, $\psi = 0$. The condition to be fulfilled by V is now

$$V = \lambda \int_\Omega \phi(R', V')\frac{dv'}{r'} + V_1, \tag{15}$$

where r' is the distance between the points R', θ', z' and R, θ, z, and $dv' = R'dR'd\theta'dz'$. Differentiating with respect to λ, we get

$$\frac{dV}{d\lambda} - \lambda \int_\Omega \frac{dV'}{d\lambda}\psi(R', V')\frac{dv'}{r'} = \int_\Omega \phi(R', V')\frac{dv'}{r'} + \frac{dV_1}{d\lambda}. \tag{16}$$

We may assume that V_1 is generated by a function ϕ_1 and a coefficient λ_1 in analogy with V; thus

$$V_1 = \lambda_1 \int_{\Omega_1} \phi_1(R', V') \frac{dv'}{r'} \tag{17}$$

and

$$\frac{dV_1}{d\lambda} = \lambda_1 \int_{\Omega_1} \frac{dV'}{d\lambda} \psi_1(R', V') \frac{dv'}{r'}. \tag{18}$$

For $\lambda = 0$ we have $V_1 = V_1^{(0)}$, and by (16) and (18),

$$\frac{dV}{d\lambda} - \lambda_1 \int_{\Omega_1} \frac{dV'}{d\lambda} \psi_1(R', V_1^{(0)\prime}) \frac{dv'}{r'} = \int_{\Omega} \phi(R', V_1^{(0)\prime}) \frac{dv'}{r'}. \tag{19}$$

This equation will have a unique solution, because we assume this to be the case when we set in the right-hand member $\phi = \phi_1$, *i.e.* when the function $\lambda\phi$ represents only an increase in the given auxiliary function $\lambda_1\phi_1$ which we assume to exist.

In the case when the velocity distribution is ellipsoidal we shall have

$$\phi(R, V) = \sum_m F_m(R) e^{\kappa V}, \tag{20}$$

and if κ is approximately the same for different m,

$$\psi(R, V) = \kappa\phi(R, V). \tag{21}$$

We cannot expect F_m and κ to remain the same when V approaches close to 0, because we assume ϕ to vanish for $V < V_0$. We assume, however, for κ a certain constant mean value for different parts of the system, and we may then write (16)

$$\frac{d(V - V_1)}{d\lambda} - \kappa \int_{\Omega} \frac{dV'}{d\lambda} \lambda\phi \frac{dv'}{r'} = \frac{V - V_1}{\lambda}. \tag{22}$$

Defining further, omitting indices,

$$\overline{\frac{dV}{d\lambda}} = \frac{\int_{\Omega} \frac{dV}{d\lambda} \lambda\phi \frac{dv}{r}}{\int_{\Omega} \lambda\phi \frac{dv}{r}}, \tag{23}$$

and observing that

$$\int_{\Omega} \lambda\phi \frac{dv}{r} = V - V_1,$$

we get

$$\frac{d(V - V_1)}{d\lambda} - \kappa \overline{\frac{dV}{d\lambda}} (V - V_1) = \frac{V - V_1}{\lambda}. \tag{24}$$

Multiplying with $\lambda\phi \frac{dv}{r}$ and integrating, we obtain with a certain approximation, if $\bar{V}_1$ may be considered as constant, and if we may identify $\overline{\overline{\frac{dV}{d\lambda}}}$ and $\overline{\frac{dV}{d\lambda}}$ with $\frac{d\bar{V}}{d\lambda}$,

$$\frac{d(\bar{V} - \bar{V}_1)}{d\lambda} [1 - \kappa(\bar{V} - \bar{V}_1)] = \frac{\bar{V} - \bar{V}_1}{\lambda}. \tag{25}$$

Finally, we get the solution

$$(\bar{V} - \bar{V}_1)e^{-\kappa(\bar{V}-\bar{V}_1)} = C\lambda. \tag{26}$$

For each value of $\bar{V}_1$ we have to determine C so that the solution fits the mean potential derived by (19) for an infinitely small λ. C will evidently in this way depend on the functions $F_m(R)$ in (20). Proceeding in this way we get the typical solution illustrated in the diagram. To each value of λ below a value λ_{max} there correspond two values of $\bar{V}$. λ_{max} will of course

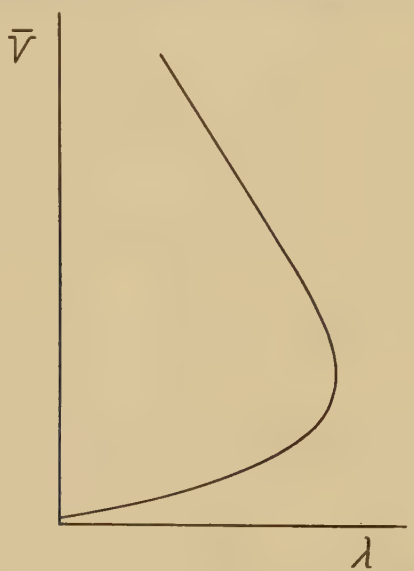

change with the functions $F_m(R)$. For $V_1 = 0$ we get by (19) and (26) $C = 0$. In the spherical case of § 4 the law $M^2\lambda = \text{const.}$ evidently corresponds to the upper branch of the curve, from λ_{max} upwards, for infinitely small C.

We must now discuss the potential V_1. Out of the distribution function $f_m(I_1, I_2)$ for the stars of mass m we may select a partial function

$$f_1(I_1), \tag{27}$$

defined within limited intervals of I_1 and I_2. The corresponding space-density may be written

$$\rho_1 = m\phi_1(V), \tag{28}$$

and we know that a spherical solution $V = V_1^{(0)}$ corresponding to this density function exists. This value has to be used for $V_1^{(0)}$ in (19). For finite λ,

$$V_1 = \lambda_1 \int_{\Omega_1} \phi_1(V') \frac{dv'}{r'}. \tag{29}$$

When forming the function $\phi(R, V)$ we have to use $f_m - f_1$ (supposed positive) instead of f_m for the stars of mass m. We may in other cases take for $V_1^{(0)}$ the potential of a circular ring where the particles move in circular orbits. This corresponds to a finite frequency for certain values of I_1 and I_2, and we take this frequency as our function f_1. In the diagram the

series of solutions for increasing λ will now correspond to a curve of steadily changing V_1. Following this curve until $\lambda = G\bar{m}$, when possible, will give the desired solution.

6. In the present case the density ρ is a function

$$\rho = \bar{m}\phi(R, V), \quad \text{where} \quad \frac{\partial \rho}{\partial V} > 0.$$

Here V is the gravitation potential, R the projection of the radius vector on the plane of rotation (invariable plane) passing through the centre of gravity. R is thus the distance from the axis of rotation. We have in several respects an analogy with the case of a heterogeneous rotating liquid in which the density is constant on the surfaces $U(x, y, z) = \text{const.}$, where

$$U(x, y, z) = \kappa V(x, y, z) + \Phi(R^2).$$

For a given R the density depends in both cases on the potential V. We may now apply to our case an analysis analogous to that carried out by Lichtenstein * for a heterogeneous liquid showing that *the system must possess symmetry with respect to the plane* $z = 0$.

7. If the system has a great degree of flattening towards this plane for a certain interval of R, it may happen that the potential V may be written in these regions approximately

$$V = V_1(R) + V_2(z). \tag{30}$$

In the case of an ellipsoidal velocity-distribution we have then, by (20) and (5),

$$\rho = \bar{m} \sum_m F_m(R) e^{\kappa(V_1 + V_2)}. \tag{31}$$

Generally we cannot satisfy Poisson's equation with this expression for the density. Assuming, however,

$$F_m(R) e^{\kappa V_1(R)} = \text{const.}, \tag{32}$$

we may write

$$\rho = \bar{m}\phi(V_2(z)), \tag{33}$$

and for Poisson's equation

$$\nabla_2 V_1(R) = 0, \qquad \nabla_2(V_2(z)) = -4\pi G\rho(z), \tag{34}$$

which gives

$$\frac{dV_1}{dR} = -\frac{C}{R}, \qquad \frac{d^2V_2}{dz^2} = -4\pi G\rho(z). \tag{35}$$

Equation (32) may be fulfilled with a close approximation within a limited interval of R if we assume that the mean motions for $z = 0$ coincide nearly with the circular motions about the centre.† In this case we may therefore assume (30) to be valid with considerable approximation within a certain

* *Gleichgewichtsfiguren rotierender Flüssigkeiten*, Berlin, p. 22, 1933.

† Cf. *Stockholms Observatoriums Annaler*, **12**, No. 4, pp. 15–17, 1936.

interval of R, and consequently have in this region another integral of the motion, namely,

$$Z_0^2 = Z^2 - 2[V(R, z) - V(R, 0)]. \tag{36}$$

We may introduce this quantity in the frequency function in order to diminish the dispersion in Z so that the axis of the velocity ellipsoid in the z direction becomes smaller than the axis in the R direction, in conformity with the conditions prevailing at our point of the galactic system. It is evident that when the integral (36) exists we may perform this change without disturbing the general equilibrium of the system. In this way we derive a quasi-steady state with a frequency function

$$f_m(I_1, I_2, Z_0^2). \tag{37}$$

In the natural motion a quasi-state of this type will be produced when the distribution of particles over the successive intersections of the surfaces

$$I_1 = \text{const.}, \qquad I_2 = \text{const.}, \qquad Z_0^2 = \text{const.}$$

may be considered as a distribution at random so that there is no correlation between the distributions over any two of these intersections, provided that we have at the same time average rotational symmetry.

We may remark incidentally that the first equation (35) determines the differential rotation in the case of a quasi-steady three-axial ellipsoidal distribution. We have for the circular motion

$$\Theta_c = \sqrt{C}, \tag{38}$$

and then get for Oort's constants A and B,

$$\left.\begin{aligned} A &= \tfrac{1}{2}\left(\frac{\Theta_c}{R} - \frac{\partial \Theta_c}{\partial R}\right) = \tfrac{1}{2}\frac{\sqrt{C}}{R} \\ B &= \tfrac{1}{2}\left(-\frac{\Theta_c}{R} - \frac{\partial \Theta_c}{\partial R}\right) = -\tfrac{1}{2}\frac{\sqrt{C}}{R} \end{aligned}\right\}. \tag{39}$$

The constants should be of the same absolute amount, but of opposite sign. This agrees well with the observed data, which give for A and B expressed in seconds of arc per year nearly

$$A = +0''{\cdot}003, \qquad B = -0''{\cdot}003.$$

The ratio of the galactic axes α and β of the velocity ellipsoid should be by a known formula in combination with (39),

$$\frac{\beta}{\alpha} = \sqrt{1 - \frac{A}{A - B}} = 0{\cdot}71, \tag{40}$$

which also agrees well with observed data, especially after correcting for the slight vertex deviation in galactic longitude. The results obtained may be considered as a further argument in favour of the general correctness of the numerical determination of the constant B, which is the most difficult one to find from observation.

These results for the circular motions must not be confused with those concerning the mean speed of rotation for a certain individual ellipsoidal distribution. This mean speed is *

$$\Theta_0 = \frac{C_1 R}{C_2 + R^2}, \tag{41}$$

as was already found by Eddington † for the "cylindrical" case. Here the ratio of the galactic axes is

$$\frac{\beta}{\alpha} = \sqrt{\frac{C_2}{C_2 + R^2}}, \tag{42}$$

and the coefficients of differential rotation,

$$A = \frac{C_1 R^2}{(C_2 + R^2)^2}, \qquad B = -\frac{C_1 C_2}{(C_2 + R^2)^2}. \tag{43}$$

In order to harmonize these results with the result for the circular motions derived above by Poisson's equation, we should have in the mean C_2 equal to the mean value of R^2 in the region. We may then write for a slight variation of R,

$$C_2 + R^2 = \overline{R^2} + R^2 = 2R_0 R, \tag{44}$$

if we replace the arithmetical with the geometrical mean, and write $R_0 = \sqrt{\overline{R^2}}$. Introducing (44) in (41) we get $\Theta_0 = \text{const.}$, as in (38). Considering the form of the function $F_m(R)$ it may further be shown directly that this is the condition for the simultaneous validity of (32) and (35) when Θ_0 is large compared with α and β.

The present results show, however, that we cannot assume three-axial ellipsoidal distributions in which (32) and (35) are valid within wide intervals of R. *The three-axial ellipsoidal distribution is an approximation for certain local intervals of R.* Special reasons for its appearance in our regions have been given in previous papers.

8. We do not consider here more special types of steady states which imply other integrals of the motion. In fact, we may assume that in the case of a natural system consisting of a great many free particles there are no uniform first integrals as long as I_1 and I_2 vary. It is true that if at a certain moment the variation of the field of force may be described as a pure rotation with the angular velocity ω, we have at this moment the Jacobi integral

$$I_1 - 2\omega I_2 = \text{const.},$$

but such a state must obviously be an exception which cannot survive for a long time. Further, in the spherical case we have two more area integrals. Still, the spherical case considered in § 4 above, in which the area integral disappears in the frequency function, is perhaps the most natural one from an evolutionary point of view.

* *Loc. cit.*

† *M.N.*, **76**, 48, 1915.

Special cases like those when the field of force is Newtonian or quasi-elastic, in so far these states are not merely limiting cases of the general case considered here, lie outside the scope of the present work, as we do not consider here the case of a prescribed central force. In our case we *define* a steady state simply as a state in which the field of force becomes stationary as a consequence of the mixing of matter in the natural motion. More special steady states under a prescribed force appear plainly artificial, except when used to describe the conditions in a local region.* The general cases of plane motion in a Newtonian or in a quasi-elastic field are, however, of a certain theoretical interest because the frequency function includes in these cases all the three possible first integrals.†

Summary

The general existence of steady states of motion of the Poincaré-Jeans type is shown. In addition to symmetry of rotation, systems in these states must possess symmetry with respect to the invariable plane. In the case of steady three-axial ellipsoidal distributions the consequences of Poisson's equation for the character of the differential rotation and for the ratio of the axes in the galactic plane are demonstrated, and it is concluded that such distributions are valid only for limited intervals of the distance from the centre. The meaning in the present case of the term steady or quasi-steady state is discussed.

* Cf. *M.N.*, **97**, 15, 1937.
† Cf. *M.N.*, **97**, 642, 1937.

Stockholm Observatory,
Saltsjöbaden :
1938 *April.*

THE INCLINATIONS OF SPIRAL NEBULÆ TO THE LINE OF SIGHT.

H. Knox-Shaw.

In a recent paper * F. G. Brown calculated the inclinations to the line of sight of the planes of the extra-galactic nebulæ of over 2′ in diameter in Reinmuth's catalogue,† and came to the conclusion that the preponderance of small inclinations could not be accounted for by observational selection, but was apparently due to a systematic orientation of the planes in space in relation to the line of sight from the Earth. This is inherently so improbable that it seemed worth while to pursue the matter further. I have consequently made a similar calculation for the objects in the Shapley-Ames catalogue,‡ adopting, however, the revised dimensions and descriptions for 448 of the nebulæ given in Part 4 of the same volume of the *Harvard Annals*. This catalogue covers the whole sky ; the dimensions of the nebulæ contained therein are taken from a number of sources ; and altogether it seems to afford the best available material for testing the point under consideration.

It is clear that the elliptical nebulæ should not be included in the discussion, as they do not satisfy the necessary condition of being discoid, it being generally accepted that they are spheroids of varying degrees of ellipticity. They would thus be expected to show a larger proportion of nearly circular images than if they were discs whose planes were distributed at random, and the figures for them given in the table show this to be the case.

Nebulæ in Shapley-Ames Catalogue
Frequency of Occurrence of Various Axis Ratios

Objects	No.	Axis Ratio		
		0 to 1/3	1/3 to 2/3	2/3 to 1
		per cent.	per cent.	per cent.
Elliptical nebulæ	229	6	32	62
Spirals, all	708	26	39	35
Spirals, 2′ and larger	574	30	40	30
Spirals, 2′ and larger, within 30° of N.G.P.	189	36	38	26

The nebulæ described as spiral, or probably so, in the Shapley-Ames catalogue were therefore counted separately. At first all such were included in the count, but as it seemed possible that among the smaller nebulæ the more elongated might have escaped detection, another count was made in which the spirals whose major axes were less than 2′ were omitted, this

* *M.N.*, **98**, 218, 1938.
† *Heidelberg Veröffentlichungen*, **9**, 1926.
‡ *Harvard Annals*, **88**, 2, 1932.

being the same limit adopted by Brown for his selection from the Reinmuth catalogue. The results for these counts are also given in the table, as percentages for the three groups of the ratio of minor to major axis which with random distribution should each contain the same number of nebulæ. It will be seen, in contradiction to Brown's results, that even when the nebulæ below 2′ in diameter are omitted there is no excess of elongated objects.

The Harvard catalogue covers the whole sky completely down to magnitude 13, and yet about one-third of its objects are within 30° of the north galactic pole. The Heidelberg catalogue, without any specified magnitude limit, goes down to declination −20° only, and so probably contains a still larger proportion of nebulæ from the polar cap. The Harvard catalogue supplies evidence that the elongated spirals are relatively a little more frequent in this region than elsewhere, so the large proportion of elongated objects found by Brown may to some extent be due to the preponderating influence of the rich polar cap. In any case, the difference between the results from the two catalogues suggests that selection of one kind or another has an important effect on the figures obtained, and gives us no cause for thinking that the planes of the spirals are in general distributed in other than a random manner.

Summary.—The frequency of apparent ellipticities of the spirals down to 2′ in diameter in the Shapley-Ames catalogue is such as would be expected from a random distribution of their planes.

ON THE FORM OF ROTATING-GAS CONFIGURATIONS. II. CONFIGURATIONS POSSESSING A REVERSAL OF THE DENSITY GRADIENT.

Zdeněk Kopal, D.Sc.

1. *Introduction.*—In a paper recently communicated to the Society * the dependence of the oblateness of a slowly rotating-gas configuration on the angular velocity of rotation was studied for three different models and different degrees of density condensations, in order to get a general idea about the dependence of the resulting oblatenesses on the whole march of density distribution. It has been found that, for values of $\frac{\rho_c}{\rho_m}$ near to unity, the oblateness depends essentially only on the density condensation, while if $\frac{\rho_c}{\rho_m}$ becomes larger, the oblatenesses of configurations with the same density condensations still depend substantially on the complete march of the density distribution.

All the three models discussed in I have been characterised by a negative density gradient throughout. But the density distributions in stellar interiors may have such special features that a reversal of the density gradient may occur within the interior, and the question arises about the effects of such reversals on the oblatenesses of slowly rotating-gas configurations. This question is not only of purely theoretical importance. As in I, our underlying aim will be to investigate whether the low density condensations arrived at in studying the ellipticities of eclipsing binaries are matters of fact, or whether they can be explained in any other way, say by the occurrence of reversals of the density gradient.

The discussion of the physical significance of such reversals is beyond the scope of the present paper, and the reader is referred to recent works of Rosseland † and Chandrasekhar.‡ As will be seen, in the present analysis we introduce the reversals of the density gradients by a formal extension of the second model discussed in I, which is most appropriate for this purpose and will enable us also to follow to some extent the mathematical procedure developed in I.

2. *The Equations of the Problem.*—It has already been shown by Clairaut § that if e denotes the oblateness of a gas spheroid and $v = \frac{\omega^2}{2\pi G\rho}$, we may for

---

* *M.N.*, **98**, 414, 1938 ; in the following it will be referred to as I.

† *Astrophysica Norvegica*, **2**, 1936.

‡ *M.N.*, **96**, 132, 1936.

§ *Cf.* Tisserand, *Traité de la Mécanique céleste*, **2**, 211–220 (Paris), 1891.

slow rotations put

$$\frac{e}{v} = C, \tag{1}$$

where C is a function of the internal density arrangement, being given by

$$C = \frac{15}{4} \cdot \frac{\phi\left(\frac{a}{a_1}\right)^3 \int_0^{a_1} \rho a^2 da}{\left(2\phi + a\frac{d\phi}{da}\right)\int_0^a \rho a^2 da - a^3 \int_a^{a_1} \rho d\phi}, \tag{2}$$

which at the boundary defined in the following by $a_1 = 1$ clearly becomes

$$C = \frac{15}{8 + \frac{4}{\phi_1}\left(\frac{d\phi}{da}\right)_1}, \tag{2.1}$$

a being the major semi-axis of the spheroid and ϕ is defined by the following equation :—

$$a^2\frac{d^2\phi}{da^2} + \frac{2\rho a^4}{\int_0^a \rho a^2 da} \cdot \frac{d\phi}{da} + 2\left(\frac{\rho a^3}{\int_0^a \rho a^2 da} - 3\right)\phi = 0. \tag{3}$$

Substitute

$$\phi = \psi \int_0^a \rho a^2 da\,; \tag{4}$$

then (3) assumes the form :

$$\frac{d^2\psi}{da^2} = \left(\frac{6}{a^2} + \frac{a^2\frac{d\rho}{da}}{\int_0^a \rho a^2 da}\right)\psi. \tag{5}$$

3. *The Density Equation.*—Let us now define the density relation by

$$\frac{a^2\frac{d\rho}{da}}{\int_0^a \rho a^2 da} = \beta - \alpha a^{2n}, \tag{6}$$

where α, β and n are arbitrary constants. The density distribution defined in this way will show the following feature :—

(i) For any value of n the equation $\frac{d\rho}{da} = 0$ has a real and positive root at $a_n = \left(\frac{\beta}{\alpha}\right)^{\frac{1}{2n}}$.

(ii) For $a=0$, and

$$n > -\tfrac{1}{2}, \qquad \left(\frac{d\rho}{da}\right)_{a=0} = 0;$$

$$n = -\tfrac{1}{2}, \qquad \left(\frac{d\rho}{da}\right)_{a=0} \neq 0, \text{ but finite};$$

$$n < -\tfrac{1}{2}, \qquad \left(\frac{d\rho}{da}\right)_{a=0} = \infty.$$

If, further, α and β are positive for $n > -\frac{1}{2}$ and negative for $n < -\frac{1}{2}$, then there is a maximum density at $a=a_n$ and a minimum at the centre for $n > -\frac{1}{2}$, while for $n < -\frac{1}{2}$ the central density vanishes. Generally speaking, the density distribution defined by (6) exhibits a reversal of the density gradient at $a=a_n$ and yields a minimal, but finite density at the centre for $n > -\frac{1}{2}$, while for $n < -\frac{1}{2}$ the density of the configuration vanishes at the centre as well as at the boundary. The constants α, β, n determine the boundary, the zone of the reversal and the density condensation; if we put $a_1 = 1$, only two of them remain arbitrary.

4. *First Model.*—Let us investigate first the behaviour of configurations with finite density at the centre, *i.e.* specified by $n > -\frac{1}{2}$.* Eq. (5) then takes the form:

$$\frac{d^2\psi}{da^2} = \left(\frac{6}{a^2} - \alpha a^{2n} + \beta\right)\psi. \tag{7}$$

Supposing n to be a positive integer,† its particular solution satisfying the condition $\psi_{a=0} = 0$ is

$$\psi = ka^3\left\{1 + \sum_{i=1}^{\infty} \frac{P_i(\alpha, \beta, n)}{\Delta(i)} a^{2i}\right\} \tag{8}$$

(k being an unimportant integration constant), where

$$\Delta(i) = 2 \cdot 7 \cdot 4 \cdot 9 \cdot \ldots \cdot 2i(2i+5),$$

and P_i's are polynomials given by

$$1 \leqslant i \leqslant n, \qquad P_i(\alpha, \beta, n) = \beta^i;$$

$$i = n+1, \qquad P_i(\alpha, \beta, n) = \beta^{i+1} - \alpha\Delta(i-1);$$

$$i > n+1, \qquad P_i(\alpha, \beta, n) = \beta P_{i-1} - \Delta_i(n) P_{i-n-1};$$

where

$$\Delta_i(n) = (2i-2n)(2i-2n+5)(2i-2n+2)(2i-2n+7) \ldots$$
$$\ldots (2i+2n-6)(2i+2n-1).$$

Let us turn now to the density equation

$$a^2\frac{d\rho}{da} = (\beta - \alpha a^{2n})\int_0^a \rho a^2 da, \tag{9}$$

and substitute

$$\int_0^a \rho a^2 da = u; \tag{10}$$

* In the limiting case $n = -\frac{1}{2}$ the solution of (6) is expressible in terms of confluent hypergeometric functions (*cf.* Whittaker and Watson, *Modern Analysis*, p. 340).

† The case $n=0$ has already been solved in I; we have only to put $\alpha - \beta = k^2$.

(9) assumes the form:

$$\frac{d^2u}{da^2}-\frac{2}{a}\frac{du}{da}+(\alpha a^{2n}-\beta)u=0. \tag{11}$$

Remembering that u (*i.e.* the mass included in the volume of the radius a) is proportional to a^3 and therefore must vanish for $a=0$, the particular solution of (11) satisfying this condition is

$$u=ka^3\left\{1+\sum_{i=1}^{\infty}\frac{Q_i(\alpha,\beta,n)}{\nabla(i)}a^{2i}\right\}, \tag{12}$$

where k is again a constant of integration,

$$\nabla(i)=2\cdot 5\cdot 4\cdot 7\ \ldots\ 2i(2i+3),$$

and, again for positive integral values of n,

$$\begin{aligned} 1\leqslant i\leqslant n, &\qquad Q_i(\alpha,\beta,n)=\beta^i;\\ i=n+1, &\qquad Q_i(\alpha,\beta,n)=\beta^i-\alpha\nabla(i-1);\\ i>n+1, &\qquad Q_i(\alpha,\beta,n)=\beta Q_{i-1}-\nabla_i(n)Q_{i-n-1}; \end{aligned}$$

where

$$\nabla_i(n)=(2i-2n)(2i-2n+3)(2i-2n+2)(2i-2n+5)\ \ldots\ \ldots\ (2i+2n-6)(2i+2n-4).$$

Now, from (10) it follows that

$$\rho=\frac{1}{a^2}\frac{du}{da}, \tag{10.1}$$

and putting

$$k=\tfrac{1}{3}\rho_c,$$

the solution of (9) finally becomes

$$\rho=\rho_c\left\{1+\sum_{i=1}^{\infty}\frac{Q_i}{(2i+1)!}a^{2i}\right\}. \tag{13}$$

Eq. (13) specifying the complete march of the density distribution of the model under consideration provides us at the same time with the relation between α and β. Imposing the condition $\rho=0$ at $a=1$, this relation assumes the form:

$$\sum_{i=1}^{\infty}\frac{Q_i}{(2i+1)!}=-1. \tag{13.1}$$

The surface density gradient is now given by

$$\left(\frac{d\rho}{da}\right)_1=\rho_c\sum_{i=1}^{\infty}\frac{Q_i}{(2i-1)\,!\,(2i+1)}, \tag{14}$$

and the density condensation

$$\frac{\rho_{\max}}{\rho_{\text{mean}}}=\frac{\beta-\alpha}{3\left(\frac{d\rho}{da}\right)_1}\cdot\frac{\rho_{\max}}{\rho_{\text{centr}}}, \tag{15}$$

where

$$\frac{\rho_{\max}}{\rho_{\text{centr}}} = 1 + \sum_{i=1}^{\infty} \frac{Q_i}{(2i+1)!} \left(\frac{\beta}{\alpha}\right)^{\frac{i}{n}}. \tag{15.1}$$

Having determined α and β we proceed to determinations of ϕ. Eq. (4) by differentiation yields

$$\frac{d\psi}{da} = \frac{\psi}{\phi}\left\{\frac{d\phi}{da} - \psi\rho a^2\right\}, \tag{16}$$

and since the density at the boundary vanishes, we see that at $a = 1$,

$$\frac{1}{\phi_1}\left(\frac{d\phi}{da}\right)_1 = \frac{1}{\psi_1}\left(\frac{d\psi}{da}\right)_1, \tag{16.1}$$

i.e. the ratios $\left(\frac{\phi'}{\phi}\right)_1$ and $\left(\frac{\psi'}{\psi}\right)_1$ become identical. Differentiating (8) we get the expression for ψ', and inserting $a = 1$, the ratios $\left(\frac{\phi'}{\phi}\right)_1$ can easily be evaluated.

Using the above results, numerical calculations have been carried out for the special case $n = 2$; Table I contains the results. The first column gives β chosen arbitrarily; col. 2, the corresponding value of α determined by eq. (13.1); col. 3, the radius of zone of the reversal $a_n = \left(\frac{\beta}{\alpha}\right)^{\frac{1}{2}}$; col. 4, the surface density gradient as given by (14) (putting $\rho_c = 1$); col. 5, the density condensation determined by use of (15) and (15.1); col. 6, the surface value of ψ given by (8); col. 7, its derivative at $a = 1$; col. 8, their ratio; and col. 9, the C's resulting from (2.1).

TABLE I

β	α	a_n	$\left(-\frac{d\rho}{da}\right)_1$	$\frac{\rho_{\max}}{\rho_{\text{mean}}}$	$\frac{\psi_1}{k}$	$\frac{\psi_1}{k}$	$\left(\frac{\phi'}{\phi}\right)_1$	C
0	22·2057	0·0000	4·7273	1·5657	0·6983	0·4816	0·6997	1·3890
0·01	22·2261	0·1457	4·7330	1·5646	0·6986	0·4813	0·6889	1·3946
0·1	22·4099	0·2585	4·7835	1·5546	0·7011	0·4784	0·6823	1·3980
0·5	23·2469	0·3830	5·0109	1·5132	0·7122	0·4655	0·6536	1·4132
1	24·2474	0·4506	5·3103	1·4592	0·7266	0·4432	0·6100	1·4368
2	26·2630	0·5254	5·9394	1·3617	0·7555	0·3927	0·5198	1·4882
3	28·2462	0·5676	6·7135	1·2535	0·7849	0·3275	0·4172	1·5514
4	30·2102	0·6032	7·6320	1·1447	0·8145	0·2483	0·3048	1·6270
5	32·1038	0·6282	8·6991	1·0385	0·8463	0·1644	0·1943	1·7090

Before discussing the results let us consider now the second model characterised by $n < -\frac{1}{2}$.

5. *Second Model.*—If in eq. (7) $n < -\frac{1}{2}$, the mathematical procedure in solving it is much the same as that developed in the preceding paragraph, and we shall not repeat it generally save for the case $n = -1$, where it can assume an essentially different form.

If $n = -1$, eq. (7) becomes

$$\frac{d^2\psi}{da^2} = \left(\frac{6}{a^2} + \frac{\alpha}{a^2} - \beta\right)\psi, \tag{7.1}$$

and its particular solution vanishing at the centre is

$$\psi = ka^{p+1}\left\{1 + \sum_{i=1}^{\infty} \frac{(-\beta)^i}{i!\,\Delta_i(p)}\left(\frac{a}{2}\right)^{2i}\right\}, \tag{17}$$ *

k being again an unimportant integration constant, and

$$\Delta_i(p) = (p+\tfrac{3}{2})(p+\tfrac{5}{2}) \ . \ . \ . \ (p+i+\tfrac{1}{2}),$$

p being the positive root of the equation

$$p(p+1) = 6 + \alpha.$$

The density equation assumes the form:

$$a^2\frac{d\rho}{da} = \left(\frac{\alpha}{a^2} - \beta\right)\int_0^a \rho a^2 da\,; \tag{9.1}$$

substituting, as in § 4,

$$\int_0^a \rho a^2 da = u, \tag{10}$$

(9.1) becomes

$$\frac{d^2u}{da^2} - \frac{2}{a}\frac{du}{da} + \left(\beta - \frac{\alpha}{a^2}\right)u = 0. \tag{11.1}$$

Its particular solution satisfying the condition $\lim_{a \to 0} u = 0$ is found to be

$$u = ka^{m+1}\left\{1 + \sum_{i=1}^{\infty} \frac{(-\beta)^i}{\Delta_i(\alpha)}a^{2i}\right\},$$

where k is an integration constant,

$$\Delta_i(\alpha) = [m(m+3) - \alpha][(m+2)(m+5) - \alpha] \ . \ . \ . \ [(m+2i-2)(m+2i+1) - \alpha],$$

and m is the positive root of the equation

$$m(m-1) = \alpha + 2.$$

Remembering again that

$$\frac{du}{da} = \rho a^2,$$

it results

$$\rho = ka^{m-2}\left\{1 + \frac{1}{m+1}\sum_{i=1}^{\infty} \frac{(2i+m+1)}{\Delta_i(\alpha)}(-\beta)^i a^{2i}\right\}.$$

---

* As the reader may verify, this can be expressed also in terms of Bessel functions with imaginary argument (*cf.* Watson, *Theory of Bessel Functions*, p. 101).

The computations of $\left(\frac{d\rho}{da}\right)_1$, $\frac{\rho_{max}}{\rho_{mean}}$, etc., follow closely the procedure developed in § 4, and the results are:

TABLE II

a	β	a_n	$\left(-\frac{d\rho}{da}\right)_1$	$\frac{\rho_{max}}{\rho_{mean}}$	$\frac{\psi_1}{k}$	$\frac{\psi_1'}{k}$	$\left(\frac{\phi'}{\phi}\right)_1$	C
0	9·8696	0·0000	1·0000	3·2899	0·4838	0·6241	1·2899	0·7599
1·75	13·6357	0·3583	0·8559	2·1791	0·3696	0·3934	1·0644	1·2237
4	17·9138	0·4725	0·7069	1·8695	0·2980	0·2646	0·8879	1·2985

6. *General Discussion.*—The nature of the problem can most conveniently be shown, as in I, diagrammatically. In the diagram the C's are plotted against $\frac{\rho_{mean}}{\rho_{max}}$, and the three lines correspond to three different models. Full line represents the second model discussed in I (negative density gradient throughout), dotted line corresponds to the first model discussed in § 4

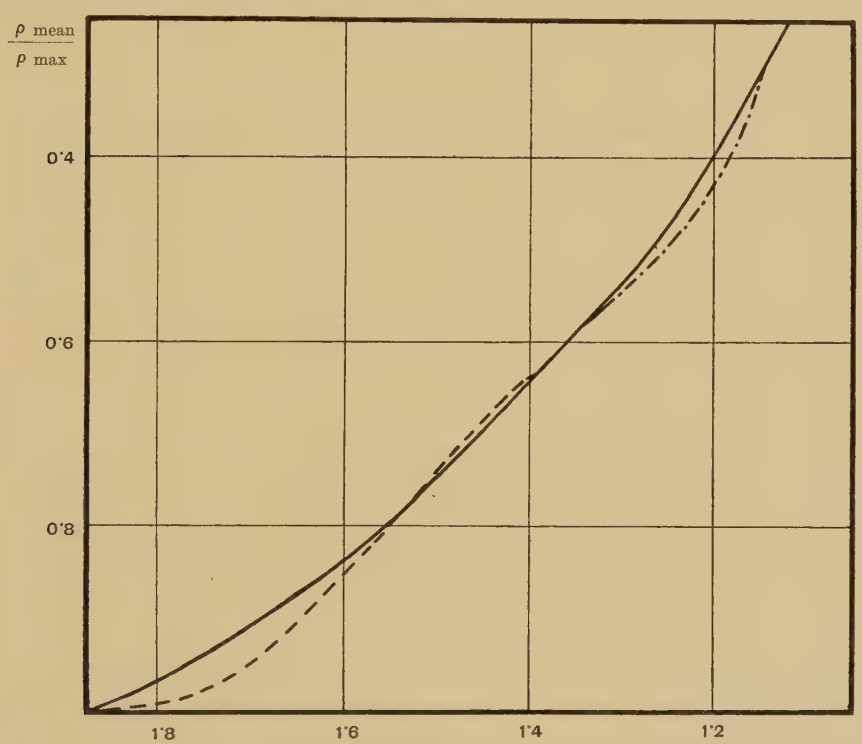

of this paper (reversal of the density gradient and the central density minimal, but finite); dots and points correspond finally to the second model treated in § 5 (reversal of the density gradient, but central density zero).

A glance at the diagram shows that the effect of the reversal on C, *i.e.* on the oblateness, is surprisingly small, even in such cases where the reversal is

exhibited at the half-distance between the surface and the centre. If two configurations with the same density condensations, but one with maximal density at the centre and the other with maximal density nearer to the surface than to the centre, rotate with the same value of v, their oblatenesses come out to be very nearly the same too. It may be objected that in the present analysis we have dealt only with moderately condensed configurations and, further, the above results are based on a rather limited number of quadratures, but in view of our underlying astrophysical problem our interest is chiefly confined to the configurations with low density condensation, and it is very probable that further quadratures would contribute to the detailed study of the special models concerned, but would scarcely change the main feature of our problem. Thus the answer to the question whether the occurrence of reversals of density gradient may account for the low density condensation arrived at in the case of eclipsing binaries seems to be definitely negative.

But so far all investigations concerned have dealt with models rotating with constant angular velocity or constant v, and there are serious reasons that this might be very far from being true.* It may be objected, however, that if the density condensation is low, the increase of the angular velocity inwards could be only moderate, but the possibility cannot be ruled out *a priori*, that low density condensations arrived at in the case of eclipsing binaries may perhaps to some extent be consequences of the improbable hypothesis, $\omega = \text{constant}$. The effect of the density condensation on the surface oblateness of a gaseous configuration rotating with the angular velocity increasing downwards has not yet been, as far as I know, the subject of any investigation. It is interesting to point out that the fundamental equations used in the present paper have a certain bearing also on this case, but its discussion would exceed widely the scope of the present analysis and is postponed to a future communication.

7. *Summary.*—The problem dealt with in the present paper may be stated as follows. Suppose we have a slowly rotating gaseous configuration with the density decreasing monotonically from the centre to the surface, which in consequence of its rotation becomes oblate. Now change the whole march of the density distribution in such a way that it will exhibit a reversal of the density gradient, and the maximal density will not be attained at the centre, but at a certain fraction of the radius. What will be the effect of the reversal on the oblateness compared with that of the initial configuration? In order to be able to give a general answer, the calculations have been carried out for two models (with central density finite or zero) in detail, and it was found that the effect of the reversal is generally small, even if it is exhibited at a considerable fraction of the radius. The oblatenesses of such configurations are very nearly the same as those of configurations with the same degree of density condensation, but possessing a negative density gradient throughout.

* *Cf.* again Rosseland, *Astrophysica Norvegica*, **2**, 1936, or Jeans, *Astronomy and Cosmogony*, Cambridge, 1928, § 249.

Concluding, I have again great pleasure in expressing my thanks to Professor Sir A. S. Eddington for allowing the very valuable privilege of enjoying the facilities offered by his observatory, where the above work was carried out. Dr. R. v. d. R. Woolley has again been kind enough to read the manuscript and assist in arranging its final English form.

Cambridge :
1938 *May*.

SUNSPOT ACTIVITY AND THE FORM OF THE SOLAR CORONA.

*W. E. Bernheimer.**

(Communicated by Professor F. J. M. Stratton)

1. This paper is a contribution to a series of studies which were devoted by several investigators to the connection between the shape of the solar corona and the general solar activity.

The greatest difficulty in dealing with this problem is the scarcity of the available material; the observations of the next few total eclipses may be of decisive value in establishing more exactly the relation under discussion.

With regard to the methods hitherto applied to our problem, and the results obtained, we refer to the full discussion by F. W. Dyson and R. v. d. R. Woolley.†

2. It has been found advisable in the present study to deduce for comparison the results for both kinds of corona-shape determination, *i.e.* for the ellipticity quantities as defined by Ludendorff (ϵ) and by Bergstrand (E_1). (The E_1-values correct the ϵ's by a veiling of the true form of the corona owing to streamers in the middle latitudes.) Both kinds of values have proved very useful for this investigation.‡

If we call ϕ the phase of an eclipse in the solar cycle ($\phi = 0$ corresponding to sunspot minimum), we find by a closer examination that appreciable differences between ϵ and E_1 appear only within the following negative phase-limits: $-0{\cdot}84 < \phi < -0{\cdot}25$. For the main conclusions drawn in the

* In accordance with the decision of the Council, this paper has been somewhat condensed by Dr. A. Beer. The paper was the last Professor Bernheimer wrote previous to his death at Vienna on 1937 December 14.

† F. W. Dyson and R. v. d. R. Woolley, *Eclipses of the Sun and Moon*, Oxford, pp. 103–108, 1937.

‡ References to previous work are as follows :—

W. J. S. Lockyer, *M.N.*, **82**, 323, 1922; **91**, 797, 1931.

H. Ludendorff, Preuss. Akademie, Berlin, *Sitzungsber Phys. Math. Kl.*, p. 185, 1928, and p. 200, 1934.

Ö. Bergstrand, *Arkiv för Mat., Astr. och Fys.*, **22** A, No. 1, and **25** A, No. 4 (or *Upsala Medd.*, Nos. 46 and 60), 1930 and 1934; *M.N.*, **95**, 436, 1935, or *Upsala Medd.*, Nr. 62, 1935.

S. A. Mitchell, *Handbuch d. Astrophysik*, **4**, 317 and 338, 1929; *Pop. Astr.*, **37**, 192, 1929; *Ap. J.*, **75**, 27, 1932, or *Philadelphia Proc. of American Philosoph. Soc.*, **71**, 344, 1932; *Science*, **81**, 463, 1935; *Handbuch d. Astrophysik*, **7**, 382, 1936; *Eclipses of the Sun* (4th ed.), pp. 399 and 497, 1935.

W. E. Bernheimer, *Arkiv för Mat., Astr. och Fys.*, **22** A, No. 25, 1931, or *Lund Medd.*, **1**, No. 126, 1931.

B. Svenonius, *K. Fys. Sällsk. Handlingar*, N.F., **48**, No. 5, or *Lund Medd.*, No. 84, p. 1, 1937.

present paper, therefore, the eclipses in this "critical region" have been excluded. But additional calculations in which they were used did not lead to any conflicting result.

3. It is the author's opinion that an adequate investigation of the material should not be performed purely graphically, but by applying an arithmetical treatment: namely, by the calculation of correlation coefficients (c.c.).*

For this purpose numerous typical series of relative sunspot numbers (r-series) have been considered and correlated with the ellipticity quantities.

The resulting correlation coefficients all reach high values.† But more important than this, for our consideration, is their relative behaviour. It appears, when sufficient r-series are used, and when the necessary precautions are taken, that their study leads to quite a number of interesting conclusions.

4. Table I collects the data of the eclipses from 1893 to 1932, arranged in order of their phases, and the corresponding measured values of ϵ and E_1. The sunspot numbers in the lower parts of the table refer to:

r_x: *Monthly Means.*—This first group of 9 values gives the monthly means taken for a date which is 3 months (r_{-3}), 2 months (r_{-2}), or 1 month (r_{-1}) before the eclipse, then for the time of eclipse itself (r_0), and for 4, 8, 12, 14, 16 months after it (r_4, r_8, r_{12}, r_{14}, r_{16}).

r_{bx}: *Half-yearly Means.*—This group represents 6 half-yearly means, centred about the date of the eclipse, 4 months after it, etc.

r_{ax}: *Yearly Means.*—These 6 annual means are grouped similarily to the r_{bx}-values.

For the purposes of discussion the r-values listed in Table I were taken as positive for the ascending and negative for the descending portions of the sunspot cycle. In calculating the correlation coefficients all those groups of the material were included, where special assumptions and weighting could be avoided. But it should be mentioned that the final results appear fully confirmed when the weighted material is used; the corresponding weights are given in § 5.

If the original values of ϵ were replaced by Mitchell's values (cf. *Handbuch*, 7, 382, 1935) (of which three are corrected: the eclipses Nos. 4, 6, 8 in Table I), the results remained unaffected, but some regularities were shown even more clearly. Thus all c.c. have been calculated using both possible ϵ-values.

5. Altogether 21 r-series have been selected (individual values are given in Table I), and in 10 different ways of grouping they have been correlated with the ellipticity. The final discussion has thus been based on 210 correlation coefficients. The groups, the weights of which are given in brackets, were formed as follows:—

I (1): Using the whole material given by Ludendorff (*cf.* 1934).

I*a* (1): The same, but with Mitchell's corrected ϵ-values for 3 eclipses (see § 4).

* *Cf., e.g.*, E. T. Whittaker and G. Robinson, *The Calculus of Observations*, London, pp. 317–342, 1929.

† Between −0·70 and −0·98.

TABLE I

Corona-Form and Sunspot Numbers

Eclipse																		
		No.	1	2	3	4	5	6	7	8	9	10	11	12	13	14	15	16
		Date	1929 May 9	1908 Jan. 3	1896 Aug. 8	1930 Oct. 21	1898 Jan. 21	1932 Aug. 31	1900 May 28	1922 Sept. 20	1901 May 17	1923 Sept. 10	1914 Aug. 21	1925 Jan. 24	1926 Jan. 14	1927 June 29	1893 Apr. 16	1905 Aug. 30
		Phase ϕ	−0·83	−0·78	−0·67	−0·57	−0·47	−0·24	−0·17	−0·15	−0·04	+0·02	+0·25	+0·31	+0·50	+0·81	+0·82	+0·85
		ϵ	0·12	0·08	0·24	0·27	0·18	0·20	0·30	0·26	0·25	0·22	0·19	0·13	0·07	0·04	0·00	0·01
		E_1	0·27	0·25	0·26	...	0·27	0·30	0·32	...	0·27	0·27	0·25	0·19	0·17	0·11	0·09	0·05
Sunspot Relative Numbers	Monthly Means	r_{-3}	57	74	26	20	10	22	6	6	2	5	2	16	75	85	71	41
		r_{-2}	59	65	49	31	12	23	7	11	5	6	14	25	57	83	72	60
		r_{-1}	53	46	52	24	30	5	22	6	0	2	4	17	100	66	64	64
		r_0	59	45	22	35	27	6	9	6	11	11	9	8	77	67	88	59
		r_4	34	41	43	43	26	11	8	5	1	1	22	43	64	63	129	56
		r_8	65	87	31	15	35	3	0	3	5	21	41	60	61	74	94	55
		r_{12}	37	57	22	10	20	0	10	13	3	25	70	72	82	91	82	48
		r_{14}	22	66	14	18	18	3	1	10	1	23	54	63	70	84	99	18
		r_{16}	32	36	33	11	8	0	1	1	8	6	35	64	79	61	70	65
	Half-yearly Means	r_b	62	48	40	27	25	11	11	8	4	7	10	20	67	68	81	67
		r_{b4}	69	48	39	29	25	11	7	7	2	6	23	34	60	62	89	63
		r_{b8}	62	55	27	22	25	8	4	4	4	16	46	59	66	73	78	60
		r_{b12}	34	46	22	15	20	3	4	7	3	23	56	67	78	87	87	55
		r_{b14}	31	43	26	14	15	2	3	6	5	20	52	69	79	79	82	58
		r_{b16}	29	38	30	14	12	4	2	6	6	20	50	60	72	73	82	60
	Yearly Means	r_a	60	50	42	31	25	12	10	11	3	5	14	27	61	70	82	60
		r_{a4}	61	50	35	26	27	10	8	7	4	10	26	36	65	70	86	61
		r_{a8}	53	52	29	22	23	7	5	7	3	15	41	54	67	75	87	60
		r_{a12}	46	49	26	16	20	5	3	5	5	17	50	61	71	75	82	60
		r_{a14}	34	45	26	15	17	4	3	7	5	23	54	65	71	75	79	62
		r_{a16}	31	43	26	14	13	5	4	10	7	27	59	67	71	71	76	60

II (3): With ϵ-values as in I, but the r-values corrected algebraically by +17,* to account for Mitchell's law (see § 8 of this paper) and to make coincide ellipticity maximum and sunspot minimum.

II*a* (3): With corrected values (see I*a*).

* The mean of the values of r (with the convention of sign given above) at the times of greatest corona ellipticity is −17.

III (4): With ϵ-values as in I, disregarding Mitchell's law, but omitting the first 5 eclipses of Table I (see § 2).
III*a* (4): With corrected values (see I*a*).
IV (6): The same as in II, but omitting the first 5 eclipses of Table I (see § 2); using ϵ.
IV*a* (6): With corrected values (see I*a*).
V (4): The same as in II, but with E_1 instead of ϵ.
VI (5): The same as in IV, but with E_1 instead of ϵ.

6. Here are the results of the discussion of all c.c.-values, derived from numerical and graphical representations:

All the highest c.c. show conclusively the absence of the r_0-series, as well as that of all other r_x-series based on 1-month means. Also r_{-3} and all other negative r-series are absent. Only positive r-series remain. They show clearly that the c.c.-values are the higher the wider their basis is, *i.e.* the highest values belong to the yearly means.

Table II gives for 5 of the 10 groups the c.c. for the series r_x, r_{bx}, r_{ax}. We consider for comparison, as an example, the 36 c.c. for the groups III*a*, IV*a*, V (*i.e.* all values given in Table II for these groups except the three r_{-3} values of the r_x-series). 34 out of these 36 cases show the result stated above, viz. that the c.c. increase with the width of their basis. (The two exceptions are r_{a4} in group IV*a* and $r_{a\,14\text{–}16}$ in group V.)

The differences between the c.c. for different ways of combination are considerable. If we take, for example, the four groups III*a*, IV, IV*a*, V, each with 21 c.c., we obtain the following order of magnitude distribution: In the first place comes r_{a4}; r_0 is not before the 14th, r_{-3} in the 16th, r_{a16} in the 18th, and r_{14} in the 21st and last place.

7. The problem, does the corona change its shape—(*a*) rapidly, *i.e.* more or less in the rhythm of the corresponding sunspot situation, or (*b*) slowly, *i.e.* more or less in the rhythm of the yearly means, has thus been decided in favour of (*b*).

8. Another group of problems is connected with "Mitchell's law," which postulates the existence of a "positive phase-shift": the extreme values of the corona-form seem to occur earlier than the extreme values of the sunspots. Mitchell states (cf. *Handbuch*, **7**, 399, 1935), using his improved curve, that the most elongated corona is found $1\frac{1}{4}$ years before minimum of spots, and that likewise the corona closest in shape to a circle takes place $1\frac{1}{4}$ years before spot maximum.

The present discussion of the correlation coefficients shows that a positive phase-shift exists indeed, *i.e.* that the corona-form is anticipating sunspots. We have the result, that Mitchell's law can be extended also to the intermediate periods.

But it is a peculiarity to be noted that, according to our r-series, the amount of this displacement appears to be 8 months at the most and zero at the least. The average of 4 months is thus only one-quarter of the displacement mentioned above, as it was observed for the extreme values. Various tests have confirmed this result.

TABLE II

The Determination of the "Positive Phase-Shift": Correlation Coefficients representing the close connection between Ellipticity of the Corona and Sunspot Number

(Selected values for 5 of the 10 groups, which were defined in § 5 : the r-series are explained in § 4.)

Groups	Series		
	r_x	r_{bx}	r_{ax}
III	r_0 −0·880 r_{-3} −0·853 r_4 −0·888 r_8, r_{12} −0·878 r_{14}, r_{16} −0·837	r_b −0·956 r_{b4} −0·966 r_{b8}, r_{b12} −0·912 r_{b14}, r_{b16} −0·905	r_a −0·947 r_{a4} −0·964 r_{a8}, r_{a12} −0·942 r_{a14}, r_{a16} −0·896
III*a*	r_0 −0·879 r_{-3} −0·780 r_4 −0·825 r_8, r_{12} −0·884 r_{14}, r_{16} −0·853	r_b −0·934 r_{b4} −0·960 r_{b8}, r_{b12} −0·915 r_{b14}, r_{b16} −0·907	r_a −0·944 r_{a4} −0·964 r_{a8}, r_{a12} −0·944 r_{a14}, r_{a16} −0·912
IV	r_0 −0·930 r_{-3} −0·872 r_4 −0·908 r_8, r_{12} −0·875 r_{14}, r_{16} −0·837	r_b −0·965 r_{b4} −0·958 r_{b8}, r_{b12} −0·901 r_{b14}, r_{b16} −0·903	r_a −0·963 r_{a4} −0·956 r_{a8}, r_{a12} −0·925 r_{a14}, r_{a16} −0·882
IV*a*	r_0 −0·720 r_{-3} −0·897 r_4 −0·921 r_8, r_{12} −0·874 r_{14}, r_{16} −0·847	r_b −0·976 r_{b4} −0·977 r_{b8}, r_{b12} −0·915 r_{b14}, r_{b16} −0·899	r_a −0·976 r_{a4} −0·976 r_{a8}, r_{a12} −0·937 r_{a14}, r_{a16} −0·912
V	r_0 −0·844 r_{-3} −0·846 r_4 −0·860 r_8, r_{12} −0·815 r_{14}, r_{16} −0·762	r_b −0·941 r_{b4} −0·950 r_{b8}, r_{b12} −0·867 r_{b14}, r_{b16} −0·813	r_a −0·981 r_{a4} −0·979 r_{a8}, r_{a12} −0·900 r_{a14}, r_{a16} −0·794

In this connection we must emphasise the fact that the closest correlation occurs just for the series r_{a4} (*i.e.* for the annual mean of the sunspot activity

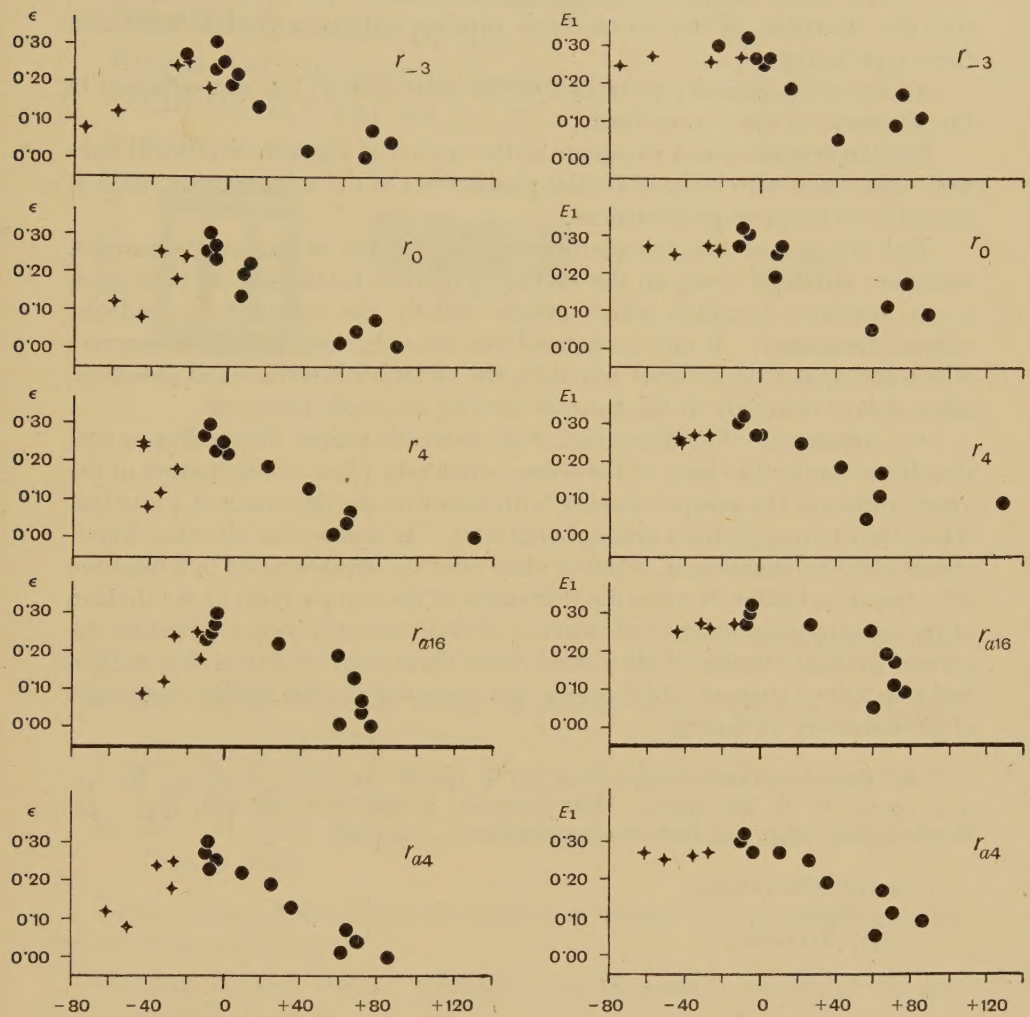

The form of the solar corona in its connection with the sunspot cycle.

The abscissæ are the relative sunspot numbers (taken negatively for eclipses with negative phases φ; see § 2).
The ordinates are the ellipticity quantities of the corona. (Ludendorff's ϵ is used in the left half of the figure, Bergstrand's E_1 in the right half; see § 2.)
The eclipses in the "critical phase-region" (see § 2) are marked with +.
The 10 small figures above represent 5 different r-series as defined in § 4. It is evident that r_{a4} furnishes the best correlation (see §§ 6 and 8).

taken symmetrically round the fourth month after the eclipse month). For the analogous half-yearly mean r_{b4}, and for the monthly mean r_4, the correlation becomes noticeably weaker.

9. An explanation of the displacement cannot be yet given. The in-

fluence of other solar phenomena has first to be studied along the lines suggested by recent papers.*

On the other hand, the existence of the phase-shift supports the view, that the alteration of the corona-form consists only in a gradual transition from type to type.

All the short-periodic variations of the solar activity are not reflected in the alteration of the corona-form.

Sudden eruptions and streamers of the corona of short duration will have to be correlated with isolated similar phenomena of the solar activity, such as flocculi and eruptive prominences.

The changes of the corona-form in the rhythm of the yearly sunspot variation, although being on the average 4 months in advance of it, suggest a yet unknown stimulus which affects equally the corona-form and the sunspot frequency. It may be noticed that the only other solar phenomenon which anticipates the sunspot activity is the variation of ultra-violet radiation, while delays relatively to the sunspot activity are more common.

10. *Summary.*—The discussion of all available eclipse data indicates that the alterations in the shape of the solar corona take place in the rhythm of the yearly means of the sunspot activity, with a positive displacement of 4 months. Thus they have a distinct gradual character. It seems that all other hypotheses must be abandoned, whether they refer to displacements in a negative direction, or whether they assume alterations of the corona-form in the rhythm of the simultaneous sunspot situation or of their monthly means. Besides the general gradual changes of the corona-form there exist doubtless also sudden and short-lived changes which appear to be associated with sudden outbreaks of prominences or flocculi.

* G. Bocchino, *Osservazioni e Mem. del R. Osserv. Astrofisico di Arcetri*, No. 51, p. 7, 1933 ; W. E. Bernheimer, *Vierteljahrsschr. d. Astr. Ges.*, **70**, 298, 1935 ; *4th Report Comm. Solar and Terrestr. Relationships*, p. 41, 1936.

University Observatory,
Vienna :
1937 *November.*

Errata

M.N., **98**, 86, No. 810. The R.A. and Dec. should be $18^h\ 10^m\ 10^s$, $-27^\circ\ 57'{\cdot}6$.

M.N., **98**, 87, No. 826. Observed Proper Motion in R.A., *for* -253 *read* $+253$.

M.N., **98**, 87, No. 832. Observed Proper Motion in R.A., *for* $+304$ *read* $+457$.